ABSTRACT

Title of Document: GEOMORPHIC, HYDRAULIC, AND BIOGEOCHEMICAL CONTROLS ON NITRATE RETENTION IN TIDAL FRESHWATER MARSHES

Emily D. Seldomridge
Doctor of Philosophy, 2012

Directed By: Dr. Karen Prestegaard
Department of Geology
University of Maryland, College Park

Tidal freshwater wetlands are ideal sites for nitrate retention because of their position within the landscape (near the head of tide); they receive water, discharge, nutrients (N and P), and sediment loads directly from contributing watersheds. Nitrate retention (the difference between nitrate inputs and outputs in an ecosystem), however, is difficult to predict due to the complex interactions between flow processes and the multiple retention processes. The goal of the study was to evaluate both external and internal controls on nitrate retention, and to determine whether scaling procedures could be identified to estimate nitrate retention for an entire ecosystem. The external controls included temperature, dissolved oxygen concentrations, and incoming nitrate concentrations. Internal controls are the interactions among geomorphic, hydrologic, and biological systems *within individual marshes* that influence nitrate retention.

This study was conducted in the upper Patuxent River Estuary where the ecosystem is composed of hundreds of individual marshes that are connected to the

estuary through tidal inlets; marsh inlet geomorphology governs water and nitrate fluxes into the marshes. This study therefore took a mass balance approach to determine geomorphic, hydrologic, and biological influences on nitrate retention. Nitrate retention was measured over a 4-year period in three tidal freshwater wetlands, selected to represent a range of marsh sizes.

An examination of the mass balance data suggest that nitrate retention is an outcome of complex interactions among inlet geomorphic characteristics, hydrologic flux, and biogeochemical processes. In cases where nitrate concentrations and temperatures are greater than critical (limiting) values, an emergent behavior in which nitrate retention is a simple function of water volume is observed. The wetland ecosystem is composed of numerous, small wetlands that process a small percentage of total nitrate; approximately 50% of retention is processed by the large marshes that comprise only 4% of the total population, but over 80% of the marsh area; therefore, any processes that affect tidal water volumes in large marshes is likely to affect net nitrate retention. The growth of vegetation in these large channels reduced ecosystem nitrate retention.

GEOMORPHIC, HYDRAULIC, AND BIOGEOCHMEICAL CONTROLS ON NITRATE RETENTION IN TIDAL FRESHWATER MARSHES

By

Emily D. Seldomridge

Dissertation submitted to the Faculty of the Graduate School of the
University of Maryland, College Park, in partial fulfillment
of the requirements for the degree of
Doctor of Philosophy
2012

Advisory Committee:
Karen Prestegaard, Chair
Jeffrey Cornwell
Sujay Kaushal
Wen-lu Zhu
Margaret Palmer

Acknowledgements

I would like to thank my committee, Drs. Karen Prestegaard, Jeff Cornwell, Sujay Kaushal, Wen-lu Zhu, and Margaret Palmer for their guidance and support. Specifically, I would like to thank Dr. Prestegaard for her close mentorship, motivation, and research insights. Also, I would like to thank Dr. Cornwell and his research assistant Mike Owens for their expertise and laboratory resources. This project wouldn't have been possible without field assistance from Dr. Prestegaard, Brittany Jenner, Marcie Occhi, and Tom Doody.

I express my deepest appreciation to my family and friends for their support. Thank you to my parents, Barry and Lisa, for encouraging me to strive for excellence, and providing love throughout this journey. My journey truly began many years ago when I was taught to explore the natural wonders of the Chesapeake Bay; I'm forever indebted. My sister, Lauren, was essential to the completion of this work. She listened as I recounted every excruciating step of my graduate career, and always managed to keep things in perspective. Lastly, I want to acknowledge all of my friends, and give a special thanks to those that participated in countless stress-reduction bike rides/spin classes.

This study was funded in part by an award from the Estuarine Reserves Division, Office of Ocean and Coastal Resource Management, National Ocean Service, National Oceanic and Atmospheric Administration. This support allowed me to finish my project within a short timeframe, and allowed me access to Jug Bay Wetland's Sanctuary and surrounding park area.

Table of Contents

Chapter 3: Use of geomorphic, hydrologic, and nitrogen mass balance data to model ecosystem nitrate retention in tidal freshwater wetlands

Chapter 4: Influence of emergent macrophytic and submerged aquatic vegetation on nitrate retention in tidal freshwater marshes

List of Tables

List of Figures

Chapter 1

Chapter 2

Chapter 3

Chapter 4

Chapter 5

Chapter 1: Introduction

1.1 Statement of purpose

1.1.1 Nutrient loads to the Chesapeake Bay

Nutrient loads to the Chesapeake Bay and many other coastal waters have been significantly increased by anthropogenic activities (Nixon, 1995). Nitrogen (N) loads derived from atmospheric (Fisher and Oppenheimer, 1991), wastewater discharges, urban/suburban runoff, and agricultural runoff (Smullen et al., 1982; Nixon, 1987; Fisher et al., 1988; Boynton et al., 1995) contribute to the development of eutrophic conditions in the Bay and other coastal waters (Boynton et al., 1995; Rabalais et al., 2001; Turner and Rabalais, 2003; Kemp et al., 2005). Significant efforts to reduce N and P (phosphorus) loads from contributing watersheds of the Chesapeake Bay are in place to mitigate these eutrophic conditions (i.e. Chesapeake Bay Agreement 1987; Chesapeake 2000). In the Mid-Atlantic region, these mitigation efforts have resulted in decreases in N and P loads to the Bay from some contributing watersheds (Langland et al., 2005); however, elevated N and P loads are still delivered into the Bay from its tributaries (Boyer et al., 2002; Testa et al., 2008).

The Chesapeake Bay receives contributions of water, nutrients, and sediments from both large and small river systems (Fig. 1.1). The large watersheds (Susquehanna and Potomac) are responsible for the vast proportion of water and nutrient loads to the Bay, whereas the small watersheds (e.g. Patuxent, Mattaponi, etc.) produce a smaller fraction of the total load. Due to their proximal location to the

Bay these small watersheds can directly affect the water quality in the sub-estuaries to which they contribute. Therefore, N reduction efforts in these watersheds can provide significant improvements on these Bay ecosystems.

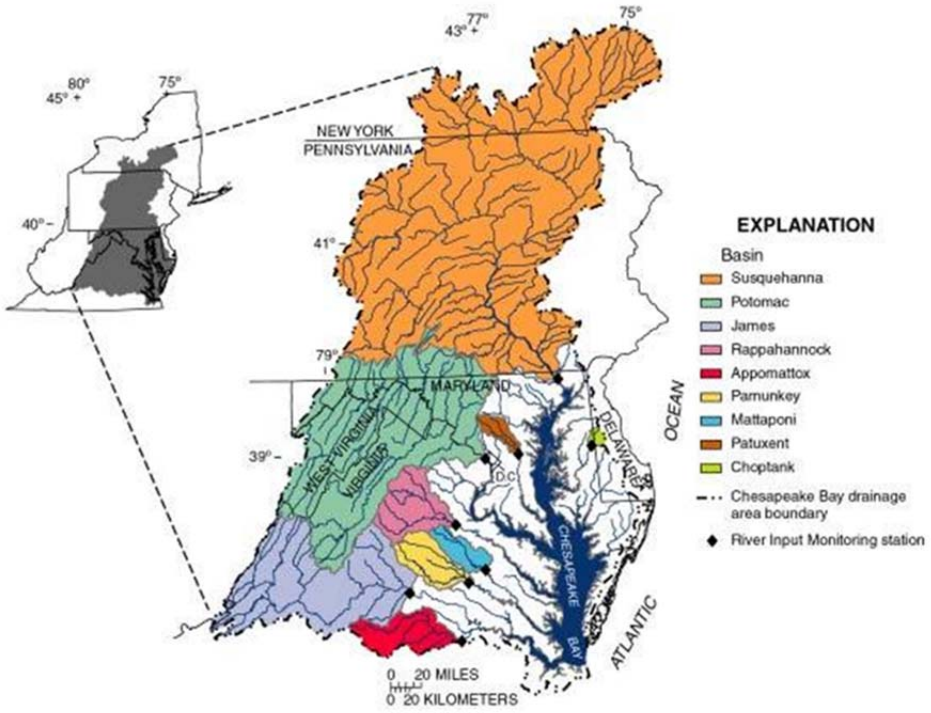

Figure 1.1. Map of the major contributing river basins of the Chesapeake Bay. The Patuxent River watershed is one of the smallest contributing basins, and is highlighted in dark orange. Dots indicate U.S. Geological Survey River Input Monitoring (RIM) stations. Image source: U.S. Geological Survey Chesapeake Bay River Input Monitoring Program.

The range in N and P contributions from the various Chesapeake Bay tributaries can be examined by comparing nutrient concentration and yield data collected through the U.S. Geological Survey Chesapeake Bay River Input Monitoring Program (RIM) stations (Fig. 1.2). In particular, the Patuxent River, which will be the focus of this paper, has high concentrations of both N and P, which lead to high yields per basin area (Fig. 1.2).

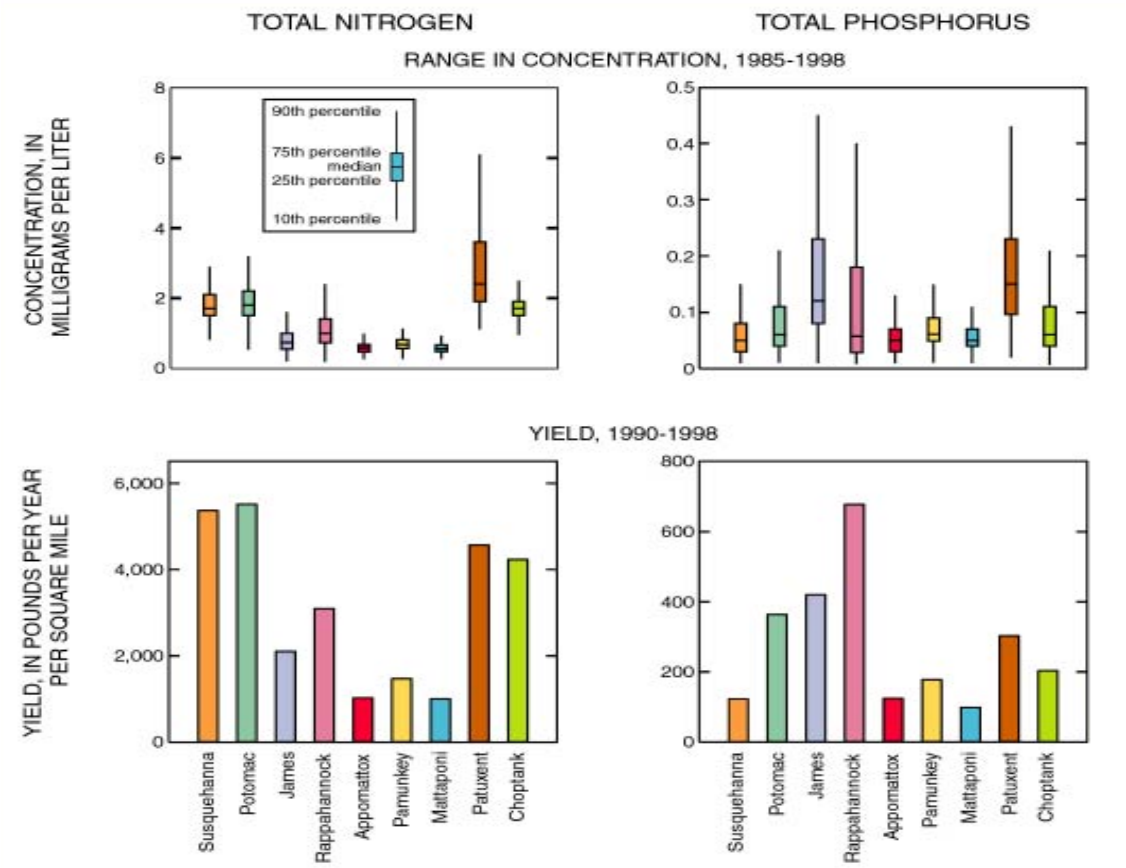

Figure 1.2. Chesapeake Bay River Input Monitoring Program nitrogen concentrations and yields (left panel) and phosphorus concentrations and yields (right panel) for 1985-1996. Image source: U.S. Geological Survey Chesapeake Bay River Input Monitoring Program.

Proximity to the Bay, however, is not the only difference between the large and small tributaries of the Chesapeake Bay; geologic and geomorphic characteristics are also significantly different between the small and large Bay tributaries. The Potomac and Susquehanna River Basins are in the Piedmont and Valley and Ridge Provinces, which are characterized by steep slopes, narrow river valleys (and floodplains), and shallow soils above bedrock. Most of the small tributaries are in the Coastal Plain Province, which is underlain by sedimentary rocks and Quaternary sediments. Coastal Plain watersheds have relatively low stream gradients, wide

floodplains, and extensive tidal freshwater wetlands (TFW) in their upper estuaries (e.g. Markewich et al., 1990). The TFW ecosystem of the Patuxent River is composed of hundreds of marshes arranged along the upper Patuxent River estuary (Fig. 1.3). These wetlands contain self-formed tidal channel networks that carry water, nutrients, and sediment into and out of marsh interiors (Rinaldo et al., 1999b). Each individual marsh is connected to the main estuary by a tidal inlet that governs the exchanges of water, solutes, and particulates with the Patuxent Estuary.

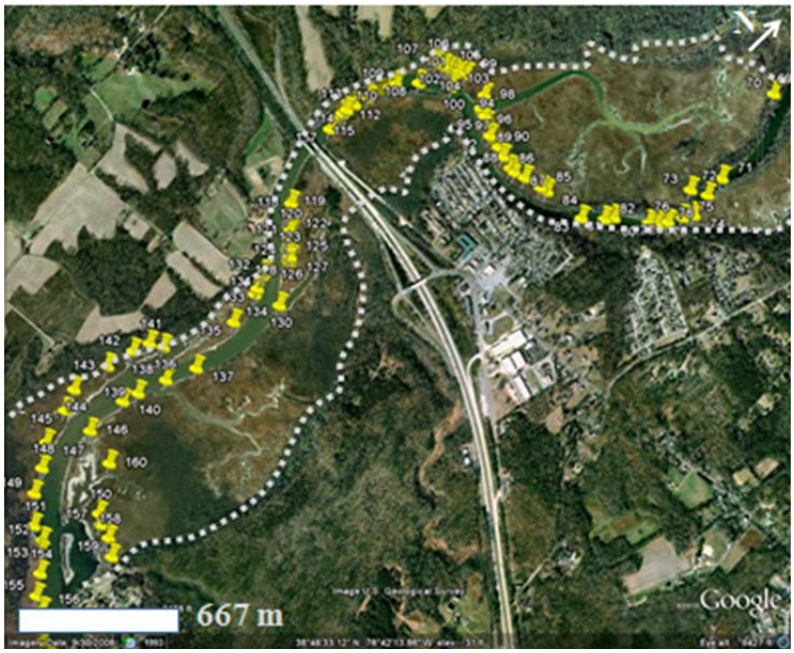

Figure 1.3. The tidal freshwater wetland ecosystem of the Patuxent River is composed of hundreds of individual marshes. Each marsh has a distinct tidal inlet (marked with a pin) that governs the water, sediment, and nutrient fluxes into and out of each marsh system. Image source: U.S. Geological Survey.

Previous work on TFW along Coastal Plain upper estuaries indicates that they process significant quantities of N and store sediment and nutrients through burial, thus can significantly improve the water quality of downstream portions of the estuary (Bowden, 1987; Seitzinger, 1988; 1994). Due to their landscape position, tidal freshwater wetlands (TFW) represent a final opportunity for attenuation of N loads

before water parcels reach the main estuary (Fig. 1.4). TFWs are bracketed between riparian (often forested) wetlands that are upstream of the TFWs. They represent the fresh end-member of a continuum of tidal marshes that extend to the salt marshes that fringe the lower estuary. Due to their position along this wetland continuum, TFW receive water, discharge, (Q), nutrients (N and P), and sediment loads directly from contributing watersheds, such as the Patuxent River (Boynton et al., 2008). Some portion of this water traverses the TFW ecosystems before entering into the lower estuary. TFWs also receive small inputs of N (often transformed into organic phases) that are transported upstream from the higher salinity portions of the estuary where sulfate reduction dominates microbial processing in these salt marsh ecosystems (Howarth and Teal, 1979).

Previous research suggests that TFW play important roles in coastal nutrient budgets. Although they account for a small fraction of the total estuary area, they are responsible for significant nutrient removal through denitrification and burial (Boynton et al., 2008). Freshwater wetlands function as critical buffers between terrestrial landscapes and estuaries due to their capacity to retain and/or transform nutrients and pollutants, particularly nitrogen (Simpson et al., 1983). As shown in figures 1.3 and 1.4, the freshwater tidal ecosystem can be composed of hundreds of individual tidal marshes that are connected to the estuary through tidal inlets. Therefore, the nitrogen processing (and other processes) within the TFW ecosystem is the sum of the processes that occur in these individual wetlands. The purpose of this research is to evaluate the linkages among the geomorphological, hydrological, and biogeochemical processes that affect N processing within this ecosystem.

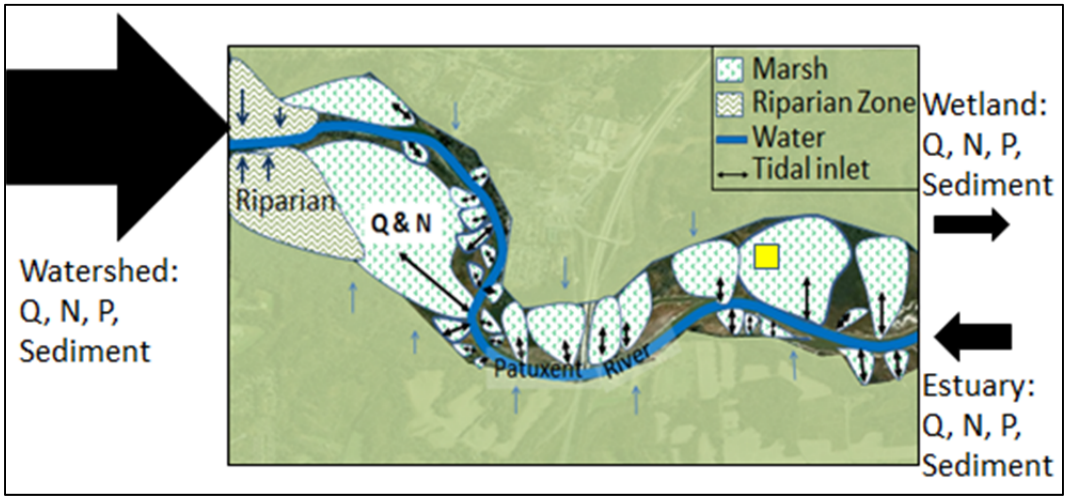

Figure 1.4. Conceptual diagram of tidal freshwater marsh ecosystem of the Patuxent River. Watershed processes deliver water, nutrients (N and P), and sediment to the head of tides. Additional inputs of groundwater (blue arrows) and stream flow occur along the length of the ecosystem; these contributions are small compared to the watershed inputs delivered to each marsh from the Patuxent. N, P, and sediment retention and biogeochemical processing occurs within the marsh ecosystem. Inset box (yellow) shows conceptual location of marsh processing diagram (Fig. 1.5).

1.1.2 The nitrogen cycle in tidal marshes and problems with up-scaling processes from individual marshes to entire TFW ecosystems

Previous work has demonstrated that the nitrogen cycle in freshwater ecosystems is complex (Fig. 1.5); it can involve multiple removal pathways, including microbially-mediated processes (e.g. denitrification and dissimilatory nitrate reduction to ammonium; Tiedje, 1988; Megonigal et al., 2009; Burgin and Hamilton, 2007), plant assimilation, and burial (Simpson et al., 1983; Bowden, 1987). Therefore, much of the previous research been designed to document N cycle processes, which are commonly measured at small spatial scales (note that a 1 m^2 plot would not be visible on images of the geomorphic setting in Fig 1.4). This detailed research on biogeochemical processes conducted in laboratory experiments or field

plots have identified dominant biochemical pathways and measured N processing rates (e.g. Jenkins and Kemp, 1984; Caffrey et al., 1993; Joye and Paerl, 1994). Recent research on N retention in marsh sediments has focused on the development of experimental techniques to produce fast, precise, and reproducible data on reaction rates in natural marsh materials. Core incubation experiments using Membrane Inlet Mass Spectrometry (MIMS; Kana et al., 1994; Kana et al., 1998), as well as acetylene inhibition experiments (Sørensen, 1978) provide these data. These measurements are often conducted under optimal conditions for denitrification that may not mimic natural environments (Seitzinger et al., 1993). Other laboratory measurements of denitrification rates have been conducted on intact, submerged marsh core samples under constant conditions (Seitzinger et al., 1980; Parkin et al., 1984; Kana et al., 1998). These experimental results should also be considered potential denitrification rates due to the constant availability of N in overlying waters. Extending the results of these core or plot-sized experiments to large, complex, natural ecosystems continues to be a problem (Petersen et al., 1999; Paola et al., 2009). In particular, N processing in natural TFW may be limited by available N or the transport of water and N from the main stream channel to marsh locations where processing takes place (Fig. 1.4).

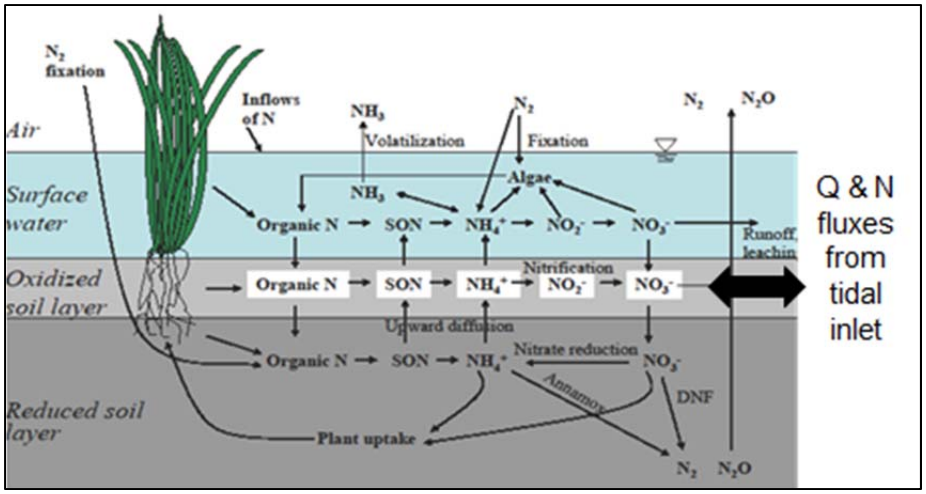

Figure 1.5. The nitrogen cycle in tidal freshwater wetlands (Mitsch and Gosselink, 2007) is highly complex. The main nitrate removal pathways are microbial processes such as denitrification (DNF) or annamox, plant uptake, and burial. These processes occur within the marshes (see highlighted inset in Fig. 1.3); therefore, the availability of N is determined by flux from tidal inlet.

Two underlying assumptions in using laboratory-scale nitrate retention rates to model ecosystem processes are that nitrogen retention is controlled by the kinetics of the biogeochemical reactions, and that this control extends *in situ* ecosystem conditions. With these assumptions, ecosystem N retention is estimated by applying these rates of biogeochemical processes to the measured quantity of sites for the processing to take place (e.g. marsh surface area). Previous research up-scaling research on other biogeochemical processes indicates that the number of processing sites may increase systematically from the laboratory to the watershed scale due to complexities of surface area (Navarre-Stitchler and Brantley, 2007). This kinetic approach to ecosystem scaling applies only if the process is not transport-limited.

As shown in figure 1.4, solutes (e.g. nitrate) and particulates are introduced into tidal freshwater wetlands by relatively low velocity transport during tidal cycles. Transport into tidal networks may be limited by flow resistance, network length, tidal cycle duration, and other process that may limit transport efficiency and thus affect biological processing. Therefore, the potential constraints introduced by nitrogen supply, kinetics of microbial reactions or plant uptake, and hydraulic controls on transport must be closely examined to determine dominant controls and to develop scaling procedures that can be used to determine ecosystem nitrate retention.

Measurements of nitrate retention in field settings may provide insight into the relationships among biological and physical processes that control N processing within an ecosystem. Should linkages between physical scaling relationships and biogeochemical processes be identified, they may be used to quantify processes such as nitrate retention at the ecosystem level. Therefore, small-scale experiments need to be complemented with field studies at a variety of physical scales to identify non-biological controls and to potentially develop scaling relationships that define ecosystem-level marsh processes (Petersen et al., 1999; Davidson and Seitzinger, 2006, Boyer et al., 2006; Seitzinger et al., 2006). Understanding the relationships and feedbacks among geomorphic, hydrologic, and ecological processes could improve our ability to predict the effects of environmental changes (e.g. invasive species or sea level rise) on marsh geomorphic structure and ecological processes.

1.1.3 Research questions

The purpose of this study is to determine the influence of geomorphic, hydrologic, and biologic processes on nitrate retention in the TFW ecosystem of the Patuxent River. Similar to other Coastal Plain sub-estuaries, the Patuxent River has an array of tidal marshes of varying size distributed along the length of the estuary. The approach of this project is to measure the spatial geomorphic organization of the tidal freshwater wetland ecosystem, select representative marshes within this geomorphic gradient in which to measure additional geomorphic characteristics and the relationship of hydrologic flux and biogeochemical processing to geomorphic controls (Fig. 1.6).

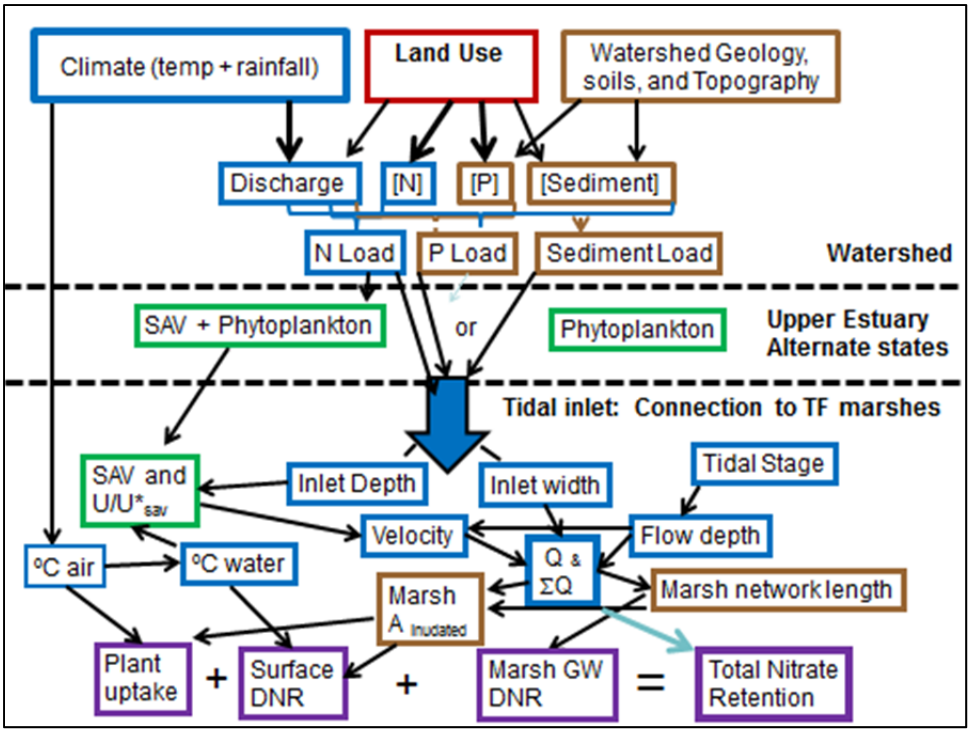

Figure 1.6. Flowchart of potential constraints on nitrate retention at a variety of scales (watershed to individual tidal marsh) in a tidal freshwater ecosystem. Fluxes into and out of the TFW ecosystem are governed by geomorphic characteristics of the tidal inlets and tidal hydrodynamics. Biological factors that may affect N uptake include microbial processes, plant uptake, and flow resistance caused by macro vegetation. Geomorphic variables are spatially distributed; tidal stage, temperature, and plant growth are temporally distributed.

Tidal freshwater wetlands ecosystems are composed of many individual marshes, which create spatial complexity. They respond to changes in astronomical tides and riverine inputs, which jointly affect tidal stage and generates temporal variability in processes. Furthermore, seasonal changes in biological processes and rates of processes result from air and water temperature changes. Therefore, I made the following simplifications of the research approach. Most of the mass balance measurements were examined only during spring (high) tidal stages. This stage should be associated with marsh inundation and therefore maximum rates of N

processing for each season. Although some characteristics of tidal marshes, such as marsh area, inlet width, and channel network length could be measured for each marsh within the ecosystem, mass balance measurements could not. Therefore, individual marshes of various sizes were selected for detailed hydrologic and N flux measurements. The research was designed to address the following questions:

1. For spring tides, does N supply, N transport, or N reaction kinetics (constrained by temperature) provide the dominant control on nitrate retention in tidal freshwater marshes?
2. What are the size distributions of geomorphic characteristics (marsh area, channel length, and inlet channel width) in the freshwater tidal wetlands?
3. In this complex system, are there emergent relationships that can be used as scaling laws to predict nitrate retention from other measured variables?
4. Does the seasonal growth of vegetation along and in tidal channels negatively affect nitrate retention within individual marshes and TFW ecosystems?

1.2. Study site and research approach

1.2.1 Study region

The Patuxent River watershed (2,260 km^2) is located between Washington, D.C. and Baltimore, Maryland. Land-uses in the basin include forest (63.5%), agriculture (20.3%), urban (15.7%), and intertidal wetlands (0.4%). Nitrate loads in the river have decreased in the past several decades largely due to reduction in point sources, but are still significantly higher than pristine watersheds (Fisher et al., 2006). The TFW ecosystem of the Patuxent River has been previously identified by Boynton

et al. (2008); it extends approximately 25 river kilometers along the upper Patuxent River (from 39° 0'N 76° 41'W to 38° 43'N 76° 41'W). This ecosystem is composed of hundreds of individual marshes with well-defined tidal creeks and marsh basin areas. The individual marshes are contained within protected parkland, Patuxent Wetland Park and Jug Bay Wetlands Sanctuary. Plant species that border tidal channels include: *Nuphar advena/leteum, Peltandra virginica, Polygonum sagittatum, Pontederia cordata*, and *Zizania aquatica*.

Tidal marshes fringe major coastal rivers; most large tidal marshes have organized networks of channels that function to bring tidal water into these marsh systems (Myrick and Leopold, 1963; Fagherazzi et al., 1999; Rinaldo et al., 1999a). The geomorphic structure of the channel network determines the amount of water, sediment, and solutes that enter the channel (Fagherazzi et al., 1999), the amount of overbank flooding that occurs, and the residence time of the water in the marsh system (Seldomridge, 2009). The tidal channel network is defined as the highly branching system of channels found within a tidal freshwater wetland. Although the mainstem of the Patuxent River flows along the marsh, natural levees between the marsh and river minimize overbank flooding directly from the main channel into back marsh areas. The marsh is primarily flooded by water that discharges through the tidal inlet, moves up the channel network, and then floods onto marsh surfaces. Most of the marsh surface area in the upper reaches of the Patuxent River lies within similar tidal network marshes. Minor fringing wetlands without tidal channels border the Patuxent River channel, but they are only inundated during extreme flooding stages (high tide + high Patuxent River flow) due to the height of the natural levees.

1.2.2 Mass balance approach to measurement of N retention

The geomorphic organization of channel network marshes affects marsh surface area and channel dimensions (Rinaldo et al., 1999b), which affect both nitrogen flux and retention. Overbank flooding of the interior marsh during the tidal cycle generates small water depths over large areas, which creates a favorable environment for nitrate processing; therefore, nutrient removal is thought to occur on the marsh surface and shallow subsurface environments adjacent to tidal creeks. The complex organization of the wetland channel network and adjacent marsh provides a series of sites for nitrate processing within the network during the tidal cycle; therefore, both hydrologic and biogeochemical processes likely affect overall ecosystem function.

A multi-scale (marsh to ecosystem-level), mass balance approach was used in this study to examine the relationships among geomorphic, hydrologic, and biogeochemical processes that determine nitrate retention in marsh networks as a function of spatial and temporal variables. By conducting the mass balance approach on a reference spring (high) tidal stage, spatial controls on nitrate retention can be examined. Moreover, the mass balance approach conducted over a three-year period allows for the identification of seasonal and inter-annual variability in N retention and its relationship to underlying physical and chemical characteristics.

Nitrate retention (NR) was determined from mass balance measurements of water and nitrogen into and out of the tidal wetlands from field measurements conducted in tidal inlets. Water chemistry was sampled at the mouth of the tidal

channel in concert with measurements of tidal stage and velocity that were used to calculate discharge. Of the three inorganic nitrogen species (NH_4-N, NO_2-N, and NO_3-N), nitrate was the only form of nitrogen that shows significant variation over the tidal cycle (Seldomridge, 2009; Seldomridge and Prestegaard, 2012). Nitrate concentration ([NO_3-N]), is measured for each time step, *Ci*. Nitrogen load (NL) is calculated for each time step (q_iC_i) and summed over the tidal cycle to obtain total nitrogen load for ingoing or outgoing tides:

$$NL = \sum(q_i\, C_i) \tag{1.1}$$

Where *NL* is nitrogen load, q_i is discharge for each time step (Ls^{-1}), C_i is nitrate concentration for each time step (μmol). A 5% discharge measurement error was propagated through all discharge and nitrate retention calculations; this error was determined by considering operator error in cross sectional area and velocity measurements (Sauer and Meyer, 1992), and error introduced by estimating average velocity from maximum velocity (Chen and Chiu, 2002). In addition, an analytical error of ±2 μmol (determined from instrumental error and reproducibility of standards) was propagated through all nitrate retention calculations (Keefe et al., 2004). Nitrate retention was determined by subtracting the outgoing nitrate load from incoming nitrate load:

$$NR = NL_{in} - NL_{out} \tag{1.2}$$

In this study, the water volume into the tidal channels was assumed to equal water volume out, and incoming nitrate concentrations were relatively constant on the incoming tide (Seldomridge and Prestegaard, 2012). One of the advantages of using

mass balance calculations of nitrate retention is that it provides measurements of nitrate retention for individual marshes for a given tidal cycle, time of year, and initial nitrate concentration.

1.2.3 Preliminary results and method refinement

An examination of tidal marshes along the Patuxent River (Seldomridge, 2009) indicates that:

i) Individual tidal marshes are of varying size.

ii) A governing inlet channel node connects each marsh network to the tidal estuary.

iii) Individual marshes contain tidal channel networks.

This indicates that there are two distinct geomorphic systems: 1) the *ecosystem* geomorphology is the distribution of tidal marshes and their inlet channels along the estuary, and 2) the *marsh* geomorphology includes the geomorphic relationships within an individual tidal marsh. The inlet channel morphology, tidal stage, and macrophyte flow resistance determine the amount of water and solutes that enter the channel, while the flow resistance of the tidal channel network and the channel morphology influence where and how much overbank flooding occurs, and the residence time of the water in the marsh system. The marsh channel network and adjacent marsh provides a series of sites for nitrate processing during the tidal cycle; however, the nutrient-rich water must reach all marsh areas for the whole system to participate in nitrate retention. Preliminary results (Seldomridge, 2009) indicate that nitrate retention per marsh area is less for large marshes than for smaller ones;

however, retention per water volume is the same for marshes of varying scale. These preliminary data suggest that hydrologic flux and marsh inundation probably limit nitrogen processing.

Field observations and previous research suggest there are likely three main interacting sets of controls that may affect nitrate retention (Fig. 1.6): tidal hydrodynamics, marsh geomorphic characteristics, and biological processes (including both the effects of macrophytes on hydraulics, plant uptake of N, and microbial biogeochemical processing). Geomorphic controls (e.g. marsh size and channel tidal channel characteristics) are spatially distributed, whereas hydraulic and biogeochemical processes are both spatially and temporally distributed. Spatial variations were characterized by determining 1) probability distributions of geomorphic characteristics that together define *ecosystem* geomorphic characteristics, 2) the relationship between geomorphic characteristics and hydrologic fluxes, and 3) the relationship between hydrologic fluxes and nitrate retention. Any variable that can be related to geomorphic or hydrologic variables can then be modeled using the geomorphic probability distributions.

The research questions posed above are examined in 3 main chapters. All chapters utilize the mass balance approach to calculate nitrate retention. Each chapter has a different goal and uses different data sets; therefore, data collection and analysis procedures are reviewed in each chapter to emphasize the approach for data interpretation. In the first results chapter, N supply, temperature (kinetic), and transport limitations on nitrate retention in tidal freshwater wetlands are examined using data collected over a three-year period. The purpose of this chapter is to

determine whether nitrate retention can be evaluated as an emergent property of the system and the conditions that govern this behavior. The second results chapter evaluates the spatial distribution of geomorphic characteristics of the TFWs in the ecosystem. Results from the first chapter are used to develop scaling relationships to estimate ecosystem nitrate retention. Due to the complexity of possible controls on nitrate retention, this scaling exercise was only conducted for a single tidal stage and season (spring (high) tides in autumn). In the third results chapter, the effects of emergent marsh macrophyte and submerged aquatic vegetation on flow hydraulics and nitrate retention were examined. Finally, in the conclusion chapter, the major findings of the dissertation are reviewed to evaluate nitrate retention in tidal freshwater wetland ecosystems level under a variety of conditions and the potential application of the results of this study to other systems.

1.3 Implications

The Patuxent River is not the only Coastal Plain River that has extensive areas of TFW that fringe upper estuaries. The upper reaches of many Mid-Atlantic and Southeastern U.S. estuaries also contain extensive riparian and tidal wetlands that formed as a result of sea-level rise in these low gradient systems (Pritchard, 1967; Dalrymple et al., 1992; Fig. 1.1 & 1.7). The hydrogeologic characteristics of the Coastal Plain are ideal for riparian and tidal freshwater wetland formation. Similar Coastal Plain wetlands extend from New Jersey south to Florida and west to Texas. Although the geomorphic-hydrologic and hydrologic-biogeochemical relationships may vary among these river systems, the approach to the investigation and some of

the results may be applicable to other TFW ecosystems if governing relationships are established.

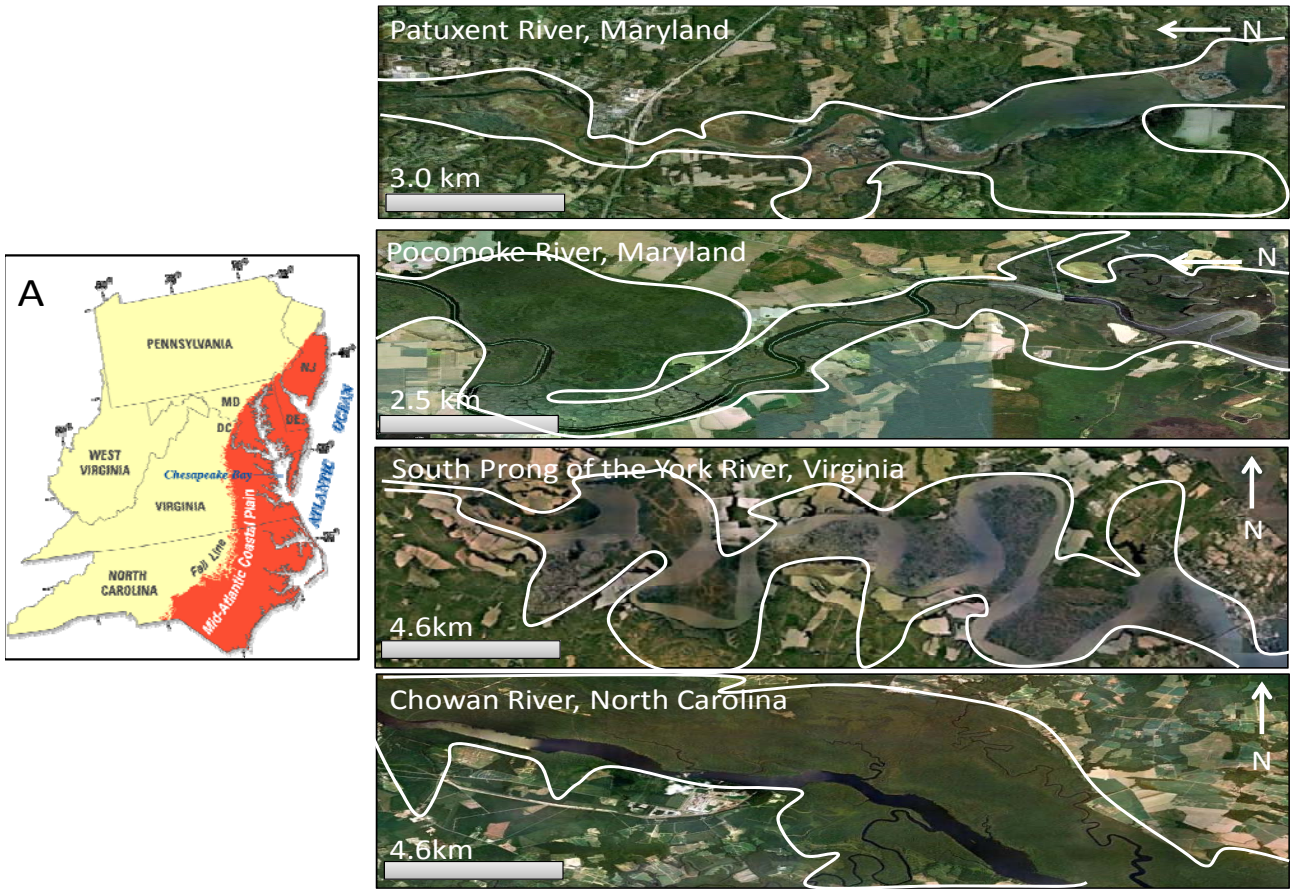

Figure 1.7. Tidal freshwater wetlands are found throughout the Coastal Plain physiographic province. (A) Map highlighting the Coastal Plain physiographic province of the Mid-Atlantic region. The area is typified by low topographic relief, an optimal environment for wetlands. Examples of the extensive wetland ecosystems throughout the Mid-Atlantic Region are outlined in the right panel. Data Source: U.S. Geological Survey.

Chapter 2:

Supply, kinetic, and transport limitations on nitrate retention in a 'biogeochemical hotspot'

2.1 Introduction

Nitrogen (N) loading from terrestrial landscapes is a major contributor to the development of eutrophic and consequently hypoxic and anoxic conditions in coastal waters (e.g. Rabalais et al., 2001; Turner and Rabalais, 2003). Tidal freshwater wetlands (TFW) have been identified as landscape elements that function as sinks for N delivered from terrestrial watershed sources (Simpson et al., 1983). TFW's appear to play important roles in coastal nutrient budgets; they account for a small fraction of the total estuarine area, yet are responsible for significant nutrient removal through denitrification and burial (Boynton et al., 2008). They share major physical and biogeochemical traits with other landscape elements that are important for nitrogen processing, including riparian zones (Naiman and Decamps, 1997; Mayer et al., 2007; Vidon, 2010), and floodplains (Brinson et al., 1984; Mulholland, 1992; Pinay et al., 2000). First, these N retention landscape elements are not sources of N; there is no external anthropogenic application of fertilizers, and there is a low net release from biomass. Second, due to their hydrogeomorphic positions, they receive or intercept water and N from other watershed locations. Third, they have biological and/or biogeochemical characteristics that favor denitrification and/or biological uptake. The N processing functions of these sites has been evaluated in terms of N removal efficiency, e.g. as % of N delivered (e.g. Nichols, 1983; Seitzinger et al., 2006). Therefore, underlying controls on N processing include hydrologic delivery

mechanisms, incoming N loads (N concentration and discharge) to or across the site for processing, and rates of N removal processes (such as denitrification), which may be site-specific and influenced by local chemistry, temperature, and microbial activity (Grimm et al., 2003; McClain et al., 2003).

Evaluation of N removal efficiencies for these sites and prediction of future behavior due to variations in climate, nutrient concentrations, or microbial communities requires a better understanding of the sensitivity of N removal to underlying controlling variables. Hydrologic flow pathways and water volumes, incoming nutrient concentrations, and local biogeochemical controls are the major parameters that could influence the amount and timing of N retention in each of these landscape elements. Although each of the N removal hotspots mentioned above has similarities in underlying controls, they also have significant differences that affect N removal functions. For example, hydrological flow paths and rates are significantly different among these N retention features. Riparian forest buffers intercept groundwater and associated N (primarily as nitrate) from the landscape before it reaches stream channels. Therefore, N removal efficiency depends upon the decrease in N loads (concentration and groundwater flux) in relation to riparian zone N retention processes (Hill, 1995). Floodplains and wetlands also receive groundwater inputs, but water distributed onto floodplains and wetlands directly from stream flow is often the main hydrological pathway that contributes N to these sites, and thus may influence N retention and storage. Due to their position at the downstream end of watersheds, TFWs primarily serve as sinks for N delivered from streamflow and from N delivered from groundwater flow along wetland margins (Bowden, 1987; Simpson

et al., 1983). In each of these landscape settings, N removal can be evaluated by tracking each major hydrologic processes and evaluating removal efficiency as the N removed from water delivered into the wetlands.

Individual types of wetlands, riparian zones, and floodplains that receive N and water from stream flow experience significant variations in the frequency and duration of flooding (Junk et al., 1989; Odum et al., 1995; Poff et al., 1997). Tidal wetlands are flooded daily during portions of the lunar cycle, whereas floodplains are inundated by seasonal high flow stages or as a consequence of individual large storms. Riparian zones can receive varying sources of hydrologic and N inputs; they intercept groundwater flow during from upland sources during some seasons and are inundated or saturated by streamflow sources during other flow stages. Due to these spatial and temporal variations in both hydrology and N content of incoming waters, characterizing the nutrient fluxes and underlying biogeochemical controls on N retention can be difficult (e.g. Grimm et al., 2003; McClain et al., 2003). Previous work in riparian zones has examined nutrient retention by collecting edge runoff (e.g. Daniels and Gilliam, 1996). Although this type of mass balance approach can be useful, hydrologic flowpaths in these systems are often not well constrained, which may inappropriately characterize N loss pathways.

The complexities of both hydrologic fluxes and biogeochemical controls on nitrogen cycling in TFWs are well recognized (e.g. Bowden, 1987; Burgin and Hamilton, 2007). Previous work on controls of nitrogen cycling in TFW has focused on identifying and measuring biogeochemical controls (e.g. denitrification rate) through plot-scale or laboratory experiments (e.g. Jenkins and Kemp, 1984; Caffrey

et al., 1993; Joye and Paerl, 1994). Although these experiments provide information on biogeochemical controls, *in situ* application is difficult because of the spatial variations in nitrogen processing rates and possible variations in the dominant biogeochemical reactions (Cornwell et al., 1999; McClain et al., 2003; Davidson and Seitzinger, 2006). Supply of N-rich water to these sites is often assumed, although the concentrations often reflect *in situ* conditions. Constraints provided by hydrological delivery mechanisms need to be studied in conjunction with measurements of N retention and assessment of other biogeochemical controls. Natural variations due to seasonal temperature changes, seasonal and storm-induced variations in stream flow and associated nitrate inputs from upstream watersheds, and both daily and seasonal variations in tidal stage may limit nitrate retention due to the influence these natural variations exert on nitrogen supply, processing rates (e.g. through temperature controls), and hydrological controls on N delivery into the wetlands. These processes are best studied under field conditions.

In this study, external controls on NR are defined as the independent variables affecting N retention processes that are external to the individual marsh setting. These N retention processes are primarily uptake by aquatic plants and denitrification. Previous work suggests that plant uptake rates are controlled by Michaelis-Menten enzyme kinetics (e.g. Michaelis and Menten, 1913; Claassen and Barber, 1974) and are thus influenced by nitrate concentration, temperature, and the plant species or plant communities that can extract nitrate from the water column for growth (phytoplankton, SAV species like *Hydrilla sp.,* some emergent macrophytes). Denitrification, which is the reduction of nitrate to N_2 or N_2O gas, requires a substrate

to be oxidized, usually labile organic carbon, and low oxygen concentrations. Therefore, the external controls examined in this system included temperature, dissolved oxygen concentrations, and incoming nitrate concentrations. Internal controls on TFW NR result from the interactions among geomorphic, hydrologic, and biological systems *within individual marshes.* Internal controls can be significantly different for each marsh due to effects of marsh size; systematic variations in internal controls may generate scaling relationships for geomorphic, hydrologic, and possibly biological variables.

2.1.1 Research questions

The purpose of this chapter is to report measurements of the amount of N removed from water distributed from watershed sources into the TFWs along the upper Patuxent River Estuary, Maryland; which is one of the major Coastal Plain tributaries to the Chesapeake Bay. The main goals of this study are to evaluate controls on hydrologic fluxes into the TFW ecosystem, measure N loads and retention rates within individual TFW, and to evaluate the effects of temperature and biogeochemical controls on N removal. To constrain the problem, all measurements were conducted during spring (high) tides: The following questions were addressed:

1. For a given tidal cycle, is there ample supply of watershed nitrate (N concentration) for biological processing/nitrate retention to occur at the potential rate? Is there a critical threshold of nitrate concentration for this processing?

2. If there is ample supply of nitrate, is there a temperature effect on the reaction kinetics (biological processing rates)? Is there a critical temperature threshold for this biological processing?
3. Do local geomorphic characteristics of inlet channels affect hydraulic fluxes and thus create transport limitations on biological processing/nitrate retention?

2.2 Methods

2.2.1 Study Site

The TFW ecosystem of the Patuxent River has been previously identified by Boynton et al. (2008); it extends approximately 25 river kilometers along the upper Patuxent River (from 39°0'N 76°41'W to 38°43'N 76°41'W). This ecosystem is composed of hundreds of individual marshes with well-defined tidal creeks and marsh basin areas (Fig. 2.1; Seldomridge and Prestegaard, 2012). Water sources to the marshes in the upper Patuxent River include direct contributions from the Patuxent River, additional inputs from smaller tributaries that contribute directly to the freshwater tidal portion of the river, groundwater flow, and direct precipitation (USGS RIM). Of these water sources, the Patuxent River watershed (2,260 km^2), which is located between Washington, D.C. and Baltimore, Maryland contributes the largest volume. Dominant N inputs include atmospheric sources into the watershed and estuary (Fisher and Oppenheimer, 1991), distributed watershed sources (fertilizers, urban runoff, and septic systems), and point sources (sewage and industrial outflows) (Smullen et al., 1982; Nixon, 1987; Fisher et al., 1988; Boynton

et al., 1995). In 2006 land-uses in the basin include forest (63.5%), agriculture (20.3%), urban-suburban (15.7%), and intertidal wetlands (0.4%; Fisher et al., 2006). Nitrate loads in the river have decreased in the past several decades largely due to reduction in agricultural land uses and in point sources, but are still significantly higher than watersheds without agricultural or urban land uses (Fisher et al., 2006; Hirsch, 2010).

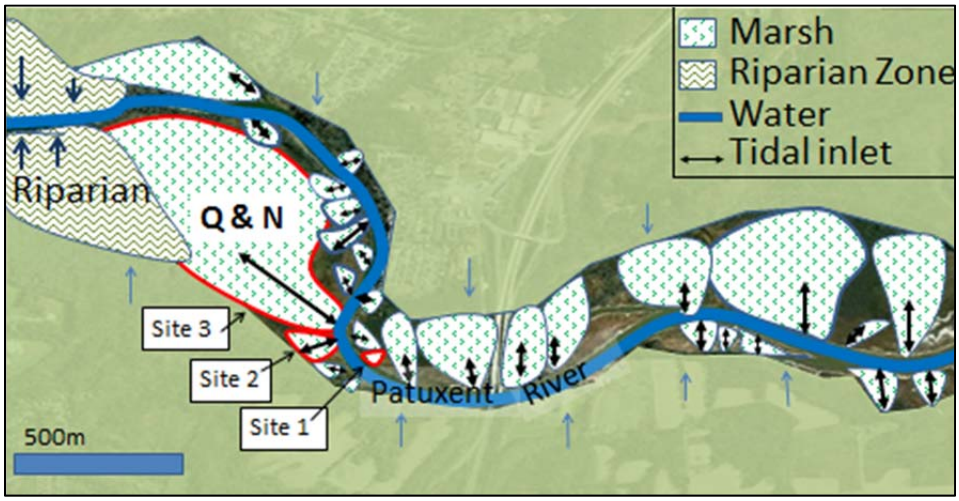

Figure 2.1. Study sites used to evaluate the effects of temperature, biogeochemical, and transport controls on N removal. Sites are located near the head of tide; therefore, they receive large inputs of watershed N. Hundreds of individual marshes line the Patuxent River, and are responsible for a large proportion of nitrate retention. The geometry of the tidal inlet governs the amount of water, sediment, and solute fluxes.

The individual marshes that compose the TFW ecosystem are contained within protected parkland, Patuxent Wetland Park and Jug Bay Wetlands Sanctuary (Fig. 2.1). Plant species that border tidal channels include: *Nuphar advena/leteum, Peltandra virginica, Polygonum sagittatum, Pontederia cordata*, and *Zizania aquatica*. The TFW is composed of hundreds of individual marshes that range in size from 225 to 675,612 m^2 (Seldomridge and Prestegaard, 2012). Each individual tidal freshwater marsh in this ecosystem connects to the tidal Patuxent River through a

well-defined inlet channel. Natural levees border the marsh boundary, which prevents direct overbank flooding from the Patuxent River into the adjacent marsh for most tidal stages. Interior marsh areas are flooded by water that enters through the tidal inlet, and moves up the tidal channel network and floods onto marsh surfaces (Seldomridge, 2009). Fringing tidal wetlands without channel networks also border the Patuxent River, but this is a smaller fraction of the total marsh area and these higher elevation marshes are inundated only during the upper 10% of tidal or flood stages (high tide ± high Patuxent River flow). Therefore, the flux of water, solutes, and particulates into these tidal marshes can be measured at these tidal inlets. In the Upper Patuxent tidal freshwater ecosystem, inlet channels vary in width from 0.2 to 60 m (Seldomridge and Prestegaard, 2012). In this study, three marshes were chosen for study that encompassed the range of tidal marsh and associated inlet sizes. Selected marshes have inlets widths of 7, 11, and 41 m and associated marsh surface areas of 671, 5705, and 536,873 m^2. These three marsh systems were chosen due to the range of marsh sizes that they represent and their proximity to one another, which made it possible to measure more than one marsh site per tidal cycle during field campaigns.

2.2.2 Incoming discharge, nitrate concentrations, and nitrate loads from the Patuxent Watershed

Discharge (daily) and N concentration data (bi-monthly samples) were obtained for the U. S. Geological Survey Patuxent River gauge near Bowie (#01594440) for the period 2008-2011. Discharge data were obtained from the National Water Information System (http://waterdata.usgs.gov/nwis/rt) and nitrogen

data were obtained from the River Input Monitoring Program (http://va.water.usgs.gov/chesbay/RIMP/). Total nitrogen was measured by the USGS on unfiltered samples as total Kjeldahl nitrogen and dissolved nitrate (NO_2+NO_3). In general, organic nitrogen accounted for 40% of the total nitrogen with the highest values in spring and early summer months. Nitrite (NO_2) accounts for a small fraction of the dissolved nitrate; however, incomplete denitrification during wastewater treatment can increase nitrite loads. For the samples measured in 2008, up to 35% of the total [NO_2+NO_3] was in the form of nitrite, but it was not significantly processed by the TFWs (Fig. 2.2); therefore, the sum of nitrate and nitrite is termed 'nitrate' in this paper. The TFWs measured in this study (Fig. 2.1) are located near the head of tide, therefore, these sites receive incoming water and nitrate fluxes directly from the Patuxent River watershed. Nitrate concentrations measured by the USGS on the Patuxent River should be similar in values to field measurements of nitrate concentrations on incoming tides into individual marsh systems.

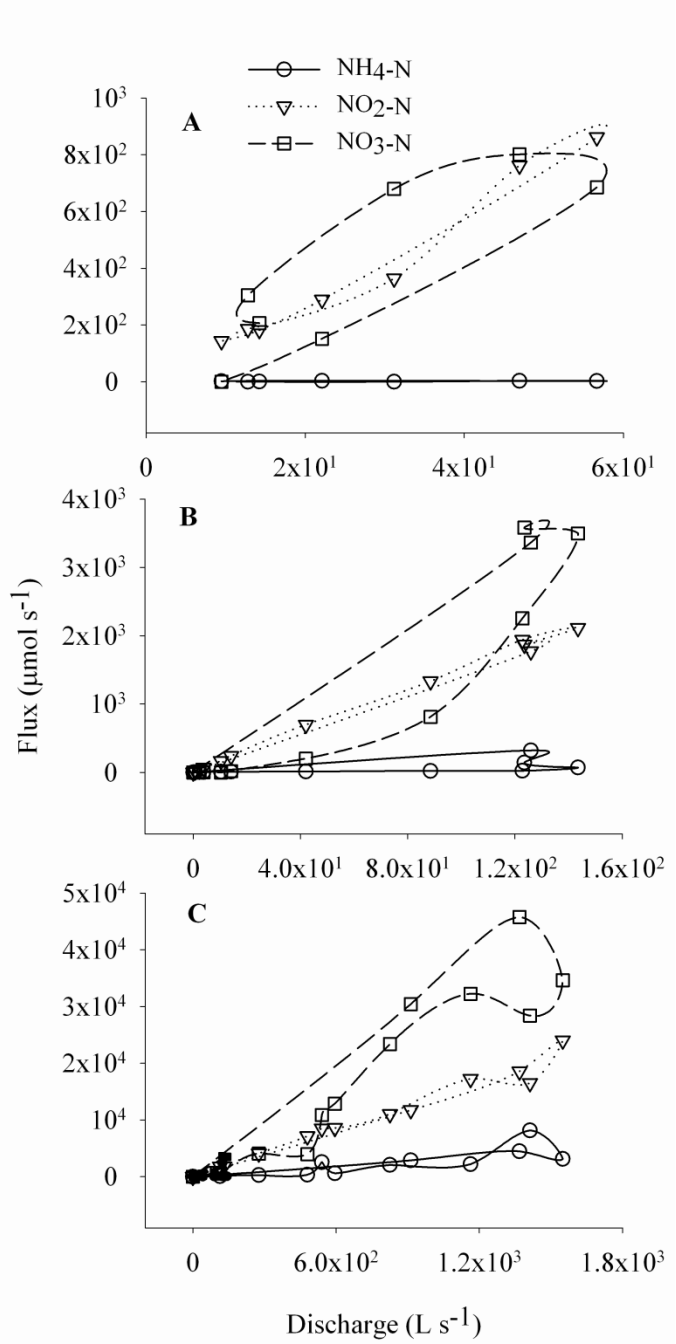

Figure 2.2. Example of water and nitrogen fluxes measured at the tidal inlets for (A) Site 1 on 10/1/2008 (B) Site 2 on 10/1/2008, and (C) Site 3 on 9/20/2008.

2.2.3 Geomorphic and hydraulic measurements

Geomorphic characteristics of inlet width and marsh surface area were measured for marshes in the tidal freshwater ecosystem. Using aerial photos from Google Earth, inlet width measurements were made for every marsh in the TFW ecosystem. Additionally, marsh surface area measurements were made for every marsh using the measuring tools on Maryland Maryland's Environmental Resources and Land Information Network (http://www.mdmerlin.net/). Probability distributions were constructed to determine the size range and frequency of the inlet width and marsh surface areas (Seldomridge and Prestegaard, 2012). These probability distributions guided site selection (described in 2.2.1) for detailed measurements of inlet cross sectional area and maximum depth.

Detailed hydraulic measurements were made at each of the 3 mass balance measurement sites at selected spring tides during the growing season (approximately March through November) for a 3-year period. Tidal stage, maximum velocity, velocity profiles, surface width, and average depth (area/width) were measured systematically between high and low tides for ebbing portions of tidal cycles. These data were used to calculate inlet discharge for each time step. Relationships were constructed between maximum velocity and average velocity (Chen and Chiu, 2002). Tidal stage was used to determine cross sectional area, A_i, for each time step in the tidal cycle. These relationships were used to calculate discharge (area * velocity) for each time step. Discharge (q_i) for each time step is defined as A_iU_i, where U_i is the average velocity. Discharge data were integrated over the tidal cycle to determine total water volume, V. A 5% error in discharge measurement for each time step was

propagated through all discharge calculations; this was determined by considering operator error in cross sectional and velocity measurements (Sauer and Meyer, 1992), and the error introduced by estimating average velocity from maximum velocity (Chen and Chiu, 2002).

2.2.4 Mass balance measurements of nitrate retention in individual marshes

As previously outlined in Seldomridge and Prestegaard (2011; 2012), nitrate retention (NR) was determined from mass balance measurements of water and nitrogen into and out of the tidal wetlands from field measurements conducted in tidal inlets. Water chemistry was sampled at the mouth of the tidal channel in concert with measurements of tidal stage and velocity that were used to calculate discharge. Of the three inorganic nitrogen species (NH_4-N, NO_2-N, and NO_3-N), nitrate was the only form of nitrogen that shows significant variation over the tidal cycle (Fig. 2.2; see also Seldomridge, 2009; Seldomridge and Prestegaard, 2012). Nitrate concentration ([NO_3-N]), is measured for each time step, *Ci*. Nitrogen load (NL) is calculated for each time step (q_iC_i) and summed over the tidal cycle to obtain total nitrogen load for ingoing or outgoing tides:

$$NL = \sum(q_i\, C_i) \tag{2.1}$$

Where NL is nitrogen load, q_i is discharge for each time step (L s^{-1}), C_i is nitrate concentration for each time step (μmol). Nitrate retention was determined by subtracting the outgoing nitrate load from incoming nitrate load:

$$NR = NL_{in} - NL_{out} \quad (2.2)$$

In this study, measured nitrate concentrations were relatively constant on the incoming tide (Seldomridge and Prestegaard, 2012). I made the simplifying assumption that total water volume that moved into the tidal channels was equal to the water volume moving out. Previous measurements indicate that these volumes might differ by 2-10% of the total volume, with higher values on the incoming tides during periods of high evapotranspiration, which can be a significant component in the water balance (Hemond et al, 1984). This assumption will therefore tend to underestimate incoming N load and thus N loss. Examples of the fluxes of N species, and the hysteresis associated with net nitrate retention is shown in figure 2.2. One of the advantages of using mass balance calculations of nitrate retention is that it provides measurements of nitrate retention for individual marshes for a given tidal cycle, time of year, and initial nitrate concentration. No assumption is made of nitrogen retention processes within each individual marsh, although previous work suggests that marsh surfaces are primary sites for nitrate retention (Seldomridge, 2009). Measurements were made during spring (high) tidal stages over the growing season of several years (2008, 2010, and 2011).

2.2.5 *Evaluation of net nitrate retention rates from mass balance measurements*

The mass balance calculations of nitrate retention described above were also used to evaluate net NR rates. This is an apparent denitrification rate, which includes additional processes such as plant uptake and burial. Nitrate retention rates can be calculated from mass balance studies as:

$$NR_{rate} = \frac{NR}{T_{inundation} \times A_m} \quad (2.3)$$

Where NR_{rate} is the retention rate (μmol $m^{-2}h^{-1}$) obtained from mass balance measurements, NR is nitrate retention (moles); $T_{inundation}$ is the inundation time (hours), which is determined from tidal dynamics and elevation of tidal inlets and marsh surfaces, and A_m is the marsh surface area (m^2). In this study, $T_{inundation}$ is estimated from tidal stages measured at tidal inlets and the elevation of marsh surfaces and tidal inlet depths relative to these tidal stages. These mass balance measurements of nitrate retention (primarily uptake and denitrification) were then compared with rates determined from laboratory core incubations and field plot studies (Table 2.1). Mass balance measurements of nitrate retention made during autumn, when plant uptake rates are minimal, were expected to most closely coincide with measured values of denitrification.

Table 2.1. Selected denitrification rates measured during the growing season for various types of freshwater marsh systems (including natural and constructed wetlands) using acetylene inhibition, core incubation, ^{15}N tracer, N_2 flux, and mass balance calculations

Denitrification Rate	**Study**	**Technique**
46 ± 15 to 107 ± 31 μM N m^{-2} h^{-1} April	Created freshwater marsh, Davis Pond, LA (DeLaune et al., 2005)	Acetylene inhibition
Max rate: 450 μM N m^{-2} h^{-1} Sept.	N. Barataria Basin Estuary receiving Davis Pond Diversion, LA (Yu et al., 2006)	^{15}N labeling; N_2:N_20 gas sampling
3.3 to 57.1 μM N m^{-2} h^{-1} March-July	Intertidal freshwater tributary Tomales Bay, CA (Joye and Paerl, 1994)	Acetylene inhibition
28 (fall) to 178 (spring) μM N m^{-2} h^{-1}	TFW, Patuxent River, MD (Merrill and Cornwell, 2000)	Core incubation
≤ 20 to 260 μM N m^{-2} h^{-1} Summer	Freshwater riparian wetlands, NJ/PA (Seitzinger, 1994)	Core incubation
Max rate in spring: 500 μM N m^{-2} h^{-1} Annual average: 110 μM N m^{-2} h^{-1}	Tidal freshwater marsh, Patuxent River, MD (Boynton et al., 2008)	Core incubations
65 to 881 ± 162 μM (NO_2+ NO_3) m^{-2} $tide^{-1}$ July-August	Intertidal freshwater emergent marsh, Upper Cooper River, SC (McKellar et al, 2007)	Tidal mass balance calculation
54 to 278 μM N m^{-2} h^{-1} April and July	Lake Waco Wetland, TX (created) (Scott et al., 2008)	Core incubations and chemical analysis of water column nutrients

2.2.6 Evaluation of nitrate removal efficiency

Nitrate supply or load into each tidal marsh system is a function of nitrate concentration and discharge integrated over the tidal cycle as described in the simple mass balance equations above (Eqs. 2.1 & 2.2). If the incoming nitrate concentration remains nearly constant, then:

$$NL_{in} = aV \tag{2.4}$$

Where *a* is the average incoming nitrate concentration (µmol), and *V* is the total incoming water volume over a tidal cycle (L). At the study sites, incoming nitrate concentration is variable due to seasonal variations, tidal stage, recent storms, point source supply, etc. Incoming nitrate concentration was measured for each of the mass balance field measurements, as well as recorded from the U.S. Geological Survey RIM stations.

To test the dependence of nitrate retention on incoming nitrate supply, I examined the relationship of both nitrate concentration and load to retention. In the Patuxent River TFWs, incoming nitrate concentration, *a*, remains nearly constant; therefore, with both *a* and *c* known, *b* can also be calculated as follows:

$$NR = aV_{in} - bV_{out} = cV \tag{2.5}$$

Where V_{in} is the incoming water volume (L), V_{out} is the outgoing water volume (L), and *b* is the integrated average nitrate concentration (µmol) on the outgoing tide. This equation is simplified when $V_{in} = V_{out}$, which is the case for tides with minimal water storage and minimal evapotranspirative losses within the marsh. Previous

research in the freshwater tidal marshes of the Patuxent River suggests that NR calculated from mass balance measurements has a linear relationship to tidal water volume:

$$NR = cV \tag{2.6}$$

Where *NR* is nitrate retention in moles, *c* is the integrated average nitrate concentration (mole L^{-1}) of the retained nitrate, and *V* is tidal water volume (L) (Seldomridge and Prestegaard, 2011; Seldomridge and Prestegaard, 2012). NR and V are calculated from mass balance considerations; therefore, the equation can be solved for *c*, which can be thought of as an integrated average nitrate concentration of the retained nitrate (moles L^{-1}).

2.2.7 Evaluation of temperature and biogeochemical controls on nitrate retention rates

If NR in TFW is controlled primarily by reaction kinetics (of both denitrification and uptake), then NR_{rate} should respond to variables that affect the rates of these biogeochemical processes. These include temperature, pH, dissolved oxygen, and/or availability of organic carbon (Patrick and Reddy, 1976; Maag, 1997; Cornwell et al., 1999). If a simplifying assumption is made that organic carbon is not limiting in this system (organic matter values have been reported as high as 70% by weight in TFW; e.g. W. Odum, 1988; Seitzinger, 1994; Neubauer, 2008; Prestegaard *unpubl*), then temperature and perhaps dissolved oxygen are the master variables that affect reaction rates. Temperature, pH, and dissolved oxygen are continuously measured on the Patuxent River Estuary by the Maryland Department of Natural

Resources Eyes on the Bay continuous monitoring program (www.eyesonthebay.net). Data are recorded at 15 minute intervals using YSI 6600 data loggers. The measurement site within the TFW portion of the estuary, and is approximately 3.25 km downstream from the study sites. Reported data are peak values recorded during the corresponding mass balance measurements.

The temperature dependence of reaction rates can be evaluated with the Arrhenius equation, which describes the relationship of the rate constant, *k,* of a chemical reaction to temperature *T* (in Kelvins) and the activation energy, $E_{a:}$

$$k = Ae^{-Ea/RT} \tag{2.7}$$

where *A* is a coefficient (the pre-factor) and *R* is the universal gas constant (8.314 x 10^{-3} kJ $mol^{-1}K^{-1}$). This equation was used to solve for *A* under a range of documented field conditions.

2.3 Results

2.3.1 Patuxent River discharge and nitrogen concentration data

Nitrate loads to the TFW study sites, located near the head of tides in the upper Patuxent River Estuary, are contributed by the flux of nitrogen ($Q \times [NO_3 - N]$) from the Patuxent River Watershed (Fig. 2.3D). Annual variations in average daily discharge for 2008 and 2010 are shown in figure 2.3C. Stream baseflow discharge is highest during the winter and early spring months when evapotranspiration is at a minimum; baseflow drops significantly during the growing season (April through September). Peak discharges are associated with storm events,

the most significant of which were associated with tropical storms and hurricanes. Annual maximum daily discharge values were 168 m^3s^{-1} in 2008, 145 m^3s^{-1} in 2010, and 354 m^3s^{-1} in 2011 (elevated by precipitation associated with Hurricane Irene).

Nitrate concentrations in the period 2008 - 2010 were seasonally variable, with higher concentrations associated with late winter-early spring baseflow. In recent years, concentrations and loads have decreased in the Patuxent River (Fisher et al., 2006; Hirsch et al., 2010; USGS RIM). Nitrate concentrations ranged from 18.2 to 106 μmol in 2008, and 30.5 to 135.5 μmol in 2010 (Fig. 2.3D). Only partial data are available at this time for 2011. Nitrate is the dominant form of the total nitrogen in the USGS measurements, but the nitrate proportion of total N concentration is seasonally variable. Nitrate proportions and concentrations are highest in winter-spring months, and drop during summer months as organic nitrogen becomes a larger proportion of the total. The low concentrations of ammonium (NH_4^+) measured in incoming tidal waters suggests that 20 to 40% of nitrate is supplied as organic N in summer months.

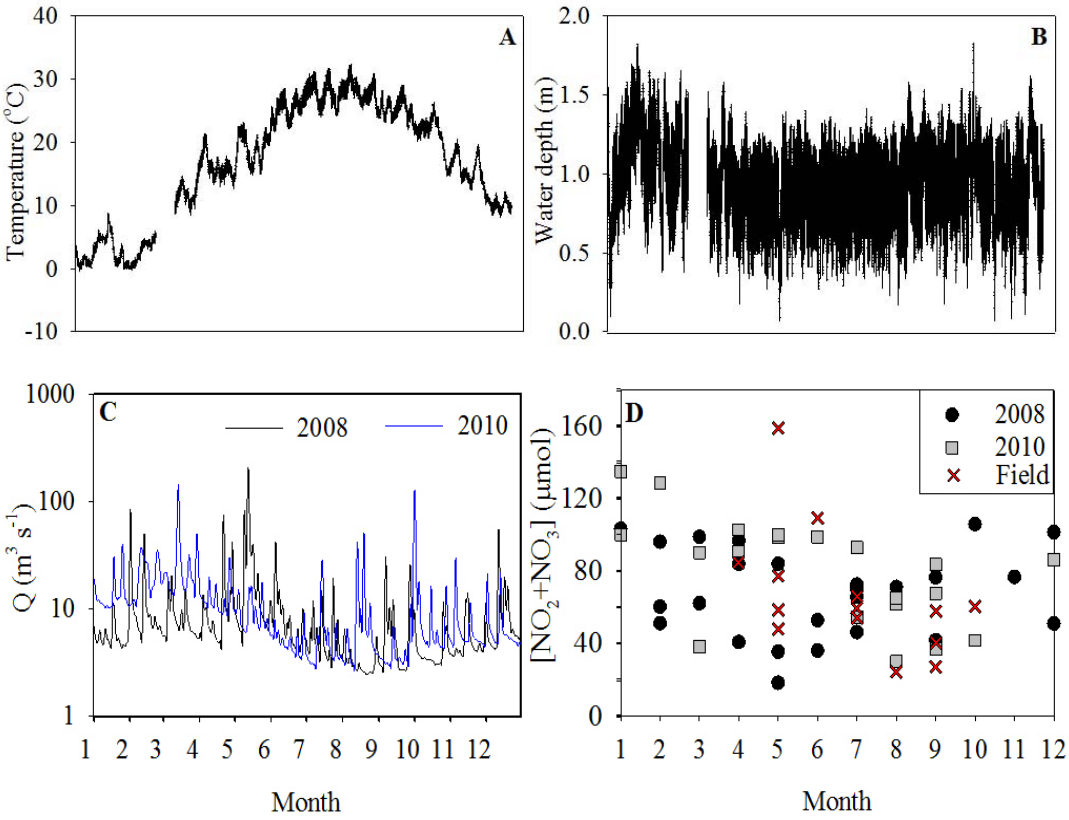

Figure 2.3. Example of seasonal variations in the Upper Patuxent River in (A) temperature in 2010, (B) tidal stage in 2010, (C) stream flow contributions, and (D) nitrate concentrations from upstream and field measurements (marked X). Sampling campaigns for nitrate retention were conducted between March and October; however, annual data allow for estimates of retention during other times of year. Data sources: temperature and water depth from Eyes on the Bay Jug Bay permanent monitoring station (A and B); discharge from U.S. Geological Survey Station 01594440, Patuxent River near Bowie, MD (C); 2008 and 2010 nitrate concentrations from Chesapeake Bay River Input Monitoring Program Patuxent River station (D).

2.3.2 Mass balance nitrate retention data

Nitrate retention values range with marsh size from less than 1 mole NO_3-N at the smallest site to 2,660 ± 212 moles NO_3-N at the largest site (Table 2.2). These retention values were normalized by total water volume and by marsh surface area. Marsh inundation time was also used to calculate NR_{rate}. At Site 1, NR per volume values ranged from 0.6 ± 0.03 to 8.1 ± 0.4 μmol L^{-1}, Site 2 ranged from 7.1 ± 0.3 to 22.2 ± 1.0 μmol L^{-1}, and Site 3 ranged from 8.8 ± 0.42 to 33.8 ± 1.6 μmol L^{-1}. At Site 1 NR_{rate} ranged from 28 ± 0.7 to 1272 ± 69 μmol m^{-2} hr^{-1}, Site 2 ranged from 280 ± 15.3 to 822 ± 22.4 μmol m^{-2} hr^{-1}, and Site 3 ranged from 25 ± 9.3 to 681 ± 29.4μmol m^{-2} hr^{-1}. These NR_{rate} values were generally higher than laboratory derived values of denitrification (Table 2.1) and they likely incorporate nitrate uptake and burial. Error was calculated for each parameter by propagating error in discharge, geomorphic, and analytical measurements.

Table 2.2. Field data (including tidal water volume flux, nitrate load into the channel, total NR, and cumulative nitrate retention per total water volume flux) for Sites 1-3, 2008-2011

Site 1					
Sampling Date	**Water Volume (m^3)**	**NL_{in}**	**Total NR (moles)**	**NR/V (µmol L^{-1})**	**NR_{rate} (µmol m^{-2} hr^{-1})**
9/20/2008	339.6 ±17	8.1 ± 0.4	2.7 ± 0.34	8.1 ± 0.4	743 ± 40
5/20/2011	576.2 ± 28.8	27.4 ± 1.4	4.7 ± 0.004	8.1 ± 0.4	1272 ± 69
7/18/2011[1]	8.2 ± 0.41	0.4 ± 0.02	0.05 ± 0.03	0.6 ± 0.3	28 ± 0.7
9/14/2011	235.1 ± 11.8	9.4 ± 0.5	1.1 ± 0.05	4.7 ± 0.2	298 ± 16.2
Site 2					
10/1/2008	1219.2 ± 61	32.4 ± 1.6	10.6 ± 0.3	8.7 ± 0.4	381 ± 20.7
5/20/2011	1459.5 ± 73	84.6 ± 4.2	16.0 ± 7	11.0 ± 0.5	574 ± 31.2
7/18/2011	517.6 ± 25.9	30.4 ± 1.5	11.5 ± 2.7	22.2 ± 1.0	822 ± 22.4
9/14/2011	1099.5 ± 54.9	44.3 ± 2.2	7.8 ± 5	7.1 ± 0.3	280 ± 15.3
Site 3					
10/1/2008	16294.6 ± 814.7	544.3 ± 27.2	144.2 ± 6	8.8 ± 0.4	110 ± 22.9
4/3/2010	65708.1 ± 3285.4	5531.9 ± 276.6	1556.2 ± 269.2	23.7 ± 1.1	374 ± 17.6
5/2/2010	78744.3 ± 3937.2	12477.0 ± 623.8	2659.6 ± 212	33.8 ± 1.6	661 ± 38
6/3/2010	72,291.2 ± 3614.6	7846.1 ± 392.3	749.0 ± 12	10.4 ± 0.5	186 ± 2.7
9/24/2010	38673.2 ± 1933.7	2318.7 ± 115.9	464.6 ± 29.4	12.0 ± 0.6	115 ± 2.5
5/21/2011	84168.0 ± 4208.4	6461.6 ± 323.1	1552.4 ± 77.6	18.4 ± 0.9	413 ± 17.5
7/17/2011	86486.9 ± 4324.3	5656.2 ± 282.8	2193.6 ± 79.1	25.4 ± 1.2	681 ± 29.4
9/16/2011	4630.3 ± 321.5	265.1 ± 13.5	92.9 ± 4.6	20.1 ± 0.9	25 ± 9.3

[1] High emergent macrophyte growth prevented direct access to channel mouth on 7/18/2011; therefore, discharge and NR values are underestimated.

2.3.3 Nitrate removal efficiency

To evaluate nitrate removal efficiency, nitrate removal must be evaluated in the context of nitrate load, which is affected by both nitrate concentration and discharge. An evaluation of the relationship between initial $[NO_3\text{-}N]_{in}$ and NR (Fig. 2.4A) suggests significant scatter between the magnitude of incoming nitrate concentrations and NR:

$$NR = 3.9[NO_3 - N]_{in}^{4.1} \qquad (n=16, R^2=0.39, p<0.01) \qquad (2.8)$$

The general pattern illustrates an increase in NR with nitrate concentration, but with little variation when concentrations exceed 70 μmol (Fig. 2.4A). This suggests that nitrate retention is not limited by incoming nitrate concentrations for some of these concentrations.

Comparing the integrated average incoming and outgoing nitrate loads suggests that 22% of the nitrate is retained in each marsh during one tidal cycle (Fig. 2.4B):

$$NR = 0.22NL_{in} \qquad (n=16, R^2=0.83, p<0.01) \qquad (2.9)$$

One data point does not follow this trend. Although it appears to indicate conditions when nitrate retention was supply-limited, further examination suggests that the low nitrate retention is an artifact of a low tidal stage. If this outlier is removed, the trend remains the same, but the correlation improves to 0.93.

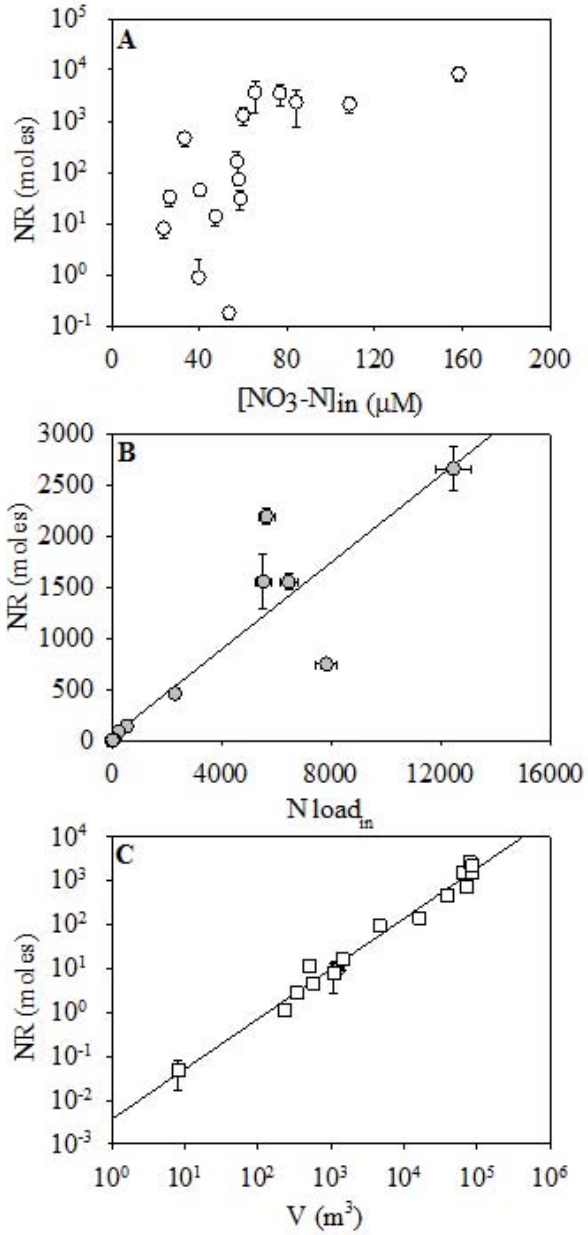

Figure 2.4. (A) A comparison of incoming [NO_3-N] and NR suggest there is no correlation between the magnitude of incoming nitrate concentrations and NR ($NR=3.9\ [NO_3\text{-}N]_{in}^{4.1}$, n=16, $R^2=0.39$, $p<0.01$). (B) A comparison of nitrate loading suggests ample nitrate supply ($NR=0.22NL_{in}$, n=16, $R^2=0.83$, $p<0.01$) and highlights the importance of discharge as a control of NR. (C) There is a strong correlation between hydrologic flux and nitrate retention ($NR=0.0045NR^{1.1}$, n=16 $R^2=0.98$, $p<0.01$). Data points without error bars have error values less than size of symbol.

2.3.4 Hydrologic flux and nitrate retention

A strong correlation exists between tidal volume during a tidal cycle and NR regardless of season (Fig. 2.4C):

$$NR = 0.0045V^{1.1} \qquad (n = 16, R^2 = 0.98, p<0.01) \qquad (2.10)$$

This trend is also evident when NR data are normalized by volume, and produce a narrow range of values (Section 2.3.3; Table 2.2). When nitrate retention is expressed as an integrated average concentration (*c*) per total volume (Eq. 2.5), this value decreases throughout the growing season (Fig. 2.5A). The lowest value reported from Site 1 in July is artificially low from dense emergent macrophyte growth in the channel; accessibility to the channel mouth was greatly reduced during this time.

The apparent nitrate retention rates calculated from the mass balance experiments are shown in figure 2.5B. These apparent rates are significantly to slightly higher than denitrification rates reported in the literature (Table 2.2). There is no strong correlation between NR_{rate} and marsh size. In particular, smaller marshes (Sites 2 and 3) with potentially higher surface area to volume ratios do not have higher nitrate retention rates. Rates are highest in May through July, which corresponds with the highest water temperatures, the macrophyte growing season, and likely the highest rates of plant uptake (Fig. 2.3A & C).

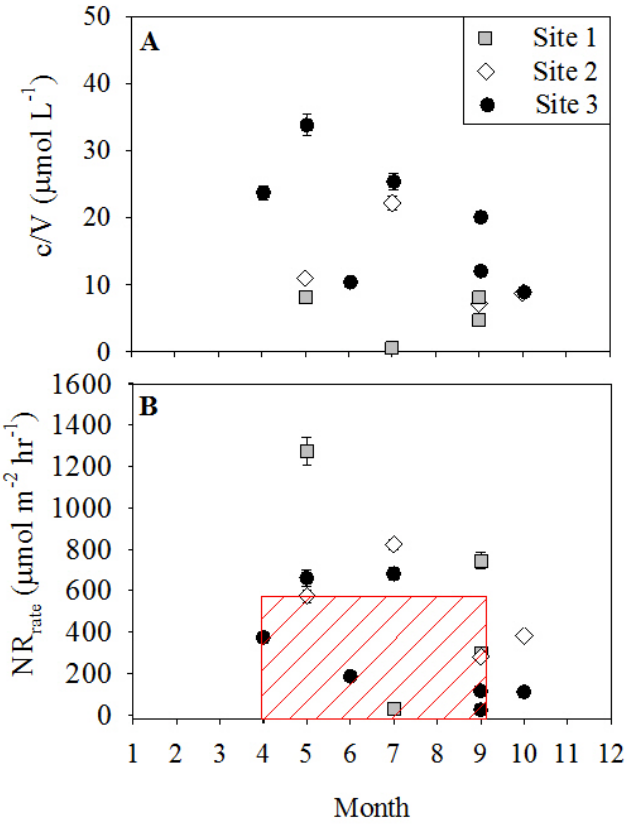

Figure 2.5. (A) Seasonal variations in nitrate retention (c values were calculated from Eq. 5) and expressed as a ratio to total tidal water volume. Values of c/V are high in spring and decrease over the growing season. (B) Nitrate retention rates calculated from field mass balance data also show declines over the growing season. Inset box shows the range of experimental data from table 1. The high apparent rates during the summer months are likely uptake by plants and/or growth of algal mats. Temperature might limit these values during the winter months (November through March), and transport during the peak summer months. Where error bars are not shown, data point size encompasses error.

2.3.5 Temperature, D.O., and pH controls on nitrate retention rates

Temperature, dissolved oxygen, and pH data that were recorded during sampling campaigns were examined as controls on NR_{rate} during mass balance measurements conducted during the growing season (Fig. 2.6). There is significant scatter (p-values were much greater than 0.05) between NR_{rate} and the three biochemical variables examined (temperature, DO, and pH). None of the variables demonstrated a correlation with NR or NR_{rate}. This suggests that, for the range of temperatures measured during the growing season (11.3℃ on 1 April 2010 to 32.4℃ on 25 July 2010), there is little influence of these parameters on apparent NR_{rate}.

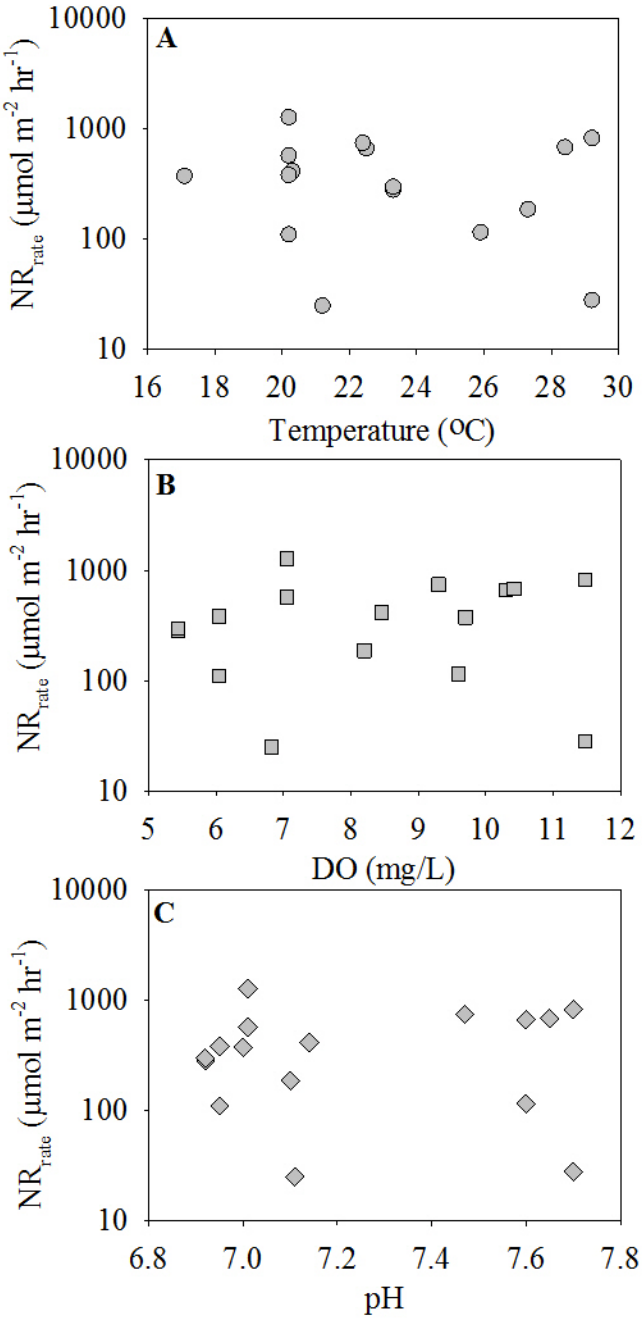

Figure 2.6. Relationship between water quality data (Eyes on the Bay, www.eyesonthebay.net), and NR_{rate} (Eq. 3): (A) temperature, (B) dissolved oxygen, and (C) pH for the Patuxent River for 2008-2011 sampling campaigns. Reported water quality data are maximum values measured during the corresponding mass balance measurements. Size of symbol encompasses error values; p-values are approximately >0.95 and therefore correlations are not statistically significant.

Temperature is an established control on reaction kinetics. Therefore, water temperatures from the field site were used to evaluate the Arrhenius equation. Field water temperatures ranged from 273.15 K (0 °C) in winter to 303.15 K (30 °C) in summer (Fig. 2.3A; Eyes on the Bay, 2010). A review of the literature provided a range of E_a values; Maag (1997) reported 49 to 89 kJ mol^{-1} (for temperatures from 5 to 15 °C), Holtan-Hartwig et al. (2002) reported from 28 to 76 kJ mol^{-1} (for 5 to 20 °C); all other studies examined fell within this range (Abdalla, 2009; Sheibley et al., 2003). Thus, for these calculations, an average E_a value of 47 kJ mol^{-1} was used. These values were used to evaluate *A* in the Arrhenius equation, which indicated the greatest sensitivity to temperature for values less than 10 °C (Fig. 2.7). Temperatures above 10 °C displayed a linear trend with a low slope (from -0.0037 to -0.0088, R^2=0.96). This analysis suggests that nitrate retention rates should fall considerably with temperatures less than 5-10 °C (Stanford et al., 1975).

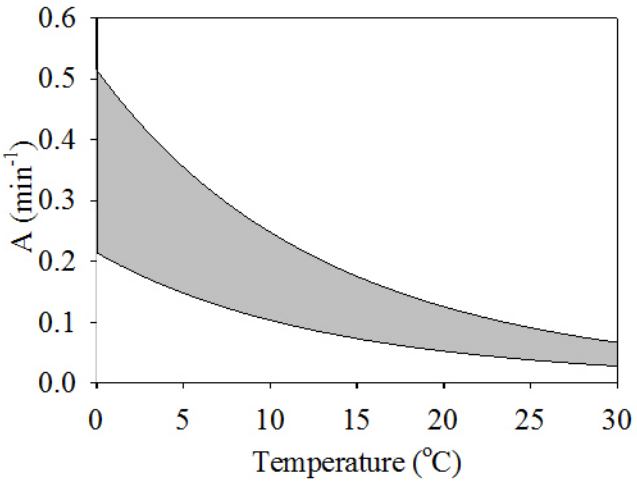

Figure 2.7. Range values for *A* in Arrhenius calculations using an average E_a of 47 kJ mol^{-1}, corresponding *k* values, and a range of recorded field water temperatures (0 to 30°C). The coefficient increases the most from 0 to 10°C; however, once above 10°C the change in values of *A* is fairly consistant. This suggests the kinetics are not a pronounced limitation during the growing season when temperatures are > 10°C.

2.4 Discussion

2.4.1 Supply limitations on nitrate retention

There are two aspects to nitrate supply that might affect the amount of nitrate retention. Nitrate delivered to sites where transformation can take place in TFWs is controlled by the nitrate concentration, discharge, and thus N load of the incoming tidal waters. At N processing sites within the marsh, local supply of nitrate may be controlled by the diffusion of water column nitrate into the sediments (Phillips et al., 1968; Patrick and Reddy, 1976), nitrification of ammonium, or advection of nitrate from groundwater (Seitzinger et al., 2006). Although local site supply may be limited by diffusion; delivery of nitrate-rich water to the site is controlled by channel inlet, channel network, and tidal marsh surface hydraulics. Furthermore, in TFW ecosystems, nitrification and denitrification are often coupled (Jenkins and Kemp, 1984; Christensen et al., 1987); therefore, nitrate supply could be limited through the nitrification of NH_4-N during times of low redox potential. Although this is possible, the continuously shifting tidal conditions minimize this microscale effect. Alternatively, groundwater NR maybe important, but this is limited by near-channel groundwater flux rates (Cooper, 1990; Hedin et al., 1998; Phemister, 2006), which are small compared with tidal flux rates.

Incoming nitrate concentration from tidal sources has a direct control on NR only if concentrations fall below a threshold level (Dodds et al., 2002). Under nitrate-limiting conditions, NR should increase proportionally as [NO_3-N] increases. In this study, there was a weak correlation (Fig. 2.4A, R^2=0.39) between nitrate

concentration and N retention. Field measurements indicated that outgoing water column nitrate concentrations were consistently above zero (Fig. 2.4C). Comparison with previous research (e.g. Seitzinger 1988; Seitzinger, 1994) suggests that these measured values of nitrate concentration are higher than required to provide nitrate for microbial processing. The shape of the concentration versus NR function strongly suggests higher concentrations do not increase NR as observed by the almost constant values of NR for the highest concentrations, which suggests the system may have reached a threshold for nitrate saturation (Ågren and Bosatta, 1988; Aber et al., 1989; Aber et al., 1998). Thus, the measured values of nitrate concentrations appear to be above a minimum threshold for processing.

The mass balance measurements were made at study sites located near the head of tides; therefore, these sites receive incoming N concentrations that should be similar to those measured on the Patuxent River by the USGS. The monthly range of nitrate concentrations measured in this study is comparable to those reported from the USGS upstream Bowie site (Fig. 2.3D). If tidal processing removes nitrate within the freshwater tidal portion of the estuary or significantly dilutes it, then nitrate concentration may be a limiting factor for freshwater tidal wetlands within other parts of this ecosystem.

2.4.2 Nitrate removal efficiency

Previous studies of nitrate removal efficiency values have focused on riparian zones through two methods: (1) measuring nitrate loss in groundwater from upgradient to the stream edge of the buffer (e.g. Jordan et al., 1993; Correll et al.,

1997; Snyder et al., 1998; Martin et al., 1999), or (2) measuring the travel distance across riparian zones required for nitrate depletion (e.g. Lowrance, 1998; Wigington et al., 2003). Although these types of studies can provide estimates of nitrate removal efficiency, they are poor at providing estimates of water and nitrate fluxes from the system (Vidon and Dosskey, 2008). In this study, I examined both water and nitrate fluxes to estimate removal efficiencies, which provided well constrained removal efficiency estimates for one tidal cycle. Total removal efficiency for the TFW ecosystem also requires evaluation of total travel times.

Mass balance studies indicate that about 22% of the incoming NO_3-N from upstream sources was retained in each TFW during one tidal cycle (Eqs. 2.8 & 2.9; Fig 2.4B). Previous studies in constructed wetland ponds have reported maximum values as high as 90% as nitrate-rich waters slowly traverse these wetlands (Cooper, 1990; Busnardo et al., 2003). The reasons for this difference in removal efficiencies may be due to the short residence time of water in the marshes and the relatively low proportion of water flooded onto marsh surfaces versus being retained within channels. In the previous studies, high removal rates were attained by creating an optimal environment with a thin film of water for an extended period (high surface area to volume ratio and extended inundation period).

Evaluation of total nitrate retention in the TFW ecosystem requires an understanding of the tidal hydrodynamics and the number of tidal marshes traversed by each parcel of water throughout the extent of the ecosystem. The fluctuating hydrodynamics add complexity to the ecosystem, and may lower the efficiency of removal (Ingersoll and Baker, 1998). In the Patuxent TFW, the same parcel of water

is involved in several tidal cycles (some at night and some during the day) before it exits the freshwater tidal ecosystem. Therefore, further examination of retention times is necessary. It is likely that semi-diurnal spring tidal cycles may double removal efficiencies, and this will be investigated in future studies.

The nitrate retention rates obtained for early fall (when plant uptake rates were minimal) were compared with laboratory and plot studies of denitrification (Fig. 2.5). These data provided apparent denitrification rates that were similar to or higher than those reported from other studies, including laboratory studies of denitrification using wetland sediment. This suggests that wetland sediments are processing N at capacity, but that delivery of N to these sediments is limited by hydrological fluxes.

2.4.3 Temperature limitations on nitrate retention

Based on the data presented in figure 2.4, kinetic controls can be evaluated by making a simplifying assumption that sufficient nitrate is available at the processing sites. Temperature is an established control on kinetics; however, the importance of temperature as an *in situ* control is difficult to discern due to variable conditions. Laboratory experiments have detailed enzyme kinetics of individual loss pathways, such as denitrification (e.g. Betlach and Tiedje, 1981; etc.); however, once extrinsic effects on denitrification (such as diversity of microbial community, quantity and quality of organic matter, diffusion rates, etc.) are considered, the basic dynamics are often masked (Seitzinger, 1988). Moreover, laboratory experiments utilize a wide range of temperatures to determine enzyme kinetics. These temperatures may not be

possible in natural systems; and a very narrow range of temperatures are reported for the Patuxent system during the growing season (Fig. 2.3A).

Application of the Arrhenius equation (Eq. 2.7) to field temperatures suggests that the rate of reaction (as demonstrated by the change in *A*) is almost unchanged once temperatures rise above 10°C (Fig. 2.7). This suggests the Patuxent TFW ecosystem exhibits a threshold behavior; once the system warms above 10°C, NR retention occurs at an optimum rate. Microbial activity is at a minimum when temperatures drop near 0°C. In the Patuxent TFW, microbial activity processes N at this optimal rate for approximately 7 months of the year; however, these high rates of processing also correspond with the lowest levels of discharge (Fig. 2.3C). During the late fall and winter months when the system receives the highest levels of streamflow, the N processing is likely at a seasonal minimum. This suggests that the elevated N loading that typically occurs between November and April are likely not processed effectively by the TFW. Therefore, temperature is a major control on nitrate retention in this system.

Field data supported this notion; seasonal apparent NR_{rate} (Table 2.2) were comparable or higher than potential denitrification rates from the literature (Table 2.1). The elevated rates are primarily in the spring, which suggest that additional loss processes (uptake by plants, etc.) other than denitrification are important. Thus, kinetic controls primarily define the difference between the dormant and growing season N processing, which is significant.

2.4.4 Hydrologic flux limitations on nitrate retention

The comparison of nitrate concentrations, loads, and retention demonstrates the importance of hydrologic flux on NR (Figs. 2.4 & 2.5). Nitrate retention appears to be limited by the amount and velocity of water entering into the marsh tidal channel network. During the supply limitation analysis (Fig. 2.4), correlations between supply and retention greatly improved once discharge was considered in the calculations. This effect has also been documented when nitrate retention was compared among various ecosystems (wetlands, rivers, and lakes); all of which indicated different values of nitrate retention until the effects of discharge were also included (Saunders and Kalff, 2001). In addition, cumulative values of NR per volume remain relatively constant regardless of season or channel/marsh size (Table 2.2; Seldomridge and Prestegaard, 2011). This is likely a result of geomorphic controls on hydrologic flux (Seldomridge, 2009). The smallest channels have steep bed elevations, which cause shorter inundation times, and proportionally less volume; therefore, during spring tides all sites have similar NR per volume.

Marsh surfaces with similar denitrification potential can be limited by local water fluxes (Cooper and Cooke, 1984; Hill, 1988; Seitzinger et al., 2002). The complex organization of tidal channel networks and adjacent marsh provides a series of sites for nitrate processing during the tidal cycle; however, marsh areas with similar elevations can experience non-synchronous behavior due long channel travel times (e.g. Wollheim et al., 2006) from increased emergent macrophyte flow resistance. Marshes with similar elevations experience different inundation times due to their distance from the main estuary. Future work is therefore necessary to refine

TFW hydraulics, since the variables are difficult to predict (e.g. Temmerman et al., 2005).

2.4.5 Synthesis of seasonal controls on nitrate retention

In this study, N concentration, temperature, and hydrologic transport all appear to affect nitrate retention; however, each operates under conditions that vary with season. In general, nutrient concentrations in the Chesapeake Bay waters are declining due to strict legislation and associated management efforts aimed at improving water quality (e.g. Fisher et al., 2006; Hirsch et al., 2010). This drop in nitrate is essential for improving the health of the Bay, but in the future, nitrate concentrations may limit NR per tidal cycle in these marshes.

This study focused on the growing season (approximately April through late September), but as evident in the annual data, a range of conditions are experienced in the tidal Patuxent. In the summer, transport limitations (tidal + flood stage) are maximized because stream baseflow is low and macrophyte flow resistance is high. Although summer storms might enhance NR, nitrate concentrations may be limiting during some of these conditions. High tidal stages are most frequent in the late winter and early spring, when temperatures are lowest. Thus temperature controls become important during these time periods when N loads have historically been high (Hirsch et al., 2010). In addition, the relative importance of temperature and hydrological controls may be altered by climate changes. For example, in 2012, water temperatures did not drop below freezing during the winter months (Eyes on the Bay). Continued warming may extend the conditions during which denitrification may be active.

Although this is could be a positive trend, increased denitrification could also lead to greater marsh decomposition (Turner et al., 2009).

2.5 Conclusion

The evidence in this study suggests that N supply, N reaction rates, and transport all affect N processing. During the growing season, when these field studies (and most other field studies) were conducted, hydrological transport, which is limited by tidal stage and the geomorphic configuration of inlet channels, provided significant limitations to N processing in the TFW Patuxent ecosystem. The reported relationships are only valid for similar spring (high) tidal stages during the growing season. This is the time period typically associated with baseflow (low) incoming stream discharge values from the Patuxent River watershed. Future work is therefore necessary to examine the relationships between hydrologic flux and nitrate retention outside of the optimal temperature window. Furthermore, these relationships must continue to be examined because they are likely to shift due to climate changes that may lengthen the growing season.

Chapter 3:

Use of geomorphic, hydrologic, and nitrogen mass balance data to model ecosystem nitrate retention in tidal freshwater wetlands

3.1 Introduction

Ecosystem functions, such as nitrate retention, are difficult to predict for entire ecosystems due to the complex interactions of linked biogeochemical and physical controls on ecosystem processes (Boyer et al., 2006; Seitzinger et al., 2006). The tidal freshwater wetland ecosystem, which is located at the interface between terrestrial and aquatic ecosystems, has been identified as an important site for nitrate retention (Simpson et al., 1983; Bowden et al., 1986; 1987). Evaluation of ecosystem nitrate retention and its distribution within this ecosystem is required to develop controls on eutrophication in coastal zones (Boyer et al., 2006; Howarth and Marino, 2006; Seitzinger et al., 2006).

Tidal freshwater wetlands (TFWs) often contain self-formed channel networks that govern water and solute fluxes into these systems (Myrick and Leopold, 1963; Rinaldo et al., 2004). Tidal channel networks are similar to fluvial networks; geomorphic relationships among stream order, length, basin area, and inlet width have been defined for both fluvial (Horton, 1945; Strahler, 1952; Shreve, 1967) and tidal channel networks (Fagherazzi et al., 1999; Rinaldo et al., 1999a; Marani et al., 2003). Geomorphic scaling parameters have been used to evaluate nitrogen (N) loads and processing in both terrestrial watersheds and tidal systems (e.g., Sferratore et al.,

2005; Seitzinger et al., 2002). Previous research on N retention in TFW has identified marsh surfaces and near-surface environments as important sites for N processing (Bowden et al., 1986, 1987; Boynton et al., 2008). Normalized kinetic rate constants (kg N/year) obtained from laboratory or field plot studies (e.g., Jenkins and Kemp, 1984; Caffrey et al., 1993; Joye and Paerl, 1994) have been used along with marsh surface area measurements and inundation times to upscale nitrogen retention for entire ecosystems (Boynton et al., 2008). Scaling nitrate retention to marsh surface area requires the following assumptions: marsh surface and near surface substrates are the dominant sites for nitrate retention; N processing rates are spatially homogeneous within marshes; and there is synchronous flooding of marsh surfaces of equal elevation. Several studies suggest that near-surface marsh sediments are relatively homogeneous with little spatial variation in hydraulic properties (Harvey et al., 1987; Phemister, 2006) and nitrogen processing rates measured on marsh cores do not show systematic spatial variability (Cornwell et al., 1999; Merrill and Cornwell, 2000). Marsh-scale field studies of nitrate retention, however, indicate that in situ controls including inundation times may be complex and may involve parameters in addition to marsh surface area (e.g., Cornwell et al., 1999). Previous work on the Patuxent TFW ecosystem suggests that nitrate retention may be closely related to hydrologic flux in this system (Seldomridge and Prestegaard, 2011).

3.1.1 Research questions

The purpose of this study is to evaluate geomorphic scaling parameters and to estimate total nitrate retention in TFW ecosystems. I obtained N retention data from field measurements of water fluxes and N species mass balance in marshes of varying

sizes. These data were combined with geomorphic data for all marshes in the ecosystem to develop 3 equations (one for each geomorphic scaling parameter) to predict nitrate retention. Criteria used to evaluate geomorphic scaling parameters for nitrate retention are: a) accuracy of measurement of each geomorphic feature, b) relationship between each geomorphic parameter and hydrologic flux, and c) the ability to adjust the geomorphic parameters to varying tidal stages and hydrologic fluxes. The following questions were addressed:

1. What are the spatial distributions of geomorphic characteristics (marsh area, channel length, and inlet channel width) in the freshwater tidal wetlands?
2. Can all geomorphic characteristics be measured to the same high degree of accuracy?
3. Do relationships exist between the geomorphic characteristics and hydrologic flux?
4. If relationships exist, can they be adjusted to varying tidal stages and hydrologic flux conditions?

3.2 Methods

3.2.1 Study regions and approach

The Patuxent River watershed (2,260 km^2) is located between Washington, D.C. and Baltimore, Maryland (Fig. 3.1). The TFW ecosystem of the Patuxent River has been previously identified by Boynton et al. (2008); it extends approximately 25 river kilometers along the upper Patuxent River (from 39° 0'N 76° 41'W to 38°43'N

76° 41'W). This ecosystem is composed of hundreds of individual marshes with well-defined tidal creeks and marsh basin areas.

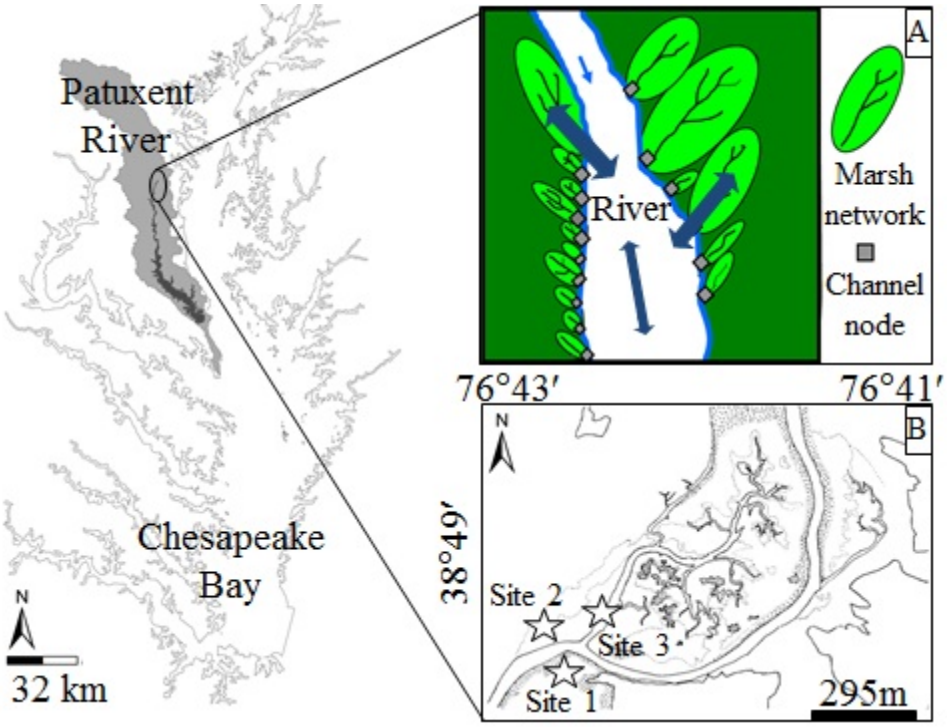

Figure 3.1. Study area located in the tidal freshwater portion of the Upper Patuxent River, Maryland. A) Schematic diagram showing the organization of tidal marshes along the river. Tidal fluxes are controlled by inlet channel geomorphology (governing node). B) Map of selected marshes for mass balance measurements. Marsh areas (m^2) are: Site 1: 670.6, Site 2: 5705, and Site 3: 536,873.4.

Each individual tidal freshwater marsh in this ecosystem connects to the tidal Patuxent River through a well-defined inlet channel (Fig. 3.1B). Natural levees border the marsh boundary, which prevents direct overbank flooding from the Patuxent River into the adjacent marsh for most tidal stages. Interior marsh areas are flooded by water that enters through the tidal inlet, and then moves up the tidal network, where it floods onto marsh surfaces (Seldomridge, 2009). Fringing tidal wetlands

without channel networks also border the Patuxent River, but these higher elevation marshes are inundated only during the upper 10% of tidal or flood stages (high tide ± high Patuxent River flow). Due to this geomorphic arrangement of marshes along the tidal Patuxent River, water and solute fluxes can be measured at the inlet of each individual marsh. Nitrate retention calculated from fluxes (e.g. Nitrate $flux_{in}$ - Nitrate $flux_{out}$) measured at channel inlets represent the consequences of net nitrate retention processes within each individual marsh system.

3.2.2 Geomorphic measurements and analysis

Marsh surface area, channel length, inlet channel width, and channel order were measured from high resolution air photos for every marsh and associated channel network in the tidal freshwater portion of the Patuxent River. Photo sources included: United States Department of Agriculture, 2006 and U.S. Geological Survey, 2002-2005; 2007-2010. Measurements were made from autumn and winter photographs to minimize measurement error due to vegetation cover. Channel order was determined following the Horton (1945) numbering scheme. Measurements of inlet channel widths and lengths from air photos were compared with field measurements of the same features to determine accuracy of measurement and the resolution of measurement (e.g. smallest measurable channel width). Marsh surface area for each tidal basin was determined from vegetation patterns and associated elevation changes, which were often subtle on images of the smallest tidal marshes (highest elevation). Thus, a subset of the smallest marshes (with areas less than $55m^2$) could not accurately be determined. Operator error was determined from triplicate measurements of each geomorphic parameter. Operator error for channel width

ranged from 1.72% for the smallest measured channel (0.2 meters) to 1.29% for the largest measured channel (93.4 meters); for channel length ranged from 1.5% for the smallest channel (2.13 meters) to 0.03% for the largest channel (3,773.1 meters); and for marsh area ranged from 6.2% for the smallest measured areas (225.6m^2) to 0.15% for the largest measured areas (675,611.9 m^2).

To investigate ecosystem geomorphic characteristics, I evaluated cumulative size distributions of the geomorphic data. A cumulative distribution is determined by sorting the data from largest to smallest and plotting the cumulative number against size of the geomorphic characteristic on a log-log plot. These distributions were evaluated to determine whether they exhibited power law behavior. The probability that an inlet width (W) greater than or equal to W_i can be written as:

$$P(W \geq W_i) \tag{3.1}$$

Data exhibit an inverse power law if $P(W \geq W_i)=\alpha W^{-\beta}$, where α and β are empirically-derived coefficient and exponent, respectively (Rinaldo et al., 1993; Scanlon et al., 2007). These distributions of geomorphic parameters were used to choose mass balance sampling locations, identify missing data, and assess the suitability of geomorphic parameters for modeling ecosystem nitrate retention.

3.2.3 Site selection for inlet cross section and nitrate mass balance measurements

Sites for field measurements of channel dimensions, water flux, and nitrogen mass balance measurements were chosen from the geomorphic probability

distributions to represent a large range of tidal marsh sizes. Cross section measurements were made on 18 inlet channels, also chosen to represent the entire range of inlet channel sizes. Cross sections were measured at slack high tide of spring tidal stage conditions. Channel depth data were referenced to the high tide marsh platform elevations and tide gauge data.

Nitrate retention measured by mass balance procedures may be sensitive to tidal water volumes, incoming nitrate concentration, and height of marsh vegetation; therefore, measurements of individual marshes were conducted during high (spring) tides during the same or sequential tidal cycles (Seldomridge, 2009). Mass balance measurements were made at the inlets of 3 individual marshes that were in close proximity to one another with areas of 671, 5705, and 536,873 m^2 respectively (Fig. 3.1C). Additional geomorphic characteristics for each mass balance measurement site are given in Table 1. Although mass balance measurements of nitrate retention were made for varying seasons and tides (from 2008-2011), only the data for flooding tides of spring tidal conditions in early autumn (20 September 2008, 1 October 2008, 14 September 2011, and 16 September 2011) were used in the ecosystem evaluation in this paper. In this system, the invasive submerged aquatic vegetation *Hydrilla verticillata* influences vegetative flow resistance during spring and summer months (Jenner and Prestegaard, *unpubl*), and thus affects water flux and nitrate retention. The autumn, spring tides represent a maximum water flux condition for which I examined geomorphic influences on nitrate retention.

Table 3.1. Geomorphic characteristics of marshes and mass balance measurements for Fall 2008

	Site 1	**Site 2**	**Site 3**
Marsh surface area (m^2)[a]	670.6	5705	536,873.4
Total channel length (m)[a]	21.6	124.6	1577.3
Inlet channel width (m)[a]	4.15	6.5	41.7
Stream order[b]	2	3	7
Inlet maximum depth (m)[c]	0.59	0.79	2.0
Inlet channel area (m^2)[c]	1.26	2.5	41.1
Water volume (m^3)[d]	353 ± 14	1218 ± 49	16,524
NR (moles)[e]	3.4 ± 0.3	10.6 ± 0.2	144.2 ± 6
NR_{rate} per area (μmol m^{-2})	4439	1822	326
NR_{rate} per volume (μmol L^{-1})	8.5 ± 0.6	8.7 ± 0.02	8.7 ± 0.1
Incoming nitrate (moles)	9	32	430

a- Measured using remotely sensed images.
b- Determined following Horton (1945) channel numbering scheme.
c- Determined from field measurements of inlet channel dimensions.
d- Field measurements of discharge were measured at 30 minute intervals at the inlet channel mouth, and integrated to determine the total water volume fluxed over a spring tidal cycle.
e- Nitrate retention was determined by subtracting the outgoing flux of nitrate from incoming nitrate flux for each tidal marsh for each time increment (Eq. 3).

3.2.4 Measurement of hydrologic flux during spring (high) tides

Hydrologic flux over a tidal cycle was determined by measuring tidal stage, associated channel cross sectional area, and velocity at time steps during tidal cycles. Tidal stage was measured at each inlet. These local tidal stage measurements were referenced to continuously monitored gauges at Jug Bay Wetlands Sanctuary (Maryland Department of Natural Resources Eyes on the Bay). Bankfull (maximum) channel cross sectional area was measured at slack high tides during spring tidal conditions. Velocity was measured at 10-12 intervals in the channel cross sections to determine discharge and average channel velocity (Q/A_c). Due to the rapid change in velocity with tidal stage, a relationship between average and maximum velocity was developed for each channel (Chen and Chiu, 2002), and from field measurements of maximum velocity, this relationship was used to determine average velocity for each time step (30 min). Discharge calculations for each time step were integrated to determine total water volume transported over the tidal cycle. A 5% error was propagated through all discharge calculations; this was determined by considering operator error in cross sectional and velocity measurements (Sauer and Meyer, 1992), and error introduced by estimating average velocity from maximum velocity (Chen and Chiu, 2002).

3.2.5 Calculation of tidal prism from tidal stage and geomorphic data

Field measurements of water volume for spring tidal cycles were compared with values of spring tidal prism calculated for each marsh:

$$V_p = T_r A_{ws} \quad (3.2)$$

where V_p is spring tidal prism (m^3), T_r is spring tidal range (m), and A_{ws} is waterway surface area (m^2). Waterway surface area was determined from air photos. Local tidal range (and tidal period) for each individual marsh system is controlled by tidal stage and the elevation of the inlet channel relative to the marsh platform. For the smaller channels, inlet depth limits tidal stage and inundation time. Maximum channel depth for each inlet was determined from the inlet width (W) to inlet area (A_c) relationship, and assuming triangular geometry that was indicated by field measurements. The relationship of spring tidal prism to geomorphic parameters (inlet cross sectional area and marsh surface area) was also examined and compared to field measurements of spring tide water volume.

3.2.6 Field mass balance measurements of nitrate retention over spring tidal cycles

Water sampling for N species (NH_4-N;NO_2-N;NO_3-N) was conducted over spring tidal cycles. This maximum flooding condition was chosen to provide comparisons with laboratory conditions of marsh surface flooding, which produce maximum nitrate retention rates (Reddy et al., 1984). Water samples for the outgoing tidal cycle were measured in concert with gauge height and velocity measurements. Samples taken during flooding tides indicate that concentrations of N species remain nearly constant on the rising stage (Fig. 3.2A); therefore, sampling schemes were adopted that included only a portion of the flooding tide to obtain average incoming concentrations, along with the entire falling tide at each channel inlet sampling (Fig.

3.2B-D). Water samples were taken at 30 minute intervals and filtered in the field with 45 μm syringe filters. The samples were immediately frozen and analyzed within several weeks for dissolved inorganic nitrogen series (NH_4-N;NO_2-N;NO_3-N) using standard photometric methods and ion chromatography (Solorzano, 1969; Keefe et al., 2004). Analytical error of ± 2 μmol, determined by the mechanical specifications of the equipment, was considered in all nitrate retention calculations. Nitrate was the only form of nitrogen that shows significant variation over the tidal cycle, and is therefore the focus of this study (Fig. 3.2B-D). Nitrate retention was determined by subtracting the outgoing flux of nitrate from the average incoming nitrate flux for each tidal marsh for each time increment:

$$NR = \sum[Q_t\,(N_{i(t)} - N_{o(t)})] \tag{3.3}$$

where *NR* is nitrate retention (moles); Q_t is discharge (Ls^{-1}); $N_{i(t)}$ is initial [NO_3-N] of tidally introduced water (μmol), and $N_{o(t)}$ is [NO_3-N] of outgoing tidal water at time *t* (μmol). One of the advantages of using mass balance calculations of nitrate retention is that it provides measurements of nitrate retention for individual marshes for a given tidal cycle, time of year, and initial nitrate concentration. No assumption is made of nitrogen retention processes within each individual marsh, although previous work suggests that marsh surfaces are primary sites for nitrate retention (Seldomridge, 2009).

Nitrate retention data were compared with both measured water volumes over a tidal cycle and marsh area to determine whether nitrate retention could be expressed as simple functions of either parameter. These results then guided the development of relationships between nitrate retention and geomorphic parameters.

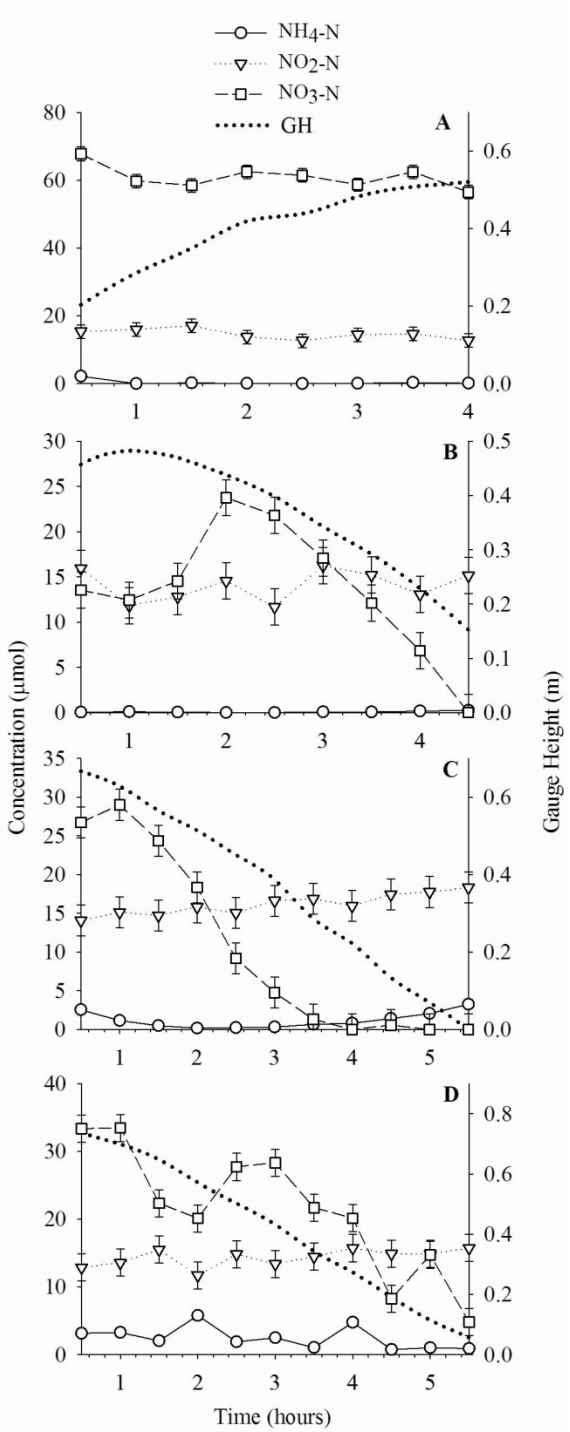

Figure 3.2. Examples of water chemistry measurements. A) Constant concentrations on incoming tides at Site 1 on 24 September 2008. B) Nitrogen concentrations and tidal stage for the ebbing tidal cycle at Site 1 on 20 September 2008. The nitrate concentrations decrease with the dropping tidal stage. C) Data for the ebbing tide at Site 2 on 1 October 2008. D) Data for the ebbing tide at Site 3 on 1 October 2008.

3.3. Results

3.3.1 Cumulative geomorphic distributions

The data in the cumulative distributions can be described as inverse power law functions (Fig. 3.3). The power law for the cumulative number of marsh surface area is:

$$N_{Am} = 4712.3A^{-0.54} \qquad \text{n = 142; } R^2 = 0.97 \qquad (3.4)$$

where N is the cumulative number of marshes with area > A. The power law for the cumulative number of channel lengths is:

$$N_L = 2224.2L^{-0.78} \qquad \text{n = 242; } R^2 = 0.90 \qquad (3.5)$$

where N is the cumulative number of channels with lengths > L. Finally, the power law for the cumulative number of inlet widths is:

$$N_W = 133.2W^{-0.59} \qquad \text{n = 267; } R^2 = 0.92 \qquad (3.6)$$

where N is the cumulative number of inlets with a width > W. The smallest marsh inlet width measured from air photo data is 0.2 ± 0.05 meters; this lower boundary was validated by field measurements.

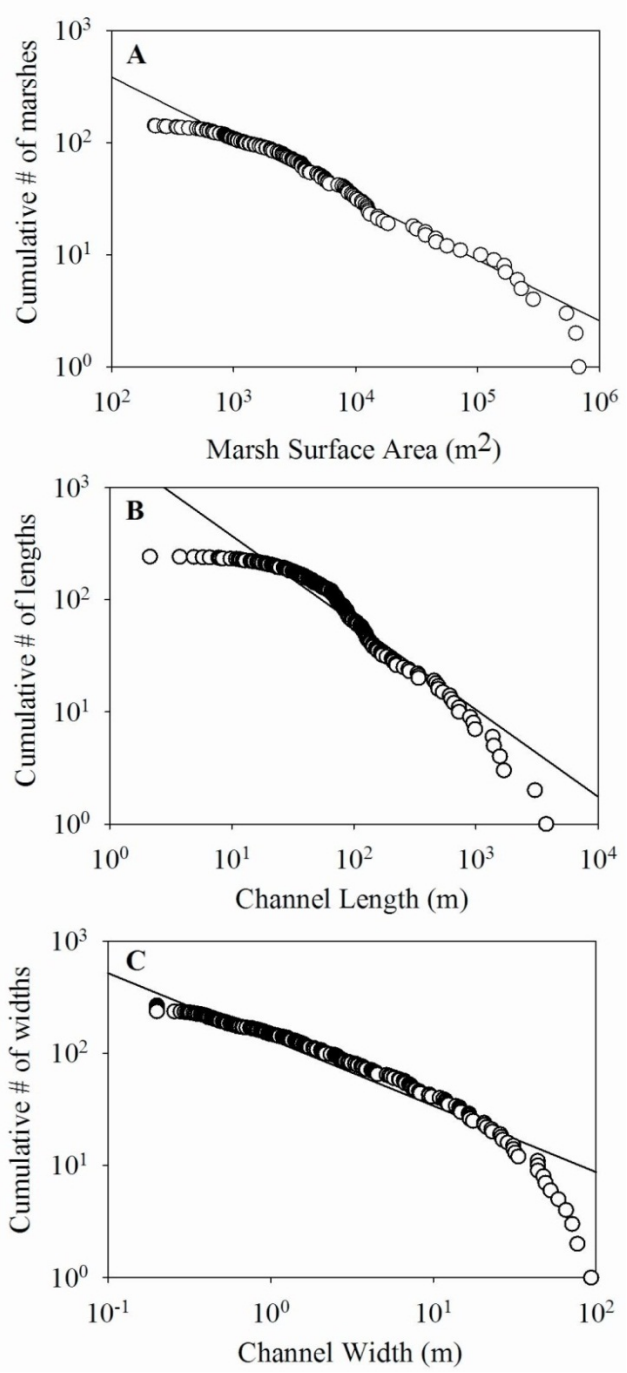

Figure 3.3. Geomorphic data for the tidal freshwater portion of the Patuxent River. A) Cumulative number of marsh areas less than or equal to indicated value ($N=4712.3A^{-0.54}$; n=142; R^2 =0.96). B) Cumulative number of channel lengths less than or equal to indicated size ($N=2224.1L^{-0.78}$; n=242; R^2 =0.90). C) Cumulative number of inlet channel widths less than or equal to indicated value ($N=133.2W^{-0.59}$; n=267; R^2 =0.92). Standard error is less than size of data points.

3.3.2 Relationships between geomorphic variables

Inlet width measurements from air photos were the most accurate of the 3 geomorphic parameters (within 1% of measured values). Visibility of small inlets on photographs provided an almost complete inventory of inlet channels; therefore, the number of marsh inlets was used to define missing data for the other geomorphic parameters. Comparison of the number of inlet widths measured with channel length and marsh area measurements indicated that 47% of the total number of marsh area measurements (for the smallest marshes) and 9% of the channel length data are missing from the measured populations although the width of the associated marsh inlet was identified. Relationships among the geomorphic variables were examined and are shown in Fig. 4; several of these relationships are given below:

$$L = 1.3{A_m}^{0.53} \qquad \text{n = 142; } R^2 = 0.79 \qquad (3.7)$$

$$W = 0.2{A_m}^{0.65} \qquad \text{n = 142; } R^2 = 0.47 \qquad (3.8)$$

Where L is the channel length, W is the inlet width, and A_m is the marsh surface area. Missing values for marsh surface area and channel length were estimated from their relationship to marsh width (e.g. Eq. 3.8).

Stream order was evaluated for each individual marsh channel network; maximum stream order for each marsh was determined, and the relationship between stream order and marsh area is shown in Fig. 3.4C. Stream order depends upon the choice of ordering system, the resolution of aerial photos and maps, and often fails to discern characteristics between network structures (Kirchner, 1993; Rinaldo and

Rodriguez-Iturbe, 1998); therefore, it was not used to model ecosystem nitrate retention in this study.

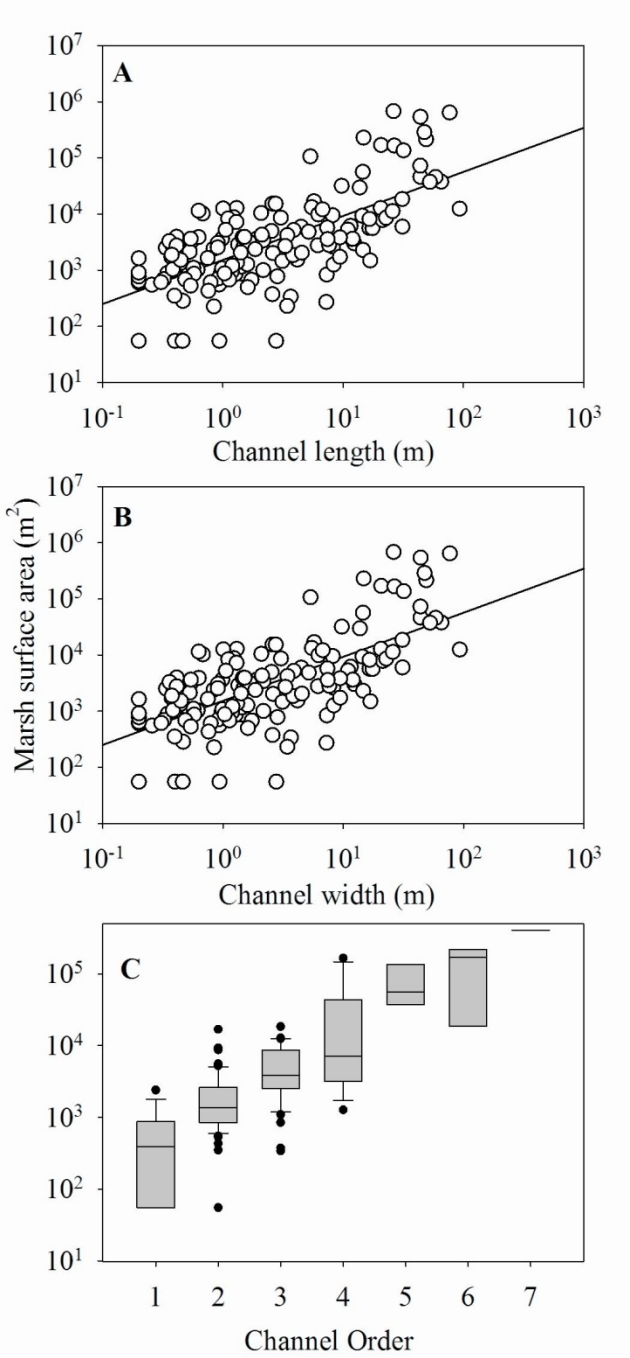

Figure 3.4. Geomorphic relationships of channel order, inlet width, and total channel length to marsh surface area of tidal freshwater marshes along the Patuxent River Estuary. A) $L=1.3A_m^{0.53}$(n=142; R^2=0.79). B) $W=0.2A_m^{0.65}$(n=142; R^2=0.47). Standard error is less than the size of each data point. C) Box plot of marsh surface areas for each stream order.

3.3.3 Relationship of spring tidal volume to geomorphic parameters

The relationships between spring tidal prism (V_p) and both marsh surface area (A), and inlet channel cross sectional area (A_c) are shown in Fig. 3.5. The relationship between bankfull inlet cross sectional area and inlet width was developed from data on 18 channel inlets (Table 3.1; Fig. 3.5A):

$$A_c = 0.20W^{1.4} \qquad \text{n = 18; } R^2 = 0.88 \tag{3.9}$$

This relationship was used to estimate average and maximum inlet depth for each channel, which can be expressed as elevation relative to mean lower low water (Fig. 3.5B). The relationship of calculated spring tidal prism to inlet channel cross sectional area (Fig. 3.5C) is:

$$V_p = 0.004{A_c}^{1.02} \qquad \text{n = 142; } R^2 = 0.65 \tag{3.10}$$

The field measurements of hydrologic volume over a tidal cycle are indicated in Fig. 3.5C as the three solid squares that plot near the central tendency of this relationship.

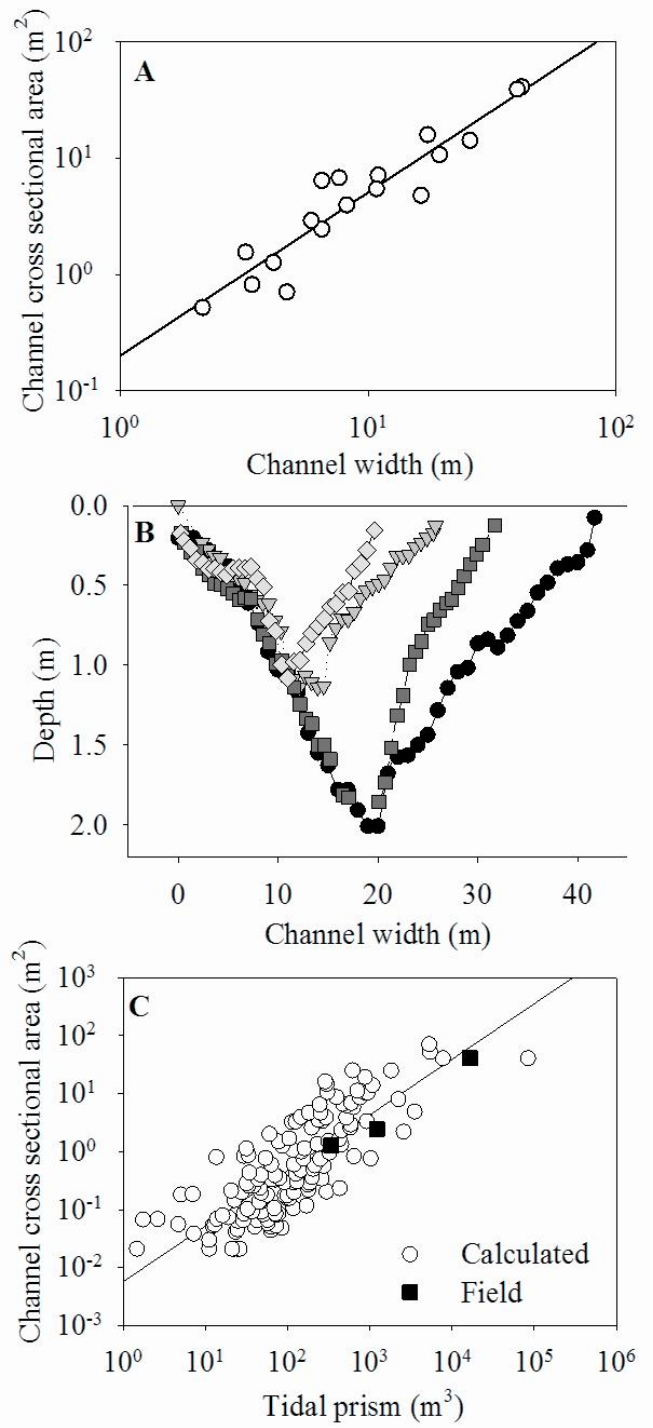

Figure 3.5. Calculated spring tidal prism for tidal freshwater wetlands. A) Relationship between inlet width and cross sectional area. B) Inlet channel cross sectional areas plotted relative to the elevation of the marsh platform. Inlets with widths > 16 m experience the entire spring tidal range, whereas tidal range in the smaller inlets is constrained by inlet elevation, so that they experience a portion of high tidal stages. C) Relationship between inlet cross sectional area and tidal prism (Eq. 10). Squares indicate field measurement of spring tide water volumes for the 3 sampling sites.

The calculated tidal prism was expressed as a power function of each of the 3 geomorphic parameters (marsh area, channel length, and inlet channel width; Fig. 3.6). Field measurements of tidal water volumes (tidal prism) for the same tidal stage are also indicated on these diagrams. These relationships indicate significant scatter between each geomorphic variable and tidal prism. In addition, there are systematic differences between the tidal prism estimates of water volume and the field measurements for all 3 geomorphic parameters (Fig. 3.6). These systematic differences suggest that the tidal prism method under-estimates the amount of water carried into small tidal systems, but over-estimates the amount carried into large tidal systems.

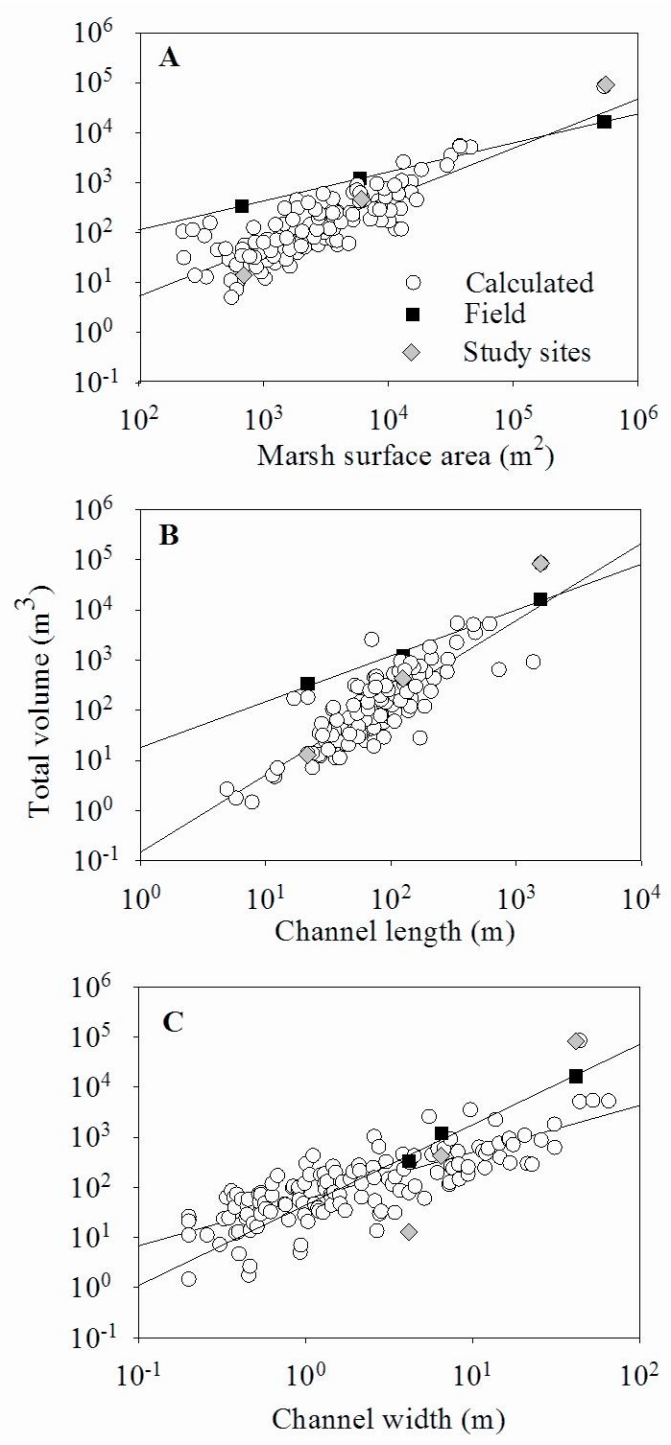

Figure 3.6. Relationship of calculated tidal prism to: A) marsh surface area, B) channel length, and C) inlet channel width. Field measurements are shown as black squares, gray diamonds highlight predicted tidal prism for the corresponding study sites.

3.3.4 Mass balance results of nitrate retention

The autumn data mass balance measurements of nitrate retention for each of the three marshes is shown in Table 3.1. These data indicate that the ratio of nitrate retention to water volume is constant for a given set of conditions. The data (Fig. 3.7) indicate a nearly linear relationship between water volume and nitrate retention for spring (high) tides, which aligns with the multi-year data for the entire growing season:

$$NR = 0.0045V^{1.1} \qquad \text{n = 6; } R^2 = 1.0 \qquad (3.11)$$

Where *NR* is nitrate retention (moles) and *V* is the tidal volume water fluxed through the inlet channel mouth (m_3). When the exponent of 1.1 is rounded to 1, the trend is linear and can be simplified to:

$$NR = aV_{in} - bV_{out} = cV \qquad (3.12)$$

Where *NR* is nitrate retention (moles), *a* is the integrated average nitrate concentration (moles) on the incoming tide, *b* is the integrated average nitrate concentration (moles) on the outgoing tide, *V* is the volume of water flux (L), and $_c$ is the concentration of retained nitrate (moles). If $V_{in} = V_{out}$, which is the case for tides with minimal water storage or evapotranspirative losses, the equation is simplified to:

$$NR = (a - b)V = cV \qquad (3.13)$$

The relatively constant incoming nitrate concentrations were used to evaluate total nitrate flux into the tidal marshes (Table 3.1). These data indicate that approximately

30% of the total nitrate flux into the marshes was retained for the measured spring tides (Table 3.1). The constant ratio of NR/V (Table 3.1; Fig. 3.7) for varying values of incoming nitrate concentration suggest that retention is not limited by the range (23 to 57 ± 2 μmol) of initial, incoming concentrations measured for this study.

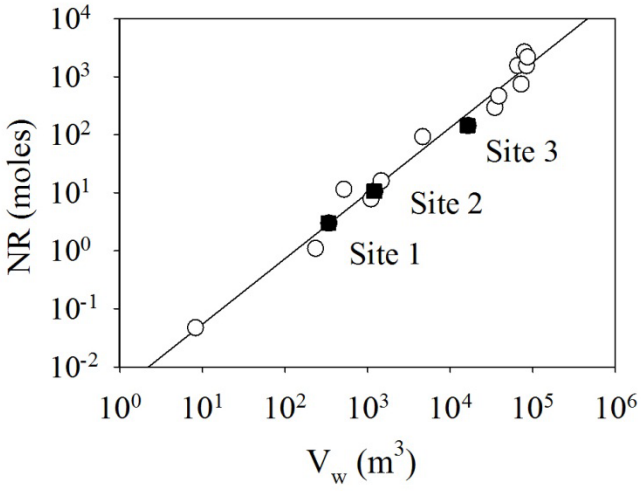

Figure 3.7. Relationship between net nitrate retention over a tidal cycle and water volume. Data are reported for the 3 sampling sites for various tides in 2008, 2010, and 2011. Nitrate retention is a simple function of hydrologic flux that varies over 5 orders of magnitude. Data for spring (high tides) in autumn 2008 are highlighted with black squares. Together data from 2008-2011 from all sites follow the relationship: $NR=0.0045V^{1.1}$ (n=16; $R^2=0.98$).

3.3.5 Comparison of ecosystem calculations of nitrate retention and evaluation of geomorphic parameters

The relationship between water volume and nitrate retention relationship (Fig. 3.7) and the field-based relationship between water volume and each geomorphic parameter (Fig. 3.6) were combined to determine an equation between each geomorphic variable and nitrate retention (Table 3.2). These equations were then applied to the entire population of each geomorphic variable (Fig. 3.3) to estimate

total nitrate retention for this TFW ecosystem (Fig. 3.8). Estimated total nitrate retention for the geomorphic parameters varied considerably; the estimate based on marsh area was only 44% of the value estimated from inlet width data. Nitrate retention for the reference spring tides (autumn 2008 and 2011) was 1738.9 ± 44.6 moles NO_3-N based on marsh area data, 2790.1 ± 31.2 moles NO_3-N based on channel length data, and 3961.2 ± 135.8 moles NO_3-N based on inlet width data. When the channel length and marsh surface area data were adjusted to account for missing measurements, the total nitrate retention is closer to the estimate based on inlet width (Fig. 3.8). The total nitrate retention based on adjusted marsh surface areas is 2254.9 ± 44:6 moles NO_3-N, and for adjusted channel length is 2892.9 ± 31.2 moles NO_3-N.

Table 3.2. List of equations describing geomorphic, hydrologic, and biogeochemical relationships

Geomorphic-hydrologic (field)	
(1) $V=7.81A_m^{0.58}$	n=3, R^2=1
(2) $V=18.15L^{0.91}$	n=3, R^2=0.99
(3) $V=44.63W^{1.6}$	n=3, R^2=0.98
Geomorphic-biogeochemical (field)	
(4) $NR=0.0045V^{1.1}$	n=13, R^2=0.98
(5) $NR=0.038A_m^{0.61}$	n=6, R^2=0.96
(6) $NR=0.09L^{0.97}$	n=6, R^2=0.96
(7) $NR=0.25W^{1.7}$	n=6, R^2=0.92

The distribution of total nitrate retention among the individual marshes as a function of channel width and marsh surface area is shown in Fig. 3.8B-C. As a function of channel width, the 8 widest channels (3% of total; ranging from 43.86 m

wide to 93.39 m wide) are responsible for 50% of the NR. As a function of marsh surface area, the 11 biggest marshes (4% of total) are responsible for 50% of the NR; in sum these marshes cover 3,227,913 m^2 or approximately 80% of the TFW ecosystem. Therefore, these largest marshes (top 4%) represent a larger proportion of the total marsh area (80%) than of total nitrate retention (50%).

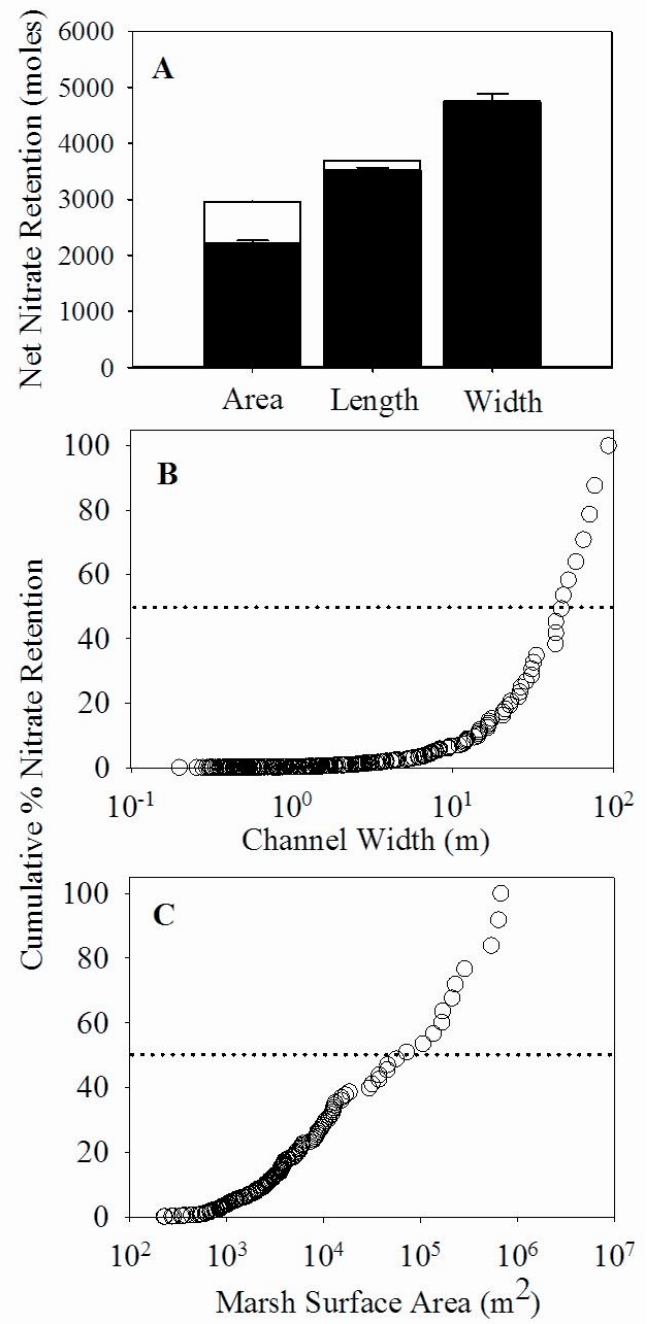

Figure 3.8. Total ecosystem nitrate retention calculated from each of the 3 geomorphic variables. A) Nitrate retention estimated from marsh surface area data is 1738.9 ± 44.6 moles NO_3-N, from channel length is 2790.1 ± 31.2 moles NO_3-N, and from channel width is 3961.2 ± 135.8 moles NO_3-N. Stacked white bars indicate additional retention calculated by adding in the missing geomorphic data, which were predicted from geomorphic relationships to inlet width. B) Spatial distribution of nitrate retention as a function of channel width; the 8 largest channels are responsible for 50% of total retention. C) Spatial distribution of nitrate retention as a function of marsh surface area; the 11 largest marshes are responsible for 50% of total retention.

3.4 Discussion

3.4.1 Geomorphic data and geomorphic relationships

In this study, the inlet width data were accurately measured from imagery data, relatively easy to field verify, and provided a nearly complete data base that could be used to evaluate the quality of the other geomorphic data bases. All of the geomorphic parameters exhibited power law behavior of cumulative data. Distributions were confined to 3 orders of magnitude for inlet width (Fig. 3.3), which suggest that minimum channel size may be affected by external controls, such as vegetation growth (Hickin, 1987; Rinaldo et al., 1999a; Montgomery, 1999). The upper limit of inlet size defines the maximum size of a tidal marsh that can be sustained in this system (Jenner, 2011), which is likely controlled by tidal stage and available space along the river width.

Although total length of the main channel network provides a measure of the conduit that conveys nutrient-rich waters into marsh interiors (Myrick and Leopold, 1963; Fagherazzi et al., 1999; Rinaldo et al., 1999a), this geomorphic parameter was also difficult to measure, particularly for large, complex marshes. In this study, the geomorphic system was composed of individual marshes arrayed along the length of the tidal Patuxent River, which is not directly analogous to the geomorphic organization of a large tidal system (e.g., Rinaldo et al., 2004). In this study, I found that total channel length was more closely related to tidal prism than marsh watershed area, which is the opposite of the result obtained by Marani et al. (2003) for a large complex tidal marsh.

Previous studies have identified marsh surfaces as important sites for biogeochemical cycling (e.g., Bowden et al., 1986), and marsh area has previously been used as a scaling parameter to extend laboratory measurements of denitrification rates to field settings. Previous studies indicate that microtopography can greatly increase the overall area available for NR (Wolf et al., 2011); this study suggests that microtopography is only one of the difficulties presented in using marsh surface area as a scaling parameter. Non-synchronous flooding of surfaces of similar elevations as a function of travel time from the tidal inlet is an important issue in this system.

In this study, each freshwater tidal marsh was connected by a well-defined inlet channel to the main Patuxent River estuary. Thus, the inlet channel cross section area and tidal hydrodynamics control the amount of water, sediment, and solutes that move into the marshes (Fagherazzi et al., 1999). Using channel width as the geomorphic unit for scaling provided the highest estimate of ecosystem nitrate retention (Fig. 3.8) because every inlet channel and thus every marsh system was included in the ecosystem evaluation. This geomorphic parameter is also easily adaptable to other tidal conditions through the relationships between channel width and hydraulic parameters (depth, velocity, area, discharge; (Myrick and Leopold, 1963; Marani et al., 2003). Measurements of vegetative flow resistance can provide information to predict water fluxes with seasonally varying hydraulic conditions. Thus, for this tidal freshwater wetland ecosystem, with the simple arrangement of the marsh inlets along the sides of the estuary, inlet width provides the most complete and accurate data for estimating tidal water volumes and nitrate retention.

3.4.2 Hydrologic controls on nitrate retention

Tidal marshes are self-organized systems in which the marsh area coevolves with hydrologic flux to form the channel network system (Bak et al., 1988; H. Odum, 1988). This self-organization of tidal marsh networks generates systematic relationships between geomorphic characteristics and hydraulic characteristics (Fig. 3.4A-B). Mass balance studies indicated a nearly linear relationship between water volume and nitrate retention for spring (high) tides (Eq. 3.11), which suggests that nitrate retention is limited by hydrologic flux in this system (Seldomridge and Prestegaard, 2011). This relationship between hydrologic flux and nitrate retention relationships was similar for different seasons and tidal stages (Fig. 3.7). These data suggest that although marsh surface area may be the dominant site for nitrate retention (Seitzinger, 1988; Cornwell et al., 1999), the ability of water to move through the system, even for the highest tides with minimum channel flow resistance, is the greatest control on nitrogen processing. Marsh areas that are available for processing have limited activity due to limitations in water reaching these sites. Nitrate retention includes a variety of processes such as denitrification, biotic assimilation, burial, and/or recycling. These processes are seasonally variable and may be controlled by factors such as temperature, the availability of organic matter, amount of oxygen, nitrogen availability, and composition of the microbial community (e.g., Seitzinger, 1988, 1994; Cornwell et al., 1999; Wallenstein et al., 2006). Although these controls may be seasonally important, results from this study suggest that nitrate retention in these freshwater tidal wetlands is a relatively simple function of water volumes. Evaluation of additional hydrodynamic data is needed to use

geomorphic data (inlet width, inlet area) to predict tidal volumes, and thus nitrate retention for other tidal stages and seasons.

3.4.3 Spatial distributions of nitrate retention

Although the small-sized marshes systems are the most common (Fig. 3.3), the spatial distributions of nitrate retention indicate that a small number of the biggest marshes are responsible for the majority of retention (Fig. 3.8B-C). The largest 4% of the marshes by area represented 80% of the total area and retained 50% of the total nitrate. Although numerous, the small marshes contributed small proportions to the total nitrate retention due to the short inundation times of these high elevation surfaces. Previous studies suggest that small marshes with high surface area to volume ratios are the important sites for nitrate retention (e.g., Simpson et al., 1983; Groffman, 1994; Boynton et al., 2008). Although we also observed the largest surface area to volume ratios for the small systems (Table 3.1), it is the volume of water that limits the nitrate retention in this system, not the area to volume ratio.

3.5 Conclusion

The appropriate geomorphic unit for scaling an ecosystem function must be chosen based on both underlying controls (e.g. water volume), and also on data availability and accuracy of measurement. For this study, field measurements of *in situ* nitrogen processing rates on multiple scales were necessary to determine the appropriate scaling parameters to estimate ecosystem nitrate retention. I suggest that mass balance measurements might be appropriate as fundamental steps to determine scaling parameters in other systems. Although the results of this study appear to be

related to the geomorphic organization of TFW along the main estuary, and thus might not be directly applicable to other tidal freshwater wetlands, the integrated mass balance, geomorphic approach should be applicable to other ecosystems. In addition, any other ecosystem function that is linked to hydrologic flux, such as sediment transport and deposition, allochthonous organic carbon retention, and perhaps sulfate retention, can be analyzed using this approach. This study presents spatially distributed estimates of nitrate retention for one representative high tidal stage. Additional work is necessary to determine hydrodynamic and other data required to evaluate nitrate retention for temporally-varying conditions (e.g. seasonal and tidal variations in hydrodynamic and nitrogen processing).

Chapter 4:

Influence of emergent macrophytic and submerged aquatic vegetation on nitrate retention in tidal freshwater marshes

4.1 Introduction

4.1.1 Vegetation in tidal freshwater wetlands

Tidal freshwater wetlands (TFW) are dynamic ecosystems that experience seasonal growth and die-back of both emergent macrophytic and submerged aquatic vegetation (SAV). Emergent macrophytes dominate marsh surfaces and also grow in shallow areas along channel margins (e.g. Simpson et al., 1983), whereas submerged aquatic vegetation grows on channel beds where light penetration permits (e.g. Orth and Moore, 1984; Orth et al., 1994). Both types of vegetation facilitate nutrient retention in tidal wetlands through uptake and burial (Bowden, 1987; Mitsch and Gosselink, 2007). Tidal freshwater wetlands commonly have high species diversity (Simpson et al., 1983; W. Odum, 1988), which can enhance ecosystem services and functions such as nutrient retention (Engelhardt and Ritchie, 2001). In some systems, however, species diversity has been reduced by the invasion of non-native plants. In particular, the shallow regions of the Upper Chesapeake Bay have been invaded by non-native plants such as SAV *Hydrilla verticillata* (Naylor and Kazyak, 1995; Delgado, *unpubl*) and emergent macrophytes *Phragmites australis* (Chambers et al., 1999; Rice et al., 2000; Delgado, *unpubl*). In the Patuxent River, *H. verticillata* grows on the channel bed in dense canopies to the height of lower low tide; this vegetation affects water velocity and discharge at all tidal stages during summer months when

SAV is present (Jenner and Prestegaard, *unpubl*). Emergent plant species (e.g. *Nuphar advena/leteum, Peltandra virginica, Polygonum sagittatum, Pontederia cordata*, and *Zizania aquatica*) can grow into channel margins and constrict or occlude small channels during summer months. Both emergent macrophytes and SAV plant species can significantly alter tidal channel hydraulics and thus affect the fluxes of water and associated materials in suspension into and out of the marshes.

4.1.2 Effects of vegetation on channel morphology and hydrodynamics

Freshwater tidal marshes often contain self-organized networks of channels that convey water from the estuary into tidal marshes (Myrick and Leopold, 1963; Fagherazzi et al., 1999; Rinaldo et al., 1999). These marshes are in dynamic equilibrium when tidal water, conveyed up the tidal channels during spring tides floods marsh surfaces and provides sediment and/or organic matter accumulation that can offset subsidence and decomposition of marsh substrates (Pasternack and Brush, 1998; Neubauer et al., 2002; Neubauer, 2008). This dynamic equilibrium between marsh geomorphology and tidal channel hydraulics is sensitive to sea-level rise and to factors that affect channel capacity, such as the growth of vegetation in and along tidal channels. The geomorphic and vegetative characteristics of marsh inlets limit the fluxes of water, sediment, and solutes into the marshes where ecological processing occurs (Fagherazzi et al., 1999; Seldomridge, 2009). Previous research on unvegetated tidal channels of the Patuxent River suggests that nitrate retention is primarily a function of the flux of water into the marsh networks (Seldomridge and Prestegaard, 2011). Alteration of hydraulic regimes by SAV is likely to affect

hydrologic fluxes and thus the amount of nitrate retention (NR) that occurs in these tidal marshes over a tidal cycle.

Tidal channel hydrodynamics are spatially and temporally variable. Relationships between tidal stage and channel discharge can be affected by the growth of vegetation on marsh platforms, which can influence contained versus overbank flows. Seasonal changes in aquatic vegetation height and density can affect flow resistance and thus flow velocities (Myrick and Leopold, 1963; Bayliss-Smith, 1979; Healey et al., 1981; French and Stoddart, 1992, Nepf and Ghisalberti, 2008). There have been relatively few studies of flow resistance in tidal channels (Knight, 1981; French and Stoddart, 1992); however, there have been significant advances in our understanding of the effects of vegetation on velocity profiles, turbulence, and flow resistance (Nepf and Ghisalberti, 2008). Flume studies of model vegetation have examined the effects of vegetation on flow resistance, velocity, and discharge in shear flows (e.g. Ghisalberti and Nepf, 2002; Nepf and Ghisalberti, 2008). Although these studies provide information on the effects of model vegetation on velocity profiles, it is not clear whether scaling relationships apply directly to in situ conditions. SAV beds composed of *Hydrilla sp*. are flexible and the vegetation flattens as flow velocities increase during tidal cycles, similar to what has been observed for grasses (Kouwen, 1980; Järvelä, 2002). Flattening of the vegetation creates a sharp inflection in the velocity profile and formation of a well-developed logarithmic velocity profile above the SAV canopies (Nepf and Ghisalberti, 2008).

Nitrate retention in the tidal freshwater marshes of the upper Patuxent River estuary appears to be primarily governed by the delivery of water and solutes into

individual marshes (see previous chapters). This analysis also indicated that a small number of large marshes are responsible for most of the nitrate retention in the ecosystem (Seldomridge and Prestegaard, 2012). Research on the hydraulic effects of *H. verticillata* on channel beds indicates that this SAV species has a significant effect on mean velocities and associated discharges into a large tidal marsh located in the upper Patuxent River Estuary (Jenner and Prestegaard, *unpubl*.). This reduction in velocity reduces the magnitude of water fluxes into marsh ecosystems and alters the distribution of water within the marsh, which in turn may alter biogeochemical cycling. The purpose of this study is to evaluate the conditions under which *Hydrilla sp.* can invade tidal channels, the effects on *Hydrilla sp*. on the relationship between geomorphic and hydraulic parameters, and an evaluation of the effects of vegetation on nitrate retention, especially within the larger tidal marshes.

4.1.3 Rationale for study

In the previous chapters, I demonstrated that NR in individual marshes and an ecosystem composed of many marshes is an outcome of complex interactions among inlet geomorphic characteristics, hydrologic flux, and biogeochemical processes. In cases where nitrate concentrations and water temperatures are greater than critical (limiting) values, an emergent behavior in which NR is a simple function of water volume is observed. Moreover, the probability distribution of marsh size in the Patuxent River ecosystem indicates that marsh size can be described as truncated fractal distributions with many more small wetlands than large ones (Jenner, 2011). Although numerous, these small wetlands process a small percentage of total nitrate (Seldomridge and Prestegaard, 2012). Approximately 50% of nitrate retention in the

Patuxent River marshes is processed by the large marshes that comprise only 4% of the total population, but over 80% of the marsh area; therefore, any processes that affect tidal water volumes in these large marshes is likely to affect net nitrate retention. Thus, the purpose of this chapter is to examine the effects of vegetative growth (emergent macrophytes and SAV) on seasonal variations in tidal inlet velocities in 3 different sized systems, with particular emphasis on the large marshes. The following questions will be addressed:

1. Are tidal inlet velocities and discharges (Q) significantly lower during vegetated conditions?

2. What sized inlet channels can support SAV populations?

3. During seasons without SAV, large marshes are responsible for a significant proportion of total ecosystem NR. Does the growth of vegetation in these channels significantly affect hydrologic fluxes and N processing?

4.2 Methods

4.2.1 Site description and selection of study inlets

The Patuxent River watershed (2,260 km^2) is located between Washington, D.C. and Baltimore, Maryland (Fig. 4.1). In this study, the tidal freshwater region of the Upper Patuxent River is defined as the region that lies within 39°0'N 76°41'W to 38°43'N 76°41'W with salinities less than 0.5 ppt (Fig. 4.1). The freshwater tidal marsh ecosystem is composed of hundreds of individual marshes with well-defined

tidal creeks and marsh basin areas (Seldomridge and Prestegaard, 2012). The wetlands are located within Patuxent Wetland Park and Jug Bay Wetlands Sanctuary. Geomorphic characteristics (marsh area, channel network length, and inlet width) were measured for all of the marshes in the tidal freshwater ecosystem. These data were used to construct probability distributions to determine the frequency of occurrence of each marsh and associated inlet channel (Seldomridge and Prestegaard, 2012). Based on these distributions, eighteen sites of varying size that spanned the range of distributions were chosen for inlet cross sectional area measurements and to develop relationships between inlet morphology and inlet width.

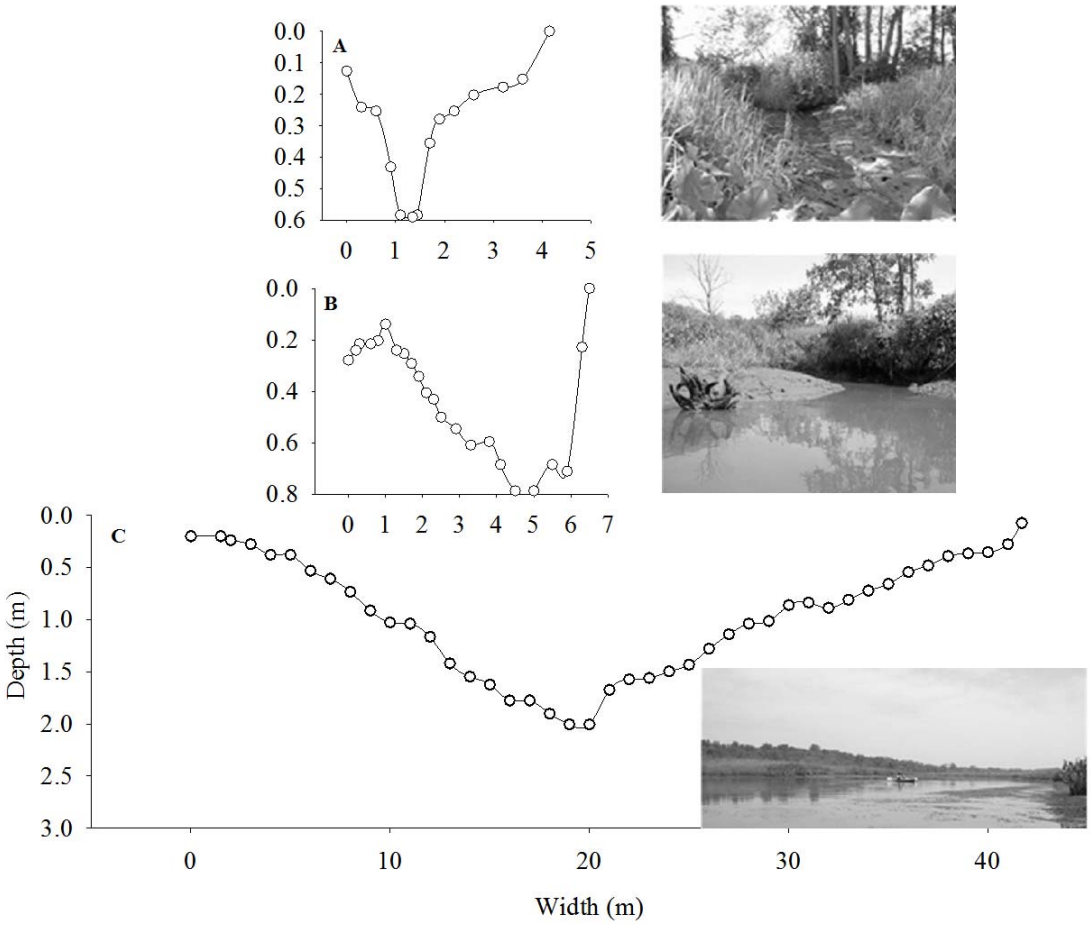

Figure 4.1. Inlet channel cross sectional profiles with corresponding field photo for (A) Site 1 (671 m^2), which is seasonally influenced by emergent macrophytes; (B) Site 2 (5705 m^2); and (C) Site 3 (536,873 m^2), which is seasonally invaded by invasive submerged aquatic vegetation *Hydrilla verticillata*. Photograph of Site 3 taken on 7 July 2008; *H. verticillata* is present and can be seen on the surface along the right bank of the channel.

Of these 18 tidal marshes, 3 were chosen for mass balance measurements of hydrologic flux and nitrate retention. The selected marshes have marsh surface areas of 671, 5705, and 536,873 m^2, and "bank full" inlet cross-sectional areas of 1.26, 2.5, and 41.1 m^2. Only three adjacent marshes were chosen for detailed study because measurements needed to be conducted on the same tidal cycles and at sites with

similar incoming nitrogen loads. Site 1 (channel width of 4.7 m) completely drains on an ebbing tidal cycle; these exposed channel beds do not support SAV growth. Site 2 is an intermediate channel (channel width of 6.5 m) that drains on some, but not all low tides, but also does not support SAV. Together, these small and intermediate channels account for 75% of the total number of tidal channels in the TFW portion of the Patuxent River. Site 3 (channel width of 41.7m) supports seasonal growth of SAV. This channel is representative of the large marshes that are responsible for a significant amount of NR in the TFW ecosystem.

4.2.2 Identification of channels that support SAV: Morphologic and hydraulic effects

Geomorphic measurements of inlet characteristics were determined from field measurements of depth at 15-20 locations along a channel cross section. These data were used to calculate bankfull cross sectional area (A_c). Measurements were made during both SAV absence (A_c) and presence (A_c') at slack tide during a bankfull tidal stage at 18 locations in the TFW ecosystem. During SAV presence, depth measurements from the water surface (adjusted for changing tidal condition) to the top of the canopy were feasible due to the water clarity, particularly during outgoing tides. These were compared to measurements made during SAV absence, and used to determine the area of the channel occupied by SAV.

During some conditions in deep channels, water clarity made canopy height measurements difficult, so the SAV canopy was characterized by near-zero values in velocity profiles measured in inlet channels (e.g. Site 3). Measurements of velocity

profiles or maximum (surface) velocity and the depth of the inflection point that defines the vegetative boundary layer velocity ($Z_{m;}$ Thom, 1971) were measured for the given tidal stage at 10-15 locations along the inlet width transect or for a half cross section if tidal conditions were changing rapidly. Cross sectional average velocity values were calculated by adjusting channel cross sectional areas by defining the vegetative boundary layer (Jenner, 2010). This method was used to determine average velocity, cross sectional area, and thus discharge for each measured time step during the tidal cycle. Relationships between geomorphic and hydraulic variables were determined using Q_{max} and U_{max}; the maximum discharge and velocity during the tidal cycle.

Cross sectional area measurements were used along with the tidal stage information to determine the maximum depth of channels that drained completely during low tides. Due to the relationship between width and cross sectional area, these measurements could be used to estimate channel depth, and to identify residual water depths at low tide (this identifies channels that can support SAV).

Geomorphic measurements of tidal inlets were made during SAV absence on 1 October 2008 and 5 April 2010. The timing of maximum heights of SAV usually occurred after mid-June and usually persisted for about 1 month (although there was considerable variability among the years). Measurements during SAV presence were made on 7 July 2009, 7 August 2009, and 27 June 2010 and 16 June 2011. Data were compiled and presented as either SAV presence or SAV absence.

4.2.3 Hydraulic measurements and hydraulic geometry calculations

4.2.3.1 At-a-station hydraulic geometry at inlet channels

Hydraulic geometry is derived from considerations of the conservation of mass (continuity equation) to either the increase in discharge in *a single channel cross section* over a hydrograph, or the *downstream* increase in discharge for a specific flow event (Leopold and Maddock, 1953; Myrick and Leopold, 1963). In this work, both these types of hydraulic geometry relationships will be examined: at-station hydraulic geometry is measured in marsh inlet channels and downstream hydraulic geometry is examined within an individual large marsh. At-a-station hydraulic geometry equations depict the changes in width, depth, and velocity with discharge at a given cross section (Leopold and Maddock, 1953; Myrick and Leopold, 1963). Channel width is determined as a function of gauge height drop and cross-sectional area change. Channel depth is derived by dividing the cross-sectional area by the channel width (A_c/W). Hydraulic geometry equations are the empirical power law relationships of width, depth and velocity to discharge data:

$$w = aQ^b \qquad d = cQ^f \qquad u = kQ^m \tag{4.1}$$

where w is water surface width, d is mean depth, u is mean velocity, Q is discharge, a, c and k are coefficients and b, f and m are exponents. Continuity places additional constraints on hydraulic geometry equations (Leopold and Maddock, 1953):

$$Q = w \cdot d \cdot u = (aQ^b)(cQ^f)(kQ^m) = (a \cdot c \cdot k)(Q^{b+f+m}) \tag{4.2}$$

where, $b + f + m = 1$ and $a \cdot c \cdot k = 1$. At an individual cross section location, the relationship of hydraulic variables to discharge depends upon both channel shape and flow resistance. Hydraulic shape, r, can be described as the f/b ratio and it increases as shapes change from triangular to rectangular (Dingman, 2007). These relationships may change seasonally in channels with emergent macrophytes as effective cross sectional area and flow resistance change (Ferguson, 1986; Dingman, 2007). Measurements were therefore made for over tidal cycles for two conditions: vegetative (SAV and emergent macrophytes) minimum and maximum. For the large marsh inlet channel, at-a-station hydraulic geometry was examined over a seasonal cycle to determine the effect of vegetation growth on hydraulic shape.

4.2.3.2 "Downstream" hydraulic geometry: Q_{max} for spring tidal stage

Downstream hydraulic geometry is similar to the at-a-station case, except the hydraulic geometry equations express the distribution of discharge within a channel network for a defined flow event (Leopold and Maddock, 1953; Myrick and Leopold, 1963; Leopold et al., 1993). Relationships were determined for the largest marsh, Site 3. Relationships of width, depth, and velocity, to Q_{max} were determined from hydraulic measurements made at cross section locations distributed throughout the channel network. For the non-vegetated case, these measurements were made during a spring tide and obtained from Jenner (2011). Measurements for the *Hydrilla sp*. maximum were made in summer, 2011. In addition to providing information on the effects of SAV vegetation on hydraulic geometry relationships within a tidal marsh, these data also provided data on Q_{max} that were used to calculate V_w and nitrate retention within various points within the tidal marsh network.

4.2.3.3 'Regional' scaling relationships: Q_{max} at tidal inlets for conditions near maximum and minimum SAV and emergent macrophytic vegetation

Regional scaling relationships were also determined for maximum discharge during spring tides at all of the measured inlets. These inlets included those of the 3 marshes used throughout this study, and 3 additional inlets measured to provide additional constraints. Measurements of Q_{max}, cross sectional area, width, depth, and average velocity at different spring tides also provided a range of values of Q_{max} and associated hydraulic parameters. Q_{max} and associated hydraulic variables were measured during vegetation maximum (late June to mid-July) and minimum (April; September-October) for predicted spring tidal stages.

4.2.3.4 Flow resistance

During times of SAV absence, flow resistance was calculated for the largest marsh, Site 3. Flow resistance is a measure of the vegetative roughness, and was calculated using the equation:

$$\frac{\bar{u}}{u*} = \frac{\bar{u}}{\sqrt{gS(H-Z_m)}} \tag{4.3}$$

where $\bar{u}$ is the mean velocity, $u*$ is the shear velocity, g is the acceleration due to gravity, S is the water surface gradient, H is the mean depth, and Z_m is the height of the plane of momentum absorption (Thom, 1971).

Water surface gradient (S) is calculated by recording tidal stage at an upstream and downstream location (200 meters apart) over time:

$$S = \frac{H_{down} - H_{up}}{\Delta L} \quad (4.4)$$

where S is the water surface gradient (or slope), H_{down} is the height of the water surface at a downstream site, H_{up} is the height of the water surface at an upstream site, and L is the distance between the two gauges (distance the water travels).

4.2.4 Mass balance measurements of hydrologic flux and nitrate retention

Hydrologic flux over a tidal cycle was determined by measuring tidal stage, associated channel cross sectional area, and velocity at time steps during tidal cycles. Local tidal stage was measured at each inlet with a staff gauge. These local tidal stage measurements were referenced to continuously logged gauges at Jug Bay Wetlands Sanctuary (Eyes on the Bay). The cross sectional area was measured at slack tide during spring (high) tidal conditions to determine maximum channel area. Relationships between tidal stage and channel cross sectional area for each measured tidal stage were developed from these data. Velocity was measured at 10-15 intervals in the channel cross sections to determine discharge and average channel velocity (Q/A). Due to the rapid change in velocity with tidal stage, a relationship between average and maximum velocity was developed for each channel (Chen and Chiu, 2002). Thereafter, maximum velocity was measured at each time step (~30 min), and this relationship was used to convert maximum velocity to average velocity.

Discharge was calculated for each time step, and the data were integrated to determine total volume of water transported over the tidal cycle (V_w). A 5% error was propagated through all discharge and nitrate retention calculations; this was determined by considering operator error in cross sectional and velocity measurements (Sauer and Meyer, 1992), and error introduced by estimating average velocity from maximum velocity (Chen and Chiu, 2002).

Dissolved inorganic nitrogen (NH_4-N, NO_2-N, and NO_3-N) was measured at all sampling sites over the tidal cycle. Sampling was conducted over the growing season from 2008-2011. Samples taken during flooding tides indicate that concentrations of N species remain nearly constant on the rising stage (Seldomridge, 2009; Seldomridge and Prestegaard, 2012); therefore, sampling schemes were adopted that included only a portion of the flooding tide along with the entire falling tide at each channel inlet sampling. Water chemistry was sampled at the mouth of each tidal channel at 30 minute intervals in concert with measurements of gauge height and velocity (Fig. 4.2). Samples were collected, filtered through 0.45 micron paper, and analyzed following standard operating procedures for ion chromatography and spectrometry (Solorzano, 1969; Keefe, 2004). Analytical error of ± 2 μmol, determined by the mechanical specifications of the equipment, was propagated throughout all nitrate retention calculations.

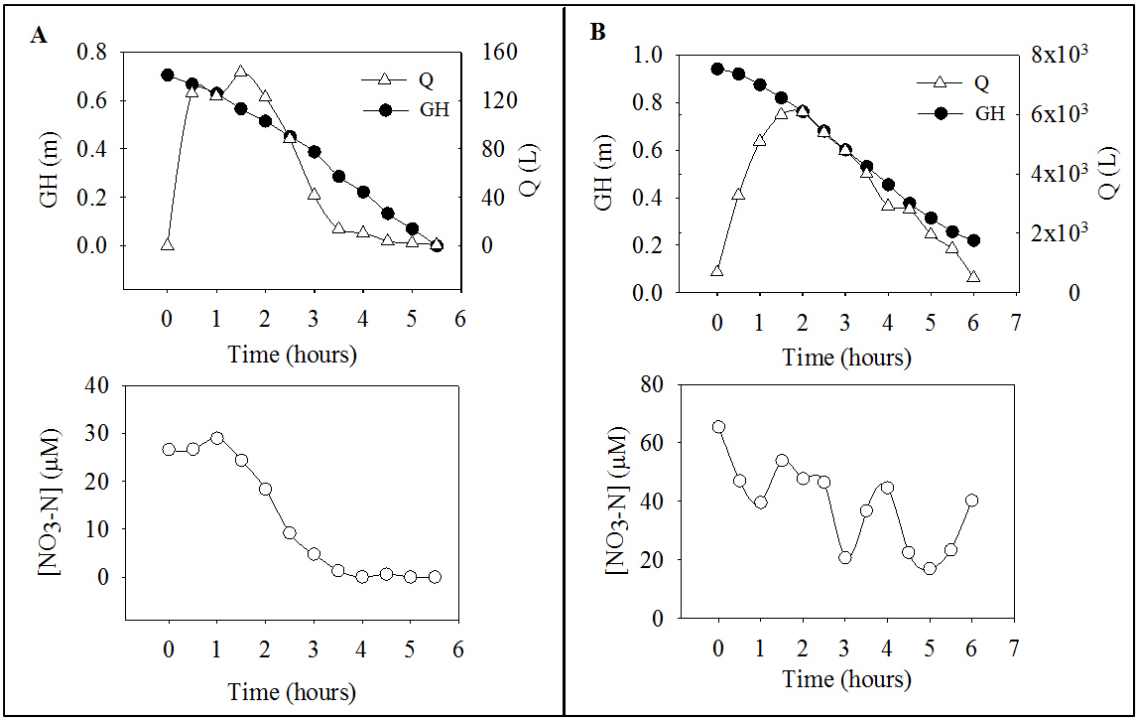

Figure 4.2. Site 3 field measurements of gauge height, discharge and nitrate water chemistry made for spring (high tidal stages) during (A) SAV absence (measurements made on 1 October 2008), and (B) SAV maximum (measurements made on 7 July 2011).

Nitrate was the only form of nitrogen that shows significant variation over the tidal cycle (Seldomridge and Prestegaard, 2012). Nitrate retention was determined by subtracting the outgoing flux of nitrate from incoming nitrate flux for each tidal marsh for each time increment:

$$NR = \Sigma[Q_t\,(N_{i(t)} - N_{o(t)})] \qquad (4.5)$$

where *NR* is nitrate retention (moles); Q_t is discharge (L s^{-1}); $N_{i(t)}$ is initial [NO_3-N] of tidally introduced water (μmol), and $N_{o(t)}$ is [NO_3-N] of outgoing tidal water at time (t) in μmol. One of the advantages of using mass balance calculations of nitrate retention is that it provides measurements of nitrate retention for individual marshes

for a given tidal cycle, time of year, and initial nitrate concentration. No assumption is made of nitrogen retention processes within each individual marsh, although previous work suggests that marsh surfaces are primary sites for nitrate retention (Seldomridge, 2009).

4.3. Results

4.3.1 At-a-station hydraulic geometry of tidal inlets

At-a-station hydraulic geometry relationships were developed for the three tidal inlets with bankfull channel widths of 4.7, 7, and 41 meters (Fig. 4.1; Appendix B). The smallest tidal inlet was at times overgrown by emergent macrophytes near the mouth (Fig. 4.1A), the intermediate-sized inlet drains completely at low tide and does not support either emergent macrophytes or SAV in the channel (Fig. 4.1B), and the largest inlet has expanses of SAV on the channel bed (Fig. 4.1C). At-a-station hydraulic geometry coefficients and exponents are shown in table 4.1. For the smallest channel, the exponent for width is significantly larger than the other channels. The at-a-station hydraulic geometry exponent for width (b) ranges from 0.661 to 0.667 for the smallest channel; this indicates that much of the increase in discharge is accommodated by the increase in channel width as the tide floods. The growth of emergent macrophytes does not significantly alter the hydraulic geometry exponents, but it does significantly decrease average flow velocities from ~ 0.1 to 0.15 ms^{-1} without emergent macrophytes to ~ 0.0015 ms^{-1} when emergent macrophytes are present (Appendix B).

The shape of the channel varies with size, which affects local at-a-station hydraulic geometry. The smallest channel has gradual channel banks that are defined by the growth of vegetation in summer. The intermediate channel also drains completely during low tides. Both of these channels have f/b ratios (r values) less than 1, indicating triangular shapes (Table 4.1). The largest channel has a less triangular shape and the hydraulic shape (f/b ratios) of the largest channel changes seasonally, from almost rectangular in early spring (possibly caused by channel erosion in winter), to triangular in September – October, as the emergent vegetation affects flow along the boundaries; however, the autumn also corresponds with times of higher discharge, which removes SAV from the center of the channel (Fig. 4.3).

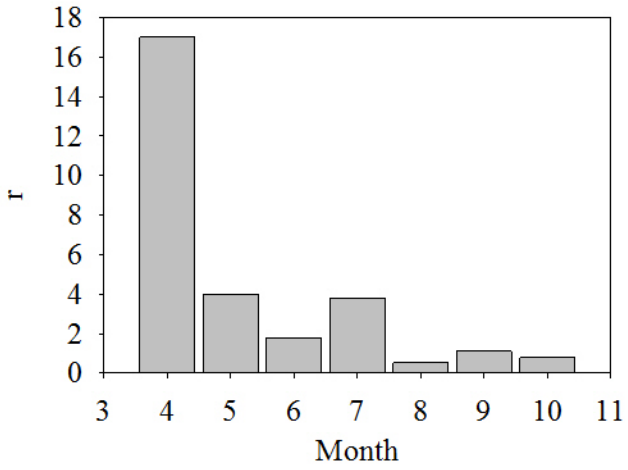

Figure 4.3. Seasonal changes in hydraulic channel shape (r = f/b; determined from exponents for at-a-station hydraulic geometry relationships) for Site 3.

Table 4.1. Seasonal at-a-station hydraulic geometry relationships

Date	b (width)	f (depth)	m (velocity)	b+f+m[a]	a (width)	c (depth)	k (velocity)	ack[a]	r[b] (shape)	Channel vegetation[c]
Site 1										
20 May 2011	0.66	0.36	-0.02	1.0	20.62	0.33	0.15	1	0.54	
18 July 2011	0.66	0.33	0	1.0	364.38	1.38	0.002	1	0.49	M
14 Sept 2011	0.88	0.15	-0.02	1.01	69.2	0.19	0.077	1	0.16	
Site 2										
20 May 2011	0.37	0.17	0.46	1.0	12.12	0.39	0.21	1.05	0.46	
18 July 2011	0.24	0.03	0.73	1.0	10.16	0.31	0.32	1	0.13	
14 Sept 2011	0.29	0.09	0.62	1.0	10.54	0.32	0.29	1	0.31	
1 Oct 2008	0.44	0.24	0.32	1.0	12.28	0.54	0.15	1	0.55	
Site 3										
3 April 2010	0.01	0.17	0.83	1.01	41.6	0.86	0.03	1.07	17	
2 May 2010	0.06	0.25	0.70	1.01	48.48	0.95	0.02	1	4.0	
21 May 2011	0.1	0.18	0.73	1.01	40.88	0.64	0.04	1	1.8	
3 June 2010	0.01	0.04	0.95	1.0	45.1	0.65	0.0005	0.01	3.8	SAV
17 July 2011	0.37	0.19	0.44	1.0	39.9	0.84	0.066	2	0.51	SAV
24 Sept 2010	0.12	0.13	0.76	1.01	44.3	0.76	0.03	1.01	1.1	SAV
1 Oct 2008	0.20	0.15	0.65	1.0	36.6	0.82	0.03	1	0.77	

a- Continuity for constraints on hydraulic geometry equations (Leopold and Maddock, 1953)
b- Channel shape (Dingman, 2007): r=(f/b)
c- Vegetative condition: M=emergent macrophyte, SAV=submerged aquatic vegetation

4.3.2 Regional hydraulic scaling relationships for inlet channels

In this analysis, the relationship between peak discharge (Q_{max}) and the associated velocity (U_{max}) for a spring tidal cycle was examined for a range of inlet channels. This analysis of the relationship of Q_{max} to A_c and U_{max} is similar to downstream hydraulic geometry. It is not exactly a downstream (or within a network) assessment; the data were obtained for Q_{max} conditions for spring tides from multiple inlet channels that were not connected to each other. The data were separated into two scenarios: 1) data collected in channels without emergent macrophytes or SAV on the channel bed (Fig. 4.4), and 2) data collected during summer months in the presence of dense emergent macrophytes or SAV on the channel bed (Fig. 4.5).

The relationship between Q_{max} and U_{max} in non-vegetated channels follows the trend:

$$U_{max} = 0.14{Q_{max}}^{0.12} \qquad (n=10, R^2=0.47) \qquad (4.6)$$

The relationship between Q_{max} and A_c in non-vegetated channels follows the trend:

$$A_c = 7.46{Q_{max}}^{0.87} \qquad (n=10, R^2=0.97) \qquad (4.7)$$

This is a regional assessment, therefore, the scaling relationships are not necessarily constrained by continuity equation that constrains hydraulic geometry exponents and coefficients for a given channel network. The exponents in these scaling relationships add to 0.99 and the coefficients multiply to 1.04, which indicates they may function as an interrelated hydraulic system. This is not surprising, because

formation and maintenance of these channels probably occurs during high tides during winter conditions when flow resistance is at a minimum and channel scour can build and maintain channels. Note, the intermediate channel was considered unvegetated, so summer data for this channel was plotted with other non-vegetated data (April-early May and September data for all channels).

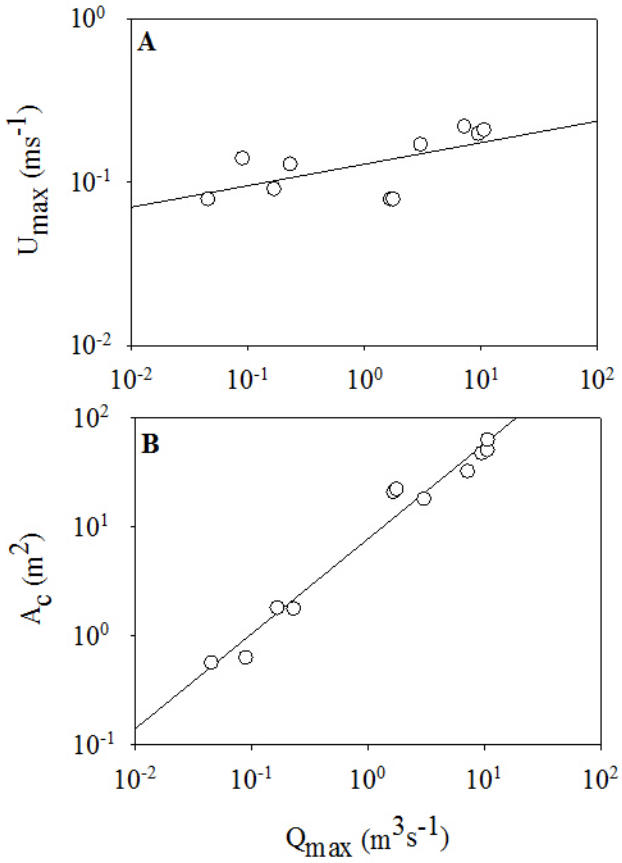

Figure 4.4. Regional scaling relationships for all inlet channels during vegetation minimum (early May and September) on a spring tidal stage indicate that velocity increases only slightly with discharge (A: $U_{max} = 0.14{Q_{max}}^{0.12}$; n=10, R^2=0.57), but discharge increases greatly with inlet cross sectional area (B: $A_c = 7.46{Q_{max}}^{0.87}$; n=11, R^2=0.97).

The relationship of Q_{max} to U_{max} for inlet channels for spring tides during mid-summer (June 30-July 30) was significantly different for channels where SAV and/or emergent macrophytes were present in significant quantities (Fig. 4.5):

$$U_{max} = 0.05 Q_{max}^{0.50} \qquad (n=10, R^2=1.0) \qquad (4.8)$$

The velocity increased significantly with an increase in Q_{max}, as demonstrated by the large exponent of 0.5 (Fig. 4.5A). Also, the small coefficient for velocity indicates the low velocities are affected by emergent macrophyte growth. For the case with emergent macrophytes and SAV, the relationship between Q_{max} and A_c follows the trend:

$$A_c = 16.57 Q_{max}^{0.49} \qquad (n=10, R^2=0.95) \qquad (4.9)$$

The exponents for velocity and area sum to 0.99, but the coefficients multiply to 0.857; this suggests that the system does not behave as a homogenous hydraulic system. This is consistent with the discontinuous presence of vegetation in the system and the variable flow velocities for channels of various sizes. It is also consistent with previous studies (e.g. French and Stoddart, 1992) that indicate formation and maintenance of channels during non-vegetated times of the year.

As mentioned above, these regional scaling relationships for vegetated cases does not include all of the channels; summer data from the intermediate channel are included on the previous diagram (Fig. 5.5A) because this size channel doesn't support SAV or emergent macrophyte growth in the channels and continues to function as a non-vegetated channel. The sizeable gap in the middle of the diagram is

caused by the lack of inlet channels in this size range with SAV (and a decrease in the associated Q with emergent macrophyte-filled first order channels).

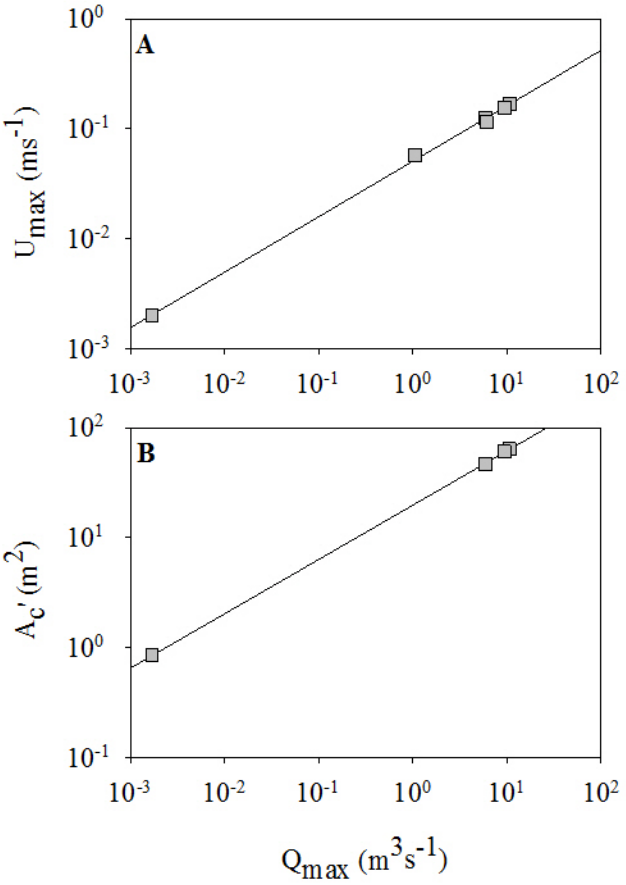

Figure 5.5. Regional scaling relationships for all inlet channels during vegetation maximum (June-July) on a spring tidal stage indicate that low velocities (A: $U_{max} = 0.052{Q_{max}}^{0.50}$; n=7, R^2=1.0) are largely affected by vegetative growth in the inlet channels (B: $A_c' = 16.6{Q_{max}}^{0.49}$; n=7, R^2=0.95). Note large gap in the data series caused by the non-vegetated inlets.

4.3.3 Regional scaling relationships: Q_{max} and V_w and A_c and Q_{max}

Data from all inlet channels (both vegetated and non-vegetated) were pooled together to examine the regional relationship between maximum discharge and water

volume (V_w; Fig. 4.6) for tidal stages the reached the elevation of the marsh platform or higher elevations, but were constrained within the channel by vegetation during the summer months:

$$V_w = 7827 Q_{max}^{1.08} \qquad (n=10, R^2=0.99) \qquad (4.10)$$

This emergent relationship includes both vegetated and non-vegetated hydraulic data; it can be used to predict water volume from maximum discharge in a tidal cycle. The regional relationships between discharge and cross sectional area can be used to estimate Q_{max}.

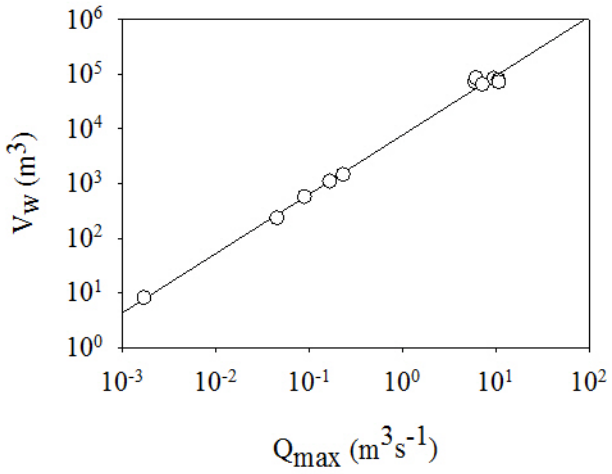

Figure 4.6. Regional scaling relationship between maximum discharge (Q_{max}) and tidal water volume for spring tides for all sites during both vegetation minimum and maximum ($V_w = 7827 Q_{max}^{1.1}$; n=11, R^2=0.99).

The scaling relationship between channel cross sectional area (A_c) and Q_{max} is shown in figure 4.7 for both vegetated (red) and unvegetated channels (black). Non-vegetated channels follow the trend:

$$Q_{max} = 0.2A_c \qquad (n=10,\ R^2=0.98) \qquad (4.11)$$

Note that some of the vegetated data points for small inlet channels fall in line with the unvegetated data. On this graph, a 14 m wide inlet channel has a maximum discharge that is smaller than the maximum discharge of the 7m wide channel. Due to the presence of SAV, a significant proportion of the A_c does not contribute to channel discharge; therefore, effective cross sectional area of the channels occupied by SAV needs to be determined. Note also that the largest cross sectional areas were measured for the large channel during vegetated conditions. Emergent macrophytes along the channel boundary constrained flows in the channel. This generated significantly higher channel flow depth at tidal stages that would cause widespread overbank flooding if the emergent macrophytes were not present.

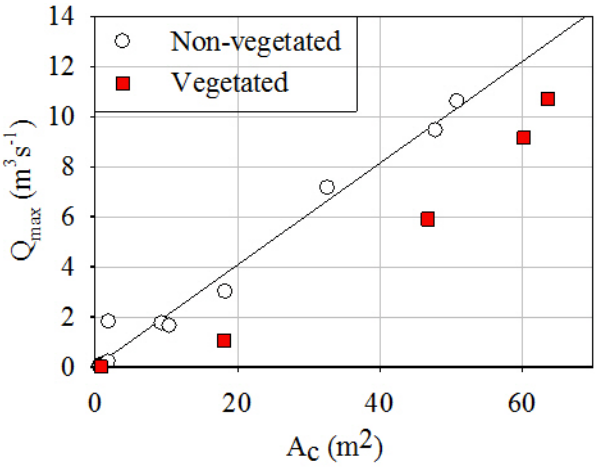

Figure 4.7. Regional scaling relationship between cross sectional area and maximum discharge during vegetated (June-July data) and unvegetated (May and September data) conditions ($Q_{max} = 0.2A_c$; n=8, R^2=0.99). During vegetated conditions, Q_{max} is greatly reduced.

4.3.4 Determination of inlet geomorphic characteristics for ungauged channels

Bankfull cross sectional area was measured for tidal channels during non-vegetated conditions. A relationship between bankfull inlet area and bankfull inlet width was developed (Fig 4.8A):

$$A_c = 0.20W^{1.4} \qquad (n=18, R^2=0.89) \tag{4.12}$$

where A_c is the channel cross sectional area (m^2) and W is the channel width (m). This relationship was used to develop another relationship for average depth. The average channel depth was calculated from channel area and width data (A_c/W; Fig. 4.8B):

$$D_A = 0.20W^{0.4} \tag{4.13}$$

The measured inlet channels have triangular channel shapes for which the maximum depth can be estimated and expressed as a function of channel width by use of the above expression. The resulting expression for maximum depth (D_{Max}) for inlet channels is:

$$D_{MAX} = 0.40W^{0.4} \tag{4.14}$$

These three relationships were used to estimate inlet channel area, inlet channel depth, and inlet channel maximum depth for all unmeasured channels.

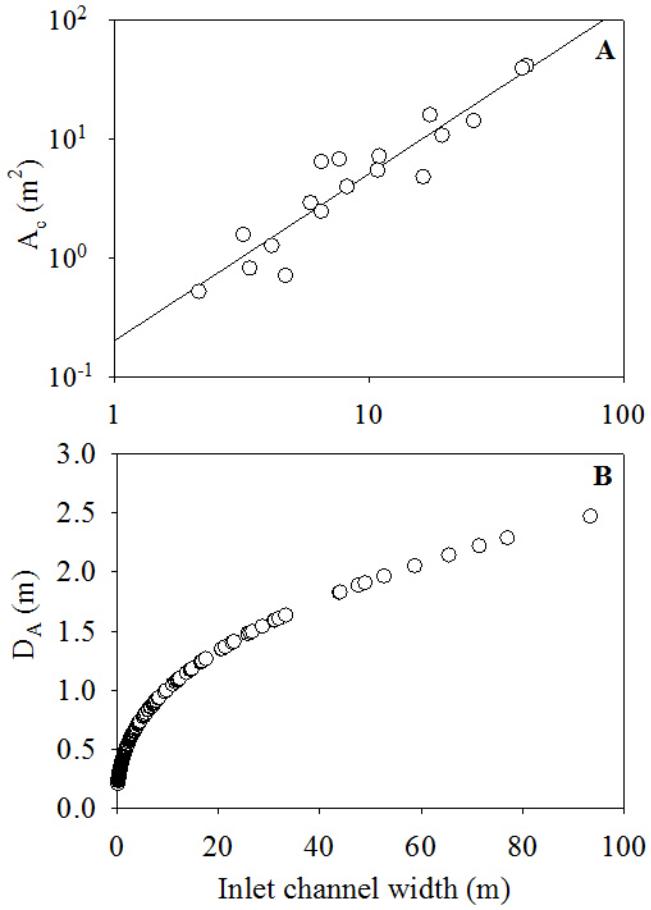

Figure 4.8. Geomorphic characteristics of tidal channels of the tidal freshwater portion of the Patuxent River: (A) inlet cross sectional area, and (B) average inlet depths. Cross sectional area increases systematically with inlet width during SAV minima, but during maxima, the effective inlet area is greatly reduced in the bigger channels that don't completely drain on the ebbing tide.

4.3.5 Identification of channels that support SAV

Field observations indicate that relative spring tidal ranges for the measured tidal inlets are 0.41(limited by channel depth) to 0.94 meters (for the larger channels); however, the tidal range of the contributing mainstem can reach as high as 2.0 to 2.5 meters (Fig. 4.9). When adjusted to the elevation of the marsh platform, tidal stages range from 0.41 to 2.01 meters.

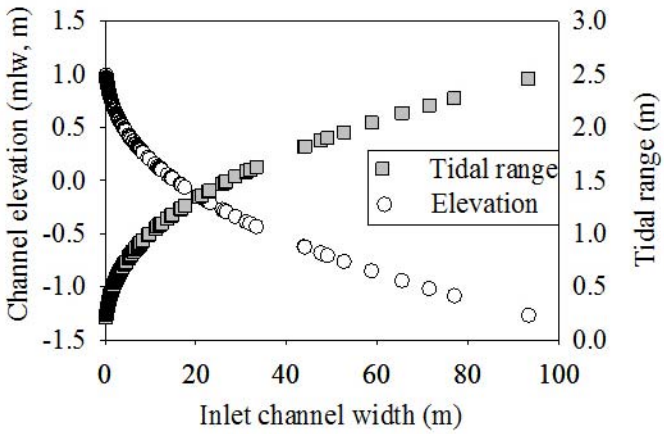

Figure 4.9. *Hydrilla verticillata*, a SAV species, can only occupy channels that do not fully drain during low tides. The smallest channel size that *H. verticillata* invades ranges between 16-20 meters in width.

Using this information on tidal range and inlet channel geomorphic characteristics (depth, bed elevation), the drainage of each channel can be predicted. The channels that drain completely are less than 16-20 meters in width (Fig. 4.9). These channels have steep bed profiles near the inlet channel. The higher bed elevation of the inlet channel restricts the tidal period to a portion of the total incoming tide and restricts the "bankfull" high tide tidal range to the depth of the inlet channel.

The larger channels (27% of the total by number) experience seasonal growth of SAV in these channels, which reduces the effective cross sectional area (Fig. 4.7) and inlet flow velocities (Fig. 4.5A). Although only 27% of the inlet channels are affected by SAV growth, these inlet channels connect to marshes that represent approximately 95% of total marsh area (Chapter 3; Seldomridge and Prestegaard, 2012).

4.3.6 Geomorphic characteristics and regional hydraulic relationships during vegetated conditions

During summer months, the growth of SAV occupies a portion of the inlet channels that do not fully drain during low tides. SAV growth was observed up to the depth of mean low water in these channels, with the densest growth along the shallow sides of the channels. The height of the canopy was estimated to be near Z_m (the depth of the approximate zero vegetative boundary layer velocity), which was determined from field measurements (Fig. 4.10). In conjunction with the non-vegetated regional hydraulic relationships (Fig. 4.7), the effective cross sectional area (A_c') for each channel was determined.

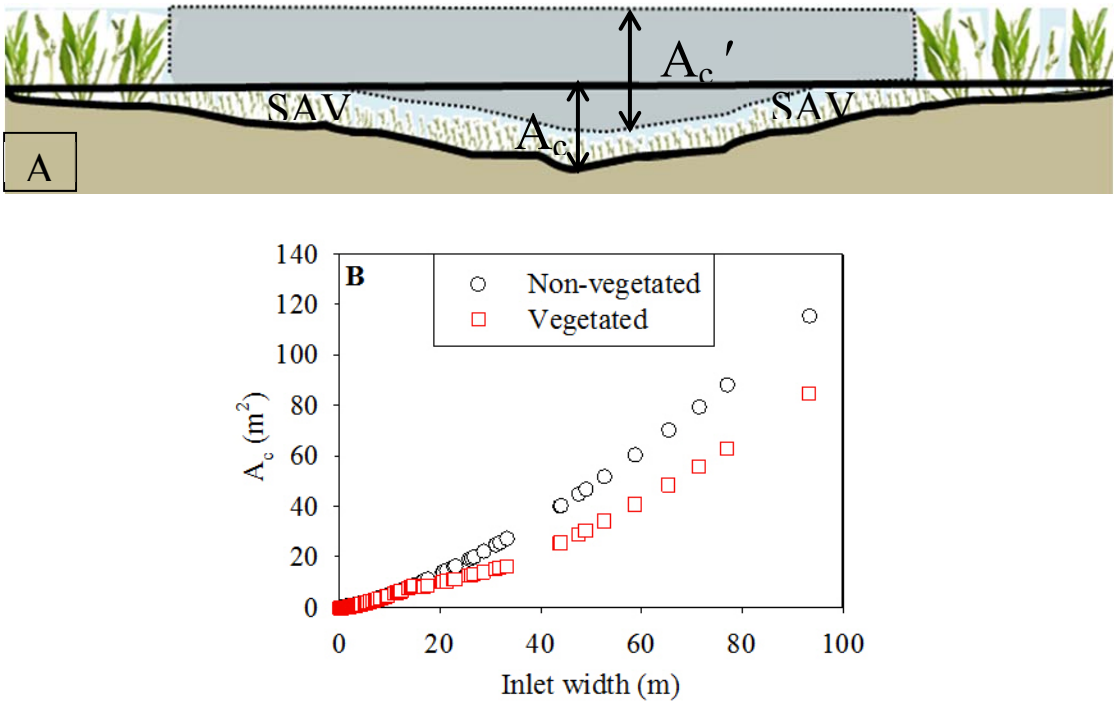

Figure 4.10. (A) Inlet channel cross sectional area during non-vegetated conditions (A_c), and vegetated conditions (A_c'). During vegetated conditions, water flow is forced over top of the dense SAV canopies, but restricted on along the channels by emergent macrophytes; this causes a higher tidal stages. (B) Inlet cross sectional area during non-vegetated (black), and vegetated (red) conditons.

4.3.7 Nitrate retention during vegetated conditions

Nitrate retention was previously demonstrated to be closely coupled with hydrologic flux during seasons when SAV was not present or abundant on inlet channel beds (Seldomridge and Prestegaard, 2011; Seldomridge and Prestegaard, 2012). Therefore, mass balance measurements of nitrate retention for the period when SAV was present were used to compare the influence of season and varying tidal ranges (Fig. 4.11). The relationship between hydrologic flux and NR within

each marsh system is not significantly affected by the presence of SAV and the peak summer tidal stage. The summer NR relationship follows the trend:

$$NR = 0.0063V_w^{1.09} \qquad (R^2 = 0.98, n = 4) \tag{4.15}$$

Similarly, combining all data, regardless of season or tidal stage, produces the following relationship:

$$NR = 0.0045V_w^{1.1} \qquad (R^2 = 0.98, n = 13) \tag{4.16}$$

These data indicate that the relationship between tidal water volume and nitrate retention does not change seasonally. This suggests that the NR would not be affected by the presence of SAV; however, the hydraulic data must also be considered. When the downstream hydraulic geometry relationships and flow resistance are considered, the effective marsh surface area decreases as a result of the altered distribution of the tidal volume (Table 4.2).

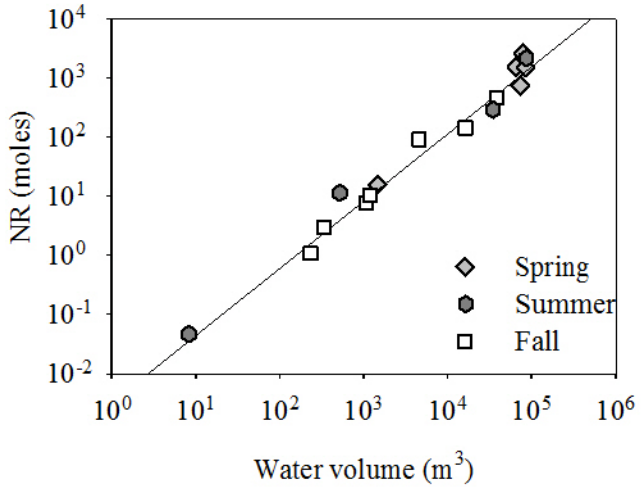

Figure 4.11. Nitrate retention values as a function of total water volume over a spring (high) tidal stage over the growing season of numerous years for all sites. Spring data follow the regression: $NR=0.38V_w^{0.72}$ ($R^2=0.91$, n=5); Summer data follow the regression: $NR=0.0063V_w^{1.1}$ ($R^2=0.98$, n=4); Fall data follow the regression: $NR=0.0064V_w^{1.05}$($R^2=0.99$, n=7); in combination the trend follows: $NR=0.0045V_w^{1.1}$($R^2=0.98$, n=16).

4.3.8 Ecosystem nitrate retention during vegetation maximum

The regional relationships between Q_{max} and A_c (Fig. 4.5), and Q_{max} and V_w (Fig. 4.6) can be combined to generate a relationship between A_c' and V_w. For spring (high) tides, the relationship between V_w and A_c' is a simple power function that includes data from vegetated and non-vegetated conditions:

$$V_w = 160A_c^{1.08} \tag{4.17}$$

As determined previously, NR is a function of hydrologic flux; therefore, the reduction in hydrologic flux during vegetation presence was examined through the regional hydraulic scaling equations reported above.

Ecosystem nitrate retention values were estimated using predicted V_w during both vegetation conditions and Eq. 4.10 (Fig. 4.12). During non-vegetated conditions, ecosystem NR is estimated to be 6512 moles NO_3-N for a "bankfull" spring tide. During SAV and marsh platform emergent macrophyte maxima, ecosystem NR is significantly reduced to 4490 moles NO_3-N; a 31% reduction. Moreover, during non-vegetated conditions, over 70% of NR occurs in the larger marshes (inlet channels > 50 meters wide), whereas during vegetated conditions, these same marshes are responsible for only 40% of total nitrate retention.

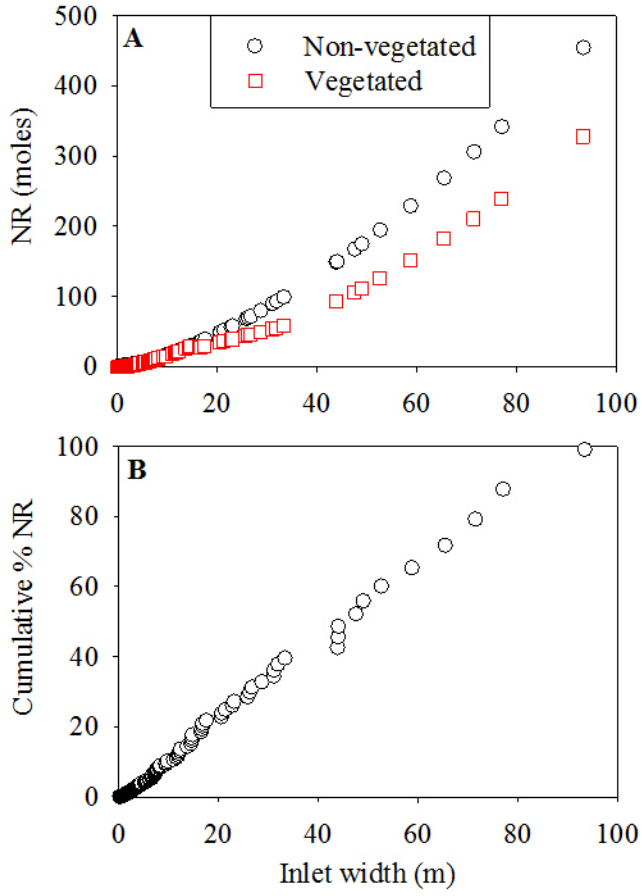

Figure 4.12. (A) Estimated nitrate retention for all marshes in the TFW Patuxent River on a spring tidal cycle and during vegetated and non-vegetated conditions. (B) Cumulative probability distribution of nitrate retention during vegetated conditions; the largest 6 marshes account for 40% of total NR.

4.3.9 Effect of vegetative flow resistance on nitrate retention within individual marshes

Vegetative flow resistance affects not only the effective marsh inlet area (A_c'), but also the velocity and discharge within tidal channel networks, which controls the propagation of water volumes into marsh interiors. Both the regional and downstream relationships suggest that when vegetation is present, channel velocity is significantly affected. This effect on flow velocity has the greatest impact on the velocity of small channels that have SAV or emergent macrophytes. Analysis of the inlet channels indicates that many of the small channels drain completely during low tides, and therefore do not support SAV on the channel bed. "Downstream" changes in flow resistance and velocity within the large channel networks affects travel times within the large channels, which appears to influence drainage on outgoing tides. Therefore, SAV vegetation grows throughout the tidal network channels of large marshes and occupies much of the channel bed in small, up-marsh channels (Fig. 4.14.B). This growth of vegetation on the channel bed throughout the channel network of large marshes significantly affects the "downstream" hydraulic geometry of these marshes (Table 4.2).

The "downstream" hydraulic geometry relationships, which describe the up-marsh changes in hydraulics for the large marsh channel network, indicate that velocity decreases significantly as water flows into the marsh network during vegetated conditions (Fig. 4.13):

$$w = 20.8Q^{0.54} \quad d = 1.05Q^{0.085} \quad u = 0.05Q^{0.36} \tag{4.18}$$

This up-marsh reduction in U_{max} would significantly increase travel times and thus reduce travel distances during a tidal cycle. As a consequence, there are highly differing NR potentials between vegetated and non-vegetated conditions (Fig. 4.14B).

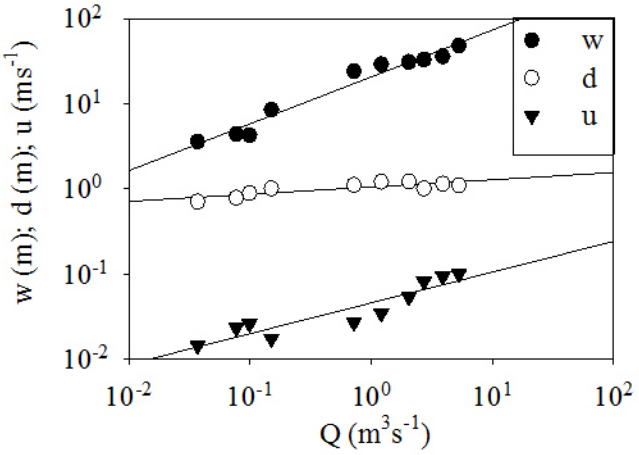

Figure 4.13. "Downstream" hydraulic geometry for the large tidal marsh network ($w = 20.8Q^{0.54}$; $d = 1.05Q^{0.085}$; $u = 0.05Q^{0.36}$). Data collected 16 June 2011.

Table 4.2. Comparison of regional scaling relationships with downstream hydraulic geometry for a marsh network (Site 3)

Relationship	***Condition***	***Width***	***Depth***	***Velocity***	***Area***
Regional	Non-vegetated			$U_{max} = 0.14Q_{max}^{0.12}$	$A=7.46Q_{max}^{0.872}$
	Vegetated			$U_{max}=.0517Q_{max}^{0.50}$	$A=16.57Q_{max}^{0.485}$
Downstream[a]	Vegetated	$w = 17.9Q^{0.70}$	$d = 0.915Q^{0.07}$	$u = 0.061Q^{0.23}$	$A = 16.29Q^{0.77}$
	Non-vegetated	$w = 6.17Q^{0.83}$	$d = 0.802Q^{0.10}$	$u = 0.202Q^{0.07}$	$A = 4.95Q^{0.93}$

a- Downstream hydraulic geometry relationships from Jenner (2010)

During vegetated conditions, the channel cross sectional area is greatly reduced in the small tidal channels in up-marsh distributary network (Fig. 4.14A). These effects on flow velocity, and channel area, greatly reduce Q_{max} and total volume flux in these up-marsh channels. The effect of these changes on nitrate retention in these up-marsh regions was estimated by using the measured values of Q_{max} at various locations within the large marsh system, the hydraulic relationship scaling relationship between V_w to Q_{max} (Eq. 4.10), and the retention relationship between NR and V_w (Eq. 4.16). These data indicate a rapid decrease in the volume conveyed up the tidal channel (Fig. 4.14B) over the dense canopies of *Hydrilla sp*. (Fig. 4.14B). This large decrease in tidal volumes would correspond with a large decrease in nitrate retention as a function of distance into the marsh (Fig. 4.14B). These data suggest that the upper half of this marsh retains only 10% of the nitrate as the lower half of the marsh due to these problems with water conveyance in the system.

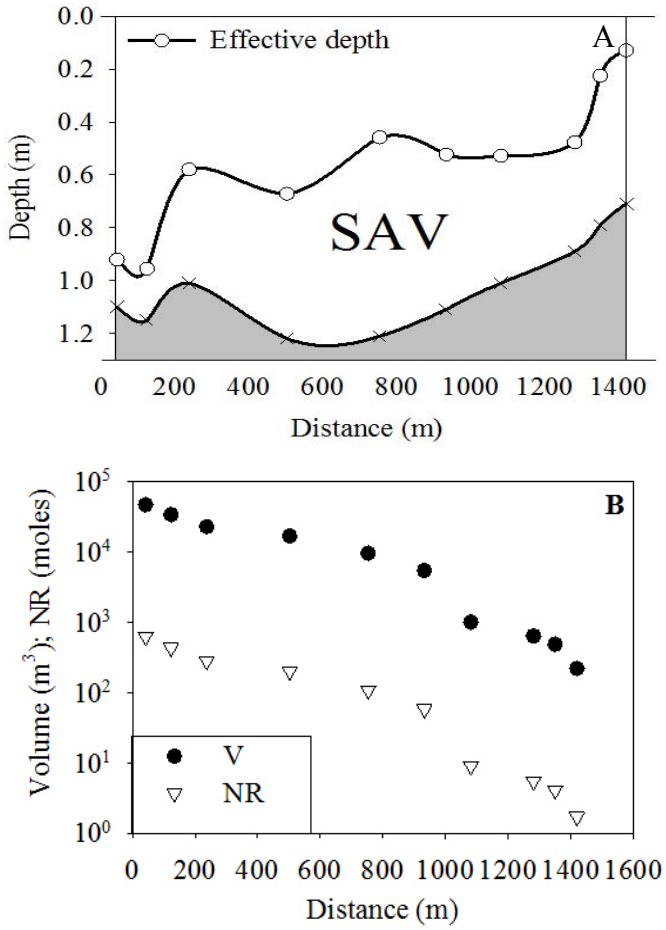

Figure 4.14. (A) The height of SAV as a function of distance upstream from the tidal inlet. (B) Up-marsh decrease in tidal volumes and associated nitrate retention during a high spring tide.

4.4 Discussion

4.4.1 Impact of SAV on effective channel geometry

The geomorphic characteristics of tidal inlets, primarily channel width and inlet elevation, influence the movement of tidal flows into inlet channels. Channels with depths greater than the tidal range do not fully drain on low tides and can support SAV species, which is currently dominated by *Hydrilla sp*. Although these channels represent only 27% of the population by number, they convey a

disproportionate share of the total water flux and thus perform much of the ecosystem nitrate retention when SAV is not present. Although SAV is often limited by light penetration, this does not appear to limit growth in the tidal marsh channels, the deepest channels of which are less than 2.5 meters deep (Van et al., 1976; Chambers and Kalff, 1984; Dennison et al., 1993). The influence of SAV on channel geometry is highly variable depending on the position within the network. Once an inlet channel is invaded, the entire interior system is consequently at risk for invasion. In particular, invasion of *H. verticillata* tends to propagate from the inlet channel node into the channel interiors through a variety of mechanisms, most common of which is vegetative propagules and tubers (Langeland and Sutton, 1980; Madsen and Smith, 1999). The propagules are tidally transported to the marsh interior, and establish new colonies. *H. verticillata* can establish new colonies with only a few whorls (3 or less; Langeland and Sutton, 1980). Once introduced into a channel network, *H. verticillata* propagates into the marsh interior (Fig. 4.14A) and establishes dense canopies that successfully trap water, sediment, and solutes.

4.4.2 Impact of SAV on channel hydrodynamics

The increased vegetative roughness not only alters the inlet cross section, but also the downstream channel hydrodynamics, and distribution of discharge. Channel hydrodynamics remain the most difficult to characterize because hydraulics vary between channels of the same size. In this study, regional hydraulic relationships were constructed to predict hydrodynamics among individual marshes (Figs. 4.4-4.7). The regional curves suggest that when SAV is not present, velocity is not sensitive to channel size. For channels with SAV on the channel bed, velocity is reduced and this

affect is most prominent in small channels. The reduction of velocity by SAV is not a homogeneous response in this ecosystem. Small inlet channels do not support either SAV or emergent channel macrophytes, and thus retain their area and velocity relationships that were observed for non-vegetated conditions; whereas small channels up-marsh of an inlet behave much differently and support dense SAV canopies.

During incoming or outgoing tides, SAV canopies flatten in the direction of flow (Kouwan, 1980), which results in velocities within the vegetative boundary layer that are very low. These conditions allow for the development of a logarithmic velocity profile that forms above the vegetation (Ghisalberti and Nepf, 2002; Nepf and Ghisalberti, 2008). Therefore, *Hydrilla sp.* effectively reduces the inlet channel cross sectional area, whereas emergent macrophyte growth within or along the channel results in a significant increase in flow resistance that reduces velocities. Marsh vegetation, therefore, greatly alters tidal flow and total volume flux into tidal channels.

This study was constrained to consider only spring (high) tidal stages; however, the relative tidal stage is largely influenced by vegetation. The effective inlet channel cross sectional area is significantly reduced during SAV presence (Fig. 4.10). During maxima vegetation growth, however, the tidal water is confined within the channel by emergent marsh surface macrophytes and is forced over the top of the canopy, which creates a higher tidal stage. This altered tidal stage and tidal volume flux consequently has implications on the sites of processing for nitrate retention. During SAV presence, the downstream hydraulic geometry relationships that describe

the flow into the marsh suggests that the velocity is decreased by a factor of four from the inlet channel to the marsh interior (Table 4.2; Jenner, 2010). SAV affects not only the velocity, but also the cross sectional area, which is also constricted up-marsh. Therefore, during SAV presence, both the distance a parcel of water can travel during a tidal cycle and the corresponding volume flux is reduced. This may cause very different biological processes in the upper and lower portions of large marshes during summer months.

4.4.3 Impact of SAV on nitrate retention

Although the physiology of *H. verticillata* is adapted to absorb nutrients from the water column (Langeland, 1996; Kennedy et al., 2009), the effect of SAV on volume reduction in the inlet channel alone caused a reduction in overall NR by approximately 30%. The development of dense *Hydrilla sp.* beds might serve to reduce exchanges of water and nutrients across the vegetative boundary layer. The significant up-marsh reductions in flow volumes may cause the marsh to bifurcate into two discrete systems: the continually flushed lower marsh, and the recycled marsh interior. In this bifurcated state, the lower marsh continues to function at a high capacity (performing nitrate retention, sediment trapping, and plankton trapping) because it is continually flushed with water, allochthonous organic carbon, and nutrients. The upper marsh, however, may become stagnant with high rates of recycling. If nutrients accumulate over time, marsh decomposition may be increased (Turner et al., 2009), which might lead to higher rates of marsh erosion when the high flows of winter and spring bring discharges over the marsh platforms.

Lastly, there is also a shift in the importance of the channel bed during vegetated conditions. During non-vegetated conditions and during the initial growth of SAV channel beds, the associated hypoheric zones are important sites for N processing through uptake and denitrification. During vegetated conditions, the vegetated boundary layer minimizes the importance of the channel bed (e.g. Nepf and Ghisalberti, 2008) and forces the processing to occur mainly on the marsh surface, in shallow groundwater, and along channel boundaries through denitrification and by plant uptake. The impact of SAV and emergent macrophytes significantly reduces NR during what might otherwise be considered optimal conditions for N processing.

4.4.4 Alternative stable states of tidal freshwater wetlands?

Freshwater tidal wetlands that border major river-estuarine systems have experienced significant changes since European settlement. Wide-spread agricultural land use, as well as storms (e.g. Tropical Storm Agnes in 1972) greatly increased sediment loads to the Bay (Orth and Moore, 1984). This increase in sediment flux, combined with a decreased SAV and sea-level rise have expanded freshwater tidal marshes. More recently, decreases in riverine sediment and nutrient loads (USGS RIM data) have allowed SAV to recover in much of the Chesapeake Bay and some of the major tributaries, including the Patuxent and Potomac River estuaries (Rybicki and Landwehr, 2007). The return of SAV beds, composed of both native and non-native species, can result in significant shifts in ecological functions with a resulting alternative stable state (Scheffer et al., 1993). Although non-native SAV species often out-compete native species (Madsen et al., 1991; Knapton and Petrie, 1999), during SAV recovery periods, it is not known whether these non-native species will remain

dominant species in this system. It is also not known whether their effects on flow resistance, water volumes, and thus important ecosystem processes such as nitrate retention are significantly different from native species. It is not clear whether the invasive SAV species such as *Hydrilla sp.* are disruptive to the functioning of the ecosystems. At the local scale, SAV slows the water velocity, which increases the rate of sedimentation and water clarity (Rybicki et al., 1997; Van Ness et al., 2002). The sediment is trapped in the SAV canopies, rather than transported and deposited on the interior marsh surfaces. This is observed in the Patuxent marshes, where the clarity of the outgoing water is quite evident during tidal cycles as is the heavy sediment cover on the *Hydrilla sp.*

These changes in the freshwater tidal marshes of the Patuxent suggest that this system has supported two alternative stable states (Duarte, 1995; Duarte et al., 2008): a) a nutrient-rich and sediment-dominated state where primary productivity is maintained on marsh surfaces and in the water column, and a SAV-dominated state facilitated by the decline of sediment and nutrients, which has prompted the regrowth of SAV. This resurgence of SAV (both native and exotic species) may have significant effects on marsh maintenance, particularly with the shifting climate. Sea level is rapidly rising in the Chesapeake Bay (IPCC, 2007, Najjar et al., 2010), which consequently requires marshes to accrete more quickly (Craft et al., 2009). Marsh accretion is accomplished by both mineral and organic matter accretion (Pasternack and Brush, 1998; Neubauer, 2008). Generally, marshes with large tidal ranges will accrete quickly enough to match sea level rise (e.g. Kirwan and Guntenspergen, 2010); however, with the presence of dense canopies of *Hydrilla sp.*, the sediment is

not reaching interior surfaces of large marshes during summer months. This may not be important if the dominant sediment transporting and depositing events occur during spring after vegetation die-back has occurred. With climate change, the growing season is becoming longer, which may allow for *Hydrilla sp.* to maintain canopies for a larger portion of the season. Under the current climate region, deposition of sediment during spring storms is responsible for a large portion of sediment loading into these tidal marshes (Pasternack and Brush, 1998; Neubauer et al., 2002), more research is necessary to determine if these pulsed events are enough to sustain marsh accretion in the face of sea level rise and seasonal *Hydrilla sp.* invasion.

4.5 Conclusion

This study was conducted during what appears to be the beginning of a climatic regime shift towards prolonged warm periods during the winter months. Since tidal freshwater wetlands are highly complex, a nonlinear response to warming temperatures is anticipated, which may decouple the hydraulic relationships among individual marshes. Future research is therefore necessary to determine if this shift may alter the timing of the growing season, which in turn may change the ecosystem functioning (services) of the vegetation. In addition, the SAV in this study were composed mainly of non-native species. More research is necessary to determine the influence of this exotic species on a suite of other ecosystem services.

Chapter 5: Synthesis
External and internal controls on nitrate retention in tidal freshwater wetlands, and identification of emergent scaling laws for ecosystem nitrate retention

5.1 Introduction

Nitrate retention is defined as the difference between nitrate inputs and outputs in an ecosystem. It is difficult to predict for many environments, including tidal freshwater wetlands, due to the complex interactions between flow processes and the multiple N retention processes, which include denitrification, uptake by aquatic plants, and sedimentation or burial. This study was conducted in the upper Patuxent River Estuary, and it was designed to determine geomorphic, hydrologic, and biological influences on nitrate retention through mass balance measurements of nitrate and water fluxes in individual marsh inlet channels. Nitrate retention (NR) was measured over a 4-year period in three tidal freshwater wetlands (TFW), selected to represent a range of marsh sizes. The goal of the study was to evaluate both external and internal controls on NR and to determine whether scaling procedures could be identified to estimate nitrate retention for an entire ecosystem.

In this study, external controls on NR are defined as independent variables that can influence the retention processes that are external to the individual marshes. The N retention processes are primarily uptake by aquatic plants and denitrification. Previous work suggests that plant uptake rates are controlled by Michaelis-Menten enzyme kinetics (e.g. Michaelis and Menten, 1913; Claassen and Barber, 1974) and are thus influenced by nitrate concentration, temperature, and the plant species or

plant communities that can extract nitrate from the water column for growth (phytoplankton, SAV species like *Hydrilla sp.,* some emergent macrophytes). Denitrification, which is the reduction of nitrate to N_2 or N_2O gas, requires a substrate to be oxidized, usually labile organic carbon, and low oxygen concentrations. Therefore, the external controls examined in this system included temperature, dissolved oxygen concentrations, and incoming nitrate concentrations. Internal controls on TFW NR are the interactions among geomorphic, hydrologic, and biological systems *within individual marshes* that influence NR. Internal controls can be significantly different for each marsh due to changes in marsh size; systematic variations in internal controls may generate scaling relationships for geomorphic, hydrologic, and possibly biological variables.

Although it is not known whether external or internal influences exert the dominant controls on NR in a given system, previous studies have primarily investigated the effects of external controls such as temperature (Holtan-Hartwig et al., 2002; Schaefer and Abler, 2007), incoming nitrate concentrations (Jensen et al., 1990; Jansson et al. 1994; Windolf et al., 1996), nitrogen retention pathways (Burgin and Hamilton, 2007), and salinity (Nowicki, 1994). The results of these studies have provided excellent data on the controls of nitrate concentration on plant uptake rates, which defines the Michaelis-Menten relationship (Michaelis and Menten, 1913; Claassen and Barber, 1974); however, these relationships are reported for specific species found in TFW (Morris, 1980; Tischner, 2000). Other studies have defined rates of denitrification (and other processes) as a function of temperature, nitrate concentrations and marsh substrate (Seitzinger, 1988; Seitzinger et al., 2006;

Wallenstein et al., 2006); and have identified variations in dominant microbial processes due to water chemistry, forms of N, and other constraints. These results are difficult to extrapolate to the ecosystem level because interactions among these processes are not known, and internal limitations of the systems are not understood.

Although nitrate retention is a result of biological processes that are kinetically controlled, the delivery of nitrate to places where these processes take place within the marshes is hydraulically controlled. Marsh inlet geomorphology may therefore govern nitrate delivery into the marshes. Thus, the approach of this project was to measure the spatial geomorphic organization of the tidal freshwater wetland ecosystem, and to examine the relationships of hydrologic flux to geomorphologic characteristics and biogeochemical processing of nitrate. As shown in figure 5.1, the tidal freshwater ecosystem can be composed of hundreds of individual marshes that are connected to the estuary through tidal inlets. Due to their position within the landscape (near the head of tide), TFW receive water, discharge, (Q), nutrients (N and P), and sediment loads directly from contributing watersheds. A portion of potentially nutrient-rich water is distributed into freshwater tidal marshes before entering the saline lower estuary where sulfate reduction dominates. Therefore, tidal freshwater marshes are ideal sites for denitrification, which represents a reduction of downstream nutrient loading. Plant uptake may contribute to net nitrate retention. As a result, the sum of processes that occur in individual wetlands can be used to estimate ecosystem retention.

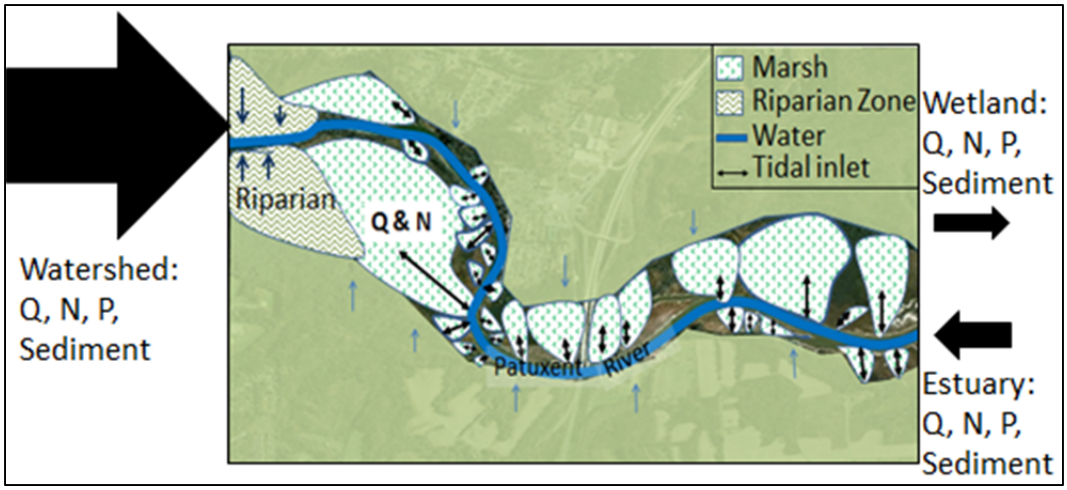

Figure 5.1. Conceptual diagram of tidal freshwater marsh ecosystem of the Patuxent River. Watershed processes deliver water, nutrients (N and P), and sediment to the head of tides. Additional inputs of groundwater (blue arrows) and stream flow occur along the length of the ecosystem; these contributions are small compared to the watershed inputs delivered to each marsh by tidal fluxes. N, P, and sediment retention and biogeochemical processing occurs within the marsh ecosystem.

5.2 External controls (temperature, D.O., nitrate concentrations, microbial pathway) on nitrate retention

Previous studies of NR by denitrification or plant uptake have primarily been conducted in laboratory or plot settings where variables can be controlled (e.g. temperature, aquatic community) where the effects of other variables (e.g. nitrate concentration) can be evaluated. Recent research indicates that results of these studies vary significantly when communities, rather than single species are used and they may be sensitive to the inclusion of relatively rare species in the population (Hooper and Vitousek, 1998; Bedford et al., 1999; Bastviken et al., 2005). In this study, the effects of temperature and nitrogen concentrations on NR were evaluated by conducting mass balance studies at various seasons throughout the year during systematic variations in water temperature (Fig 5.2A) and less systematic variations in nitrate concentration (Fig. 5.2B). Although investigation of microbial nitrogen loss

pathways was not a major part of this investigation, these data indicate that nitrate is the only inorganic N species that showed significant change of the tidal cycle. Furthermore, evaluation of the USGS Patuxent RIM data indicates that most of the incoming N is in the form of nitrate. Measurements of nitrate concentrations at the field site (located at the head of the TFW ecosystem) are similar to the USGS concentrations, which suggest little transformation of nitrate to organic N has occurred within this portion of the upper Patuxent Estuary. Experiments on core samples of marsh materials were conducted to determine nitrate loss rates (Seldomridge, 2009). These experiments indicated conversion of nitrate to N_2 gas, which is consistent with denitrification, and rates of this reaction were consistent with previous studies of denitrification rates (e.g. Greene, 2005). Therefore, the primary microbial pathway of nitrate loss at the study site was assumed to be denitrification.

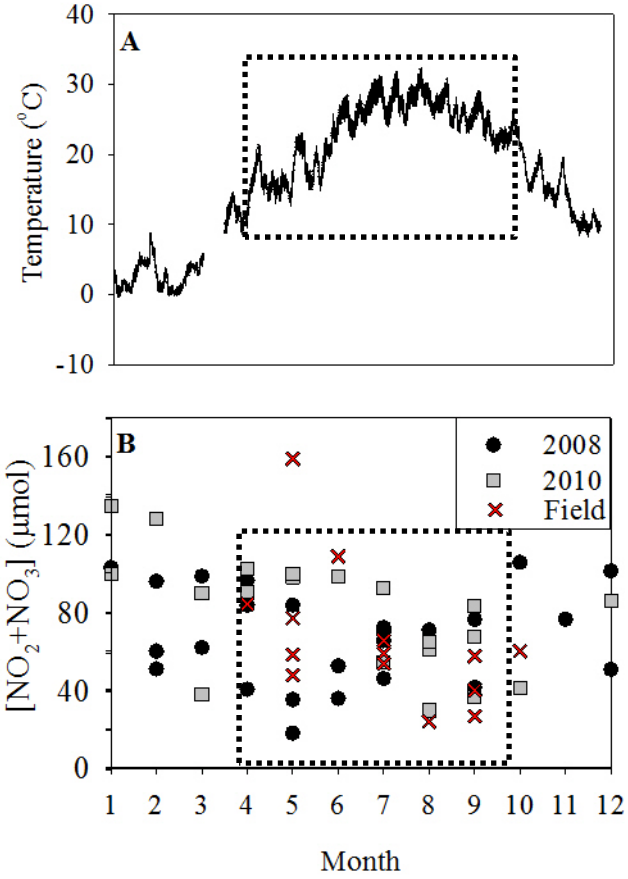

Figure 5.2. Seasonal variations in the Upper Patuxent River in (A) temperature in 2010, and (B) nitrate concentrations from upstream and field measurements (marked X). Sampling campaigns for nitrate retention were conducted between April and October; however, annual data allow for estimates of retention during other times of year. Data sources: temperature from Eyes on the Bay Jug Bay permanent monitoring station (A); 2008 and 2010 nitrate concentrations from Chesapeake Bay River Input Monitoring Program Patuxent River station (B).

The variation in temperature at the study site is shown in figure 5.2A. Although water temperature in this freshwater portion of the tidal estuary varies from 0 to 32℃, the increase in temperature occurs rapidly in the spring and declines in the fall. Evaluation of the potential effect of temperature on microbial processes through the Arrhenius equation suggests that microbial reaction rates are sensitive to temperatures in the range of 0-10℃, but there is little sensitivity of reaction rates to

temperatures between 10 and 32℃. Studies of plant uptake also suggest little effect of temperature above a threshold value (Eppley et al., 1969). Therefore, temperature appears to function primarily as a threshold effect in this wetland ecosystem.

Evaluation of incoming nitrate concentration data at the USGS RIM station and at the study site indicates that most values were between 18 and 158 μmol (average is 62 μmol, and standard deviation is 33 μmol). The results of the mass balance measurements indicate that NR is poorly correlated to nitrate concentrations (Fig. 5.3), although there is some suggestion of little additional NR at nitrate concentrations > 60-80 μmol (Fig. 5.3). Comparison with previous research (e.g. Seitzinger 1988; Seitzinger, 1994) suggests that these values of nitrate concentration are higher than required to provide nitrate for microbial processing. Comparison with Michaelis-Menten (1913) experiments of uptake by phytoplankton and *Hydrilla sp.* suggests that these values are also lower than required for maximum processing rates. Thus, these concentrations are above a minimum threshold for processing, and some values indicate nitrogen saturation. Further work is needed to elucidate the controls on microbial and plant population diversity, and interactions between populations and nitrate uptake.

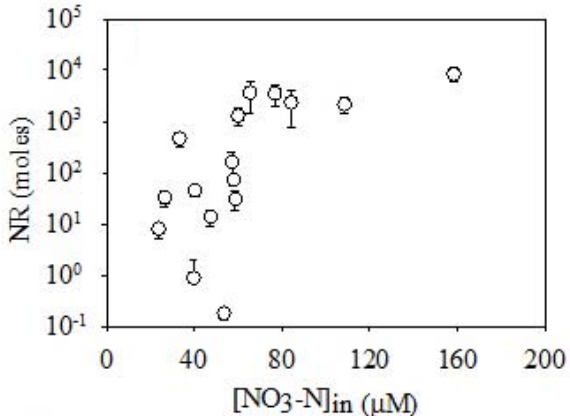

Figure 5.3. A comparison of incoming $[NO_3\text{-}N]$ and NR suggest there is no correlation between the magnitude of incoming nitrate concentrations and NR ($NR=3.9\ [NO_3\text{-}N]_{in}^{4.1}$, n=16, $R^2=0.39$, $p<0.01$). There is some suggestion of maximum processing at concentrations > 70 μmol. Data points without error bars have error values less than size of symbol.

At any time in the annual cycle, however, nitrate retention mechanisms (uptake, denitrification, or burial) may occur simultaneously or one process may dominate. Due to seasonal temperature increases and the associated growth of plants, uptake of nitrate by emergent macrophytes and *Hydrilla sp.* should vary seasonally. Nitrate uptake by emergent marsh macrophytes and SAV is likely highest in spring and early summer, while microbial denitrification may proceed throughout the period when temperatures are greater 10°C. Thus, total nitrate retention would be highest in spring to early summer, which is what the data indicate. Although *Hydrilla sp.* can take up nitrate, it also creates flow resistance and a dense canopy that creates a vegetative boundary layer (Ghilsalberti and Nepf, 2002) that may inhibit the movement of nitrate-rich flow into the canopies. Thus, uptake by *Hydrilla sp.* may be limited to the spring and early summer due to a negative feedback created by vegetative flow hydraulics. This may also lead to *Hydrilla sp.* decline, which was observed to occur by July.

Tidal stage can also be considered to be an external control because it varies without control by the local marshes. It primarily affects the volume flux of water through each tidal inlet. Although tidal stage is a major control on water flux, the total flux into each tidal inlet is also governed by the geomorphic characteristics of each tidal inlet. Thus, volume flux is controlled both by tidal stage (external control) and inlet characteristics (internal control). These controls work in synergy to create a critical tidal stage necessary for NR. During vegetated conditions, tidal waters are forced over the dense, flexible canopies of *Hydrilla sp*. Higher tidal stages are contained within the channel banks, and thus control fluxes into the marsh interior over the top of the SAV canopies because emergent macrophytes restrict overbank flooding in the lower marsh.

5.3 Internal controls: Interactions among geomorphic, hydrologic, and biological processes and development of emergent relationship to predict nitrate retention

5.3.1 Spatial geomorphic organization of marshes in the TFW ecosystem

An initial examination of interactions among geomorphic, hydraulic, and NR parameters suggested that water volumes conveyed into the marshes were a major control on NR. In this TFW ecosystem, flux into the marshes is controlled by inlet channel geometry; therefore, geomorphic characteristics of the inlet channels (width, area) are variables that can be up-scaled to estimate ecosystem NR. Marsh surface area, another parameter that might be used for ecosystem scaling, is difficult to use due to the variable proportion of the marsh area that participates in NR during changing tidal stages, and the seasonal variations in marsh and channel vegetation. In

this study, I determined that inlet channel characteristics control the amount of water and solutes fluxing to and from the marsh (Seldomridge, 2009), which is consistent with results from previous investigations (e.g. Fagherazzi et al., 1999). As is the case in many channel systems, maximum tidal discharge (Q_{max}) and total tidal water volume (V_w) are closely related to channel width (e.g. Leopold and Maddock, 1953). Thus inlet width can be used to predict tidal water volume for a bankfull tidal stage. This relationship of inlet channel width to cross sectional area is predictable for bankfull tidal stages during non-vegetated conditions (Fig. 5.4A); however, the relationship becomes less clear during higher tidal stages and during vegetated conditions (discussed below).

Accordingly, all inlet channel widths were measured from aerial photos to determine the width for marsh inlets in the TFW ecosystem (Fig. 5.4B). This produced a truncated power law distribution, which suggests there are upper and lower limits of natural self-forming channel sizes within this ecosystem. The maximum tidal channels are limited by available space and maximum travel distances during flooding tidal stages. The smallest channels are limited by vegetative growth. Channels that are approximately 20 cm in width can apparently be maintained during the growth of emergent macrophytes. No inlet channels smaller than this dimension were observed. According to the power law distribution, the majority of channels are small in size; approximately 75% of the channels are less than 5 meters wide. Although these small channels are great in number, they encompass only a small portion of the total marsh surface area; therefore, they may not represent a large proportion of ecosystem functioning. The 11 biggest marshes (upper 4% of total

number of marshes) cover 3,227,913 m^2 or approximately 80% of the TFW ecosystem. These 11 largest marshes represent 65% of the total volume of water fluxed during "bankfull" spring tides for non-vegetated conditions. The 75% of the marshes less than 5 meters wide represent 3 % of total volume flux and 7% of total marsh area.

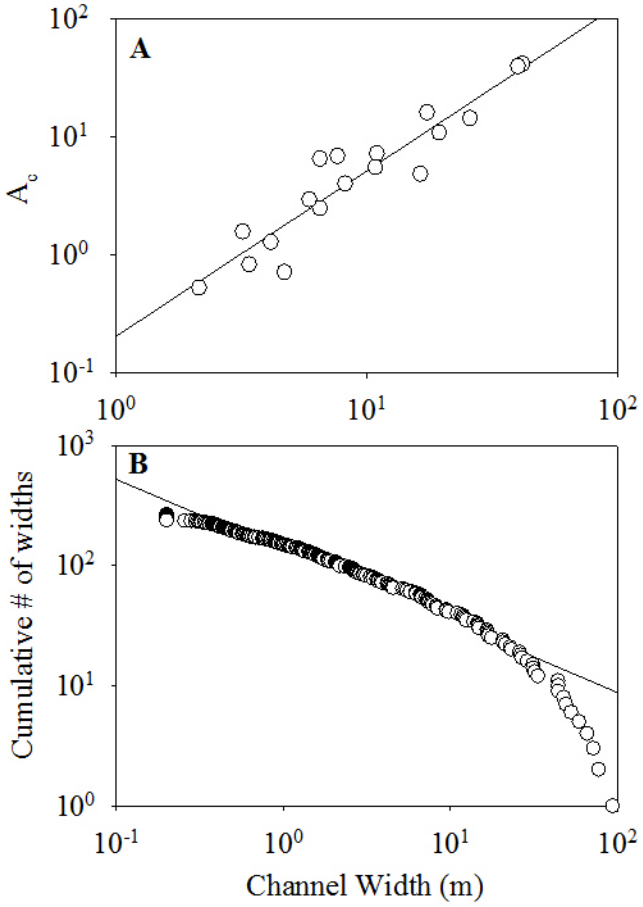

Figure 5.4. (A) Relationship between inlet width and cross sectional area. (B) Cumulative number of inlet channel widths less than or equal to indicated value ($N = 133.23W^{-0.59}$; n=267; R^2 =0.92). Standard error is less than size of data points.

5.3.2 Relationship of inlet depth to minimum tidal stage for channels

Inlet channel geometry controls the amount of water and solute fluxes into the marsh. Field observations indicated that small channels had higher bed elevations

than large inlet channels; therefore, further examination of inlet channel bed characteristics was conducted to define tidal drainage behavior of individual channels (Fig. 5.5). The maximum depth of channels therefore controls the minimum tidal stage required to initiate flow in each channel. It also identifies the channels that fully drain on ebbing tidal cycles, which appear to be channels less than 15-20 meters wide. In general, channels that do not drain during low tides can also support submerged aquatic vegetation.

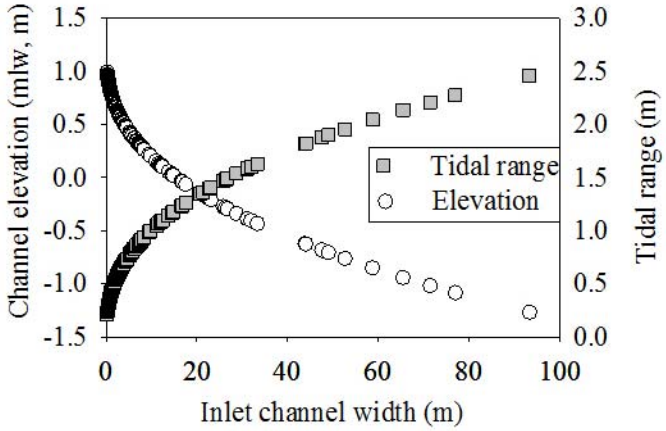

Figure 5.5. Inlet channel bed elevation defines the tidal range experienced in a given channel, and whether the channel contains water at low tide and thus can support submerged aquatic vegetation.

5.3.3 Effects of vegetation on channel geomorphic characteristics

During the growing season, both submerged aquatic vegetation and emergent macrophytes can influence inlet channel geomorphic characteristics and flow hydraulics. Furthermore, emergent macrophyte vegetation that grows on the marsh platform can contain tidal flows within the channel system. The channels that do not drain on low tides can support SAV, currently the dominant SAV species is *Hydrilla verticillata* (Delgado, *unpubl*.), which grows in dense mats to within several

decimeters of low tide. The smallest channels can be invaded by emergent macrophyte growth, primarily arrow arum (*Peltandra virginica*) and pickerelweed (*Pontederia cordata*). Most of the tidal channels that drain during low tide, however, do not support either emergent macrophytes or SAV in the channels themselves. The SAV species *Hydrilla* is dense during maximum vegetation in mid-July. During changing tides, *Hydrilla* sp. flattens in the direction of flow, which results in velocities within the vegetative boundary layer that are very low. These conditions allow for the development of a logarithmic velocity profile that forms above the vegetation (Ghisalberti and Nepf, 2002; Nepf and Ghisalberti, 2008). Therefore, SAV reduces the inlet channel cross sectional area, whereas emergent macrophyte growth within or along the channel results in a significant increase in flow resistance that reduces velocities. Marsh vegetation, therefore, greatly alters tidal flow and total volume flux into tidal channels.

In early spring, when SAV and emergent macrophyte vegetation is at a minimum, high tides can cause overbank flooding over the entire marsh network, which may be the dominant time for sediment deposition in upper interior marsh areas and/or deposition or removal of organic material. After peak vegetation growth, but before die-back, emergent macrophytes along the channel and on the marsh platform contain discharge within the channel. This containment of flows increases flow depths in the channel. The increased water depth causes water to flow over the SAV canopies and upstream into the marsh. This creates a significantly higher "bankfull" channel depth during vegetative conditions (Fig. 5.6). Therefore, the tidal

stage that causes widespread overbank flooding is much higher during summer months and may only be associated with large storms.

Moreover, the presence of SAV also shifts the location of nitrate retention within the marshes. Nitrate processing by denitrification can occur either in the channel or on the marsh surface. During non-vegetated conditions, both sites are active, whereas during vegetated conditions, only the marsh surface is active. Rapid growth of SAV during the early growing season represents significant plant uptake of nitrate, but development of the vegetative boundary layers would limit exchanges with the bed and may eventually limit contact of the canopy with nitrate-rich waters. Therefore, both flow volume constraints and formation of the vegetative boundary layer may limit mid-summer values of NR. This limitation can be significant due to the reductions in water volume distributed into the larger marshes and the spatial reduction in marsh surface denitrification due to channel and marsh platform flow resistance. The degree of inundation is additionally limited by the tidal stage. This link between internal (A_c') and external (lunar tidal stage) controls on volume flux suggests that difficulties in distributing discharge within these marshes are a major control on nitrate retention. Thus, the observed relationship between water flux and nitrate retention is an emergent property of this ecosystem.

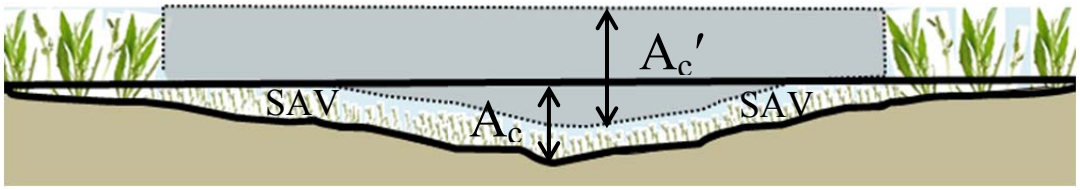

Figure 5.6. Inlet channel cross sectional area during non-vegetated conditions (A_c), and vegetated conditions (A_c'). During vegetated conditions, water flow is forced over top of the dense SAV canopies, but restricted on along the channels by emergent macrophytes; this causes a higher tidal stages.

5.3.4 Regional hydraulic scaling relationships

The geomorphic characteristics of tidal inlets, primarily channel width and inlet elevation, influence the movement of tidal flows into inlet channels. The relationship between inlet hydraulic characteristics (width, depth and velocity) to discharge was examined for each tidal inlet. These at-a-station hydraulic geometry relationships indicate that for non-vegetative conditions, the velocity is not sensitive to channel size (Appendix B); therefore, maximum discharge during a tidal cycle is closely related to channel cross sectional area (Fig. 5.7). Likewise, the relationship between Q_{max} and volume can also be determined for any defined inlet area. This becomes a powerful predictive tool for understanding ecosystem dynamics from a small number of measured channels.

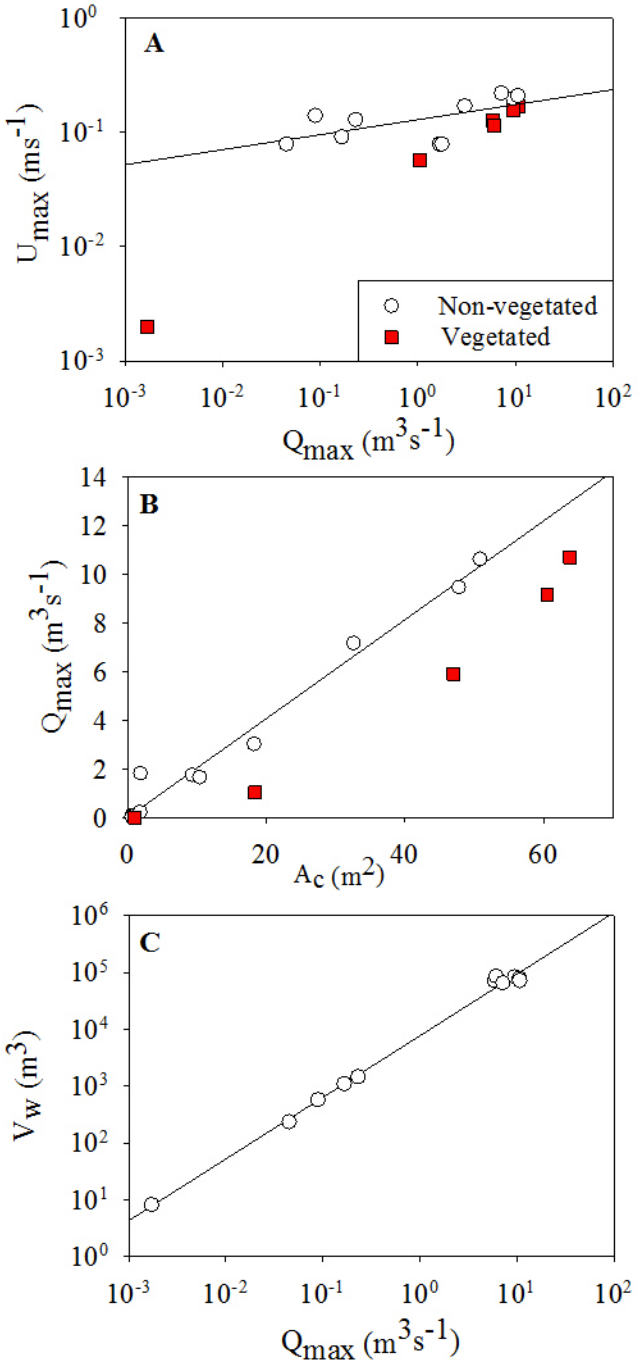

Figure 5.7. Regional hydraulic scaling relationships during vegetated and non-vegetated conditions for (A) maximum discharge (Q_{max}) to maximum velocity (U_{max}), (B) cross sectional area and maximum discharge, and (C) maximum discharge and water volume.

Vegetative flow resistance affects not only the effective marsh inlet area (A_c'), but also the velocity and distribution of flow into the network interior. Both the regional and downstream relationships suggest that when vegetation is present, small channels have much lower channel velocities than the larger channels; this is observed by the large change in the exponent for velocity in the regional and "up-marsh" hydraulic geometry exponents for velocity (Table 5.1). The regional curves suggest velocity is affected among tidal inlets of varying size. The reduction of velocity by SAV is a homogeneous response in this ecosystem because many small channels do not support either SAV or emergent channel macrophytes, and thus retain their area and velocity relationship that were observed for non-vegetated conditions. The up-marsh "downstream" hydraulic geometry relationships for the large marsh indicate that velocity decreases significantly as water flows into the marsh network. This up-marsh reduction in U_{max} would significantly increase travel times and thus travel distances during a tidal cycle. As a consequence, there are highly differing NR potentials between vegetated and non-vegetated conditions. During non-vegetated conditions, over 70% of NR occurs in the larger marshes with inlet channels > 50 meters wide).

Table 5.1. Comparison of regional scaling relationships with downstream hydraulic geometry for a marsh network (Site 3)

Case	***Condition***	***Width***	***Depth***	***Velocity***	***Area***
Regional	No veg			$U_{max} = 0.14Q_{max}^{0.12}$	$A=7.46Q_{max}^{0.87}$
	Veg			$U_{max}=.052Q_{max}^{0.50}$	$A=16.57Q_{max}^{0.48}$
Downstream[a]	Veg	$w = 17.9Q^{0.70}$	$d = 0.915Q^{0.07}$	$u = 0.061Q^{0.23}$	$A = 16.29Q^{0.77}$
	No veg	$w = 6.17Q^{0.83}$	$d = 0.802Q^{0.10}$	$u = 0.202Q^{0.07}$	$A = 4.95Q^{0.93}$

a- Downstream hydraulic geometry relationships from Jenner (2010)

5.4 Emergent relationship between nitrate retention and hydrologic flux

Results of this study suggest hydrologic flux is a dominant control on NR in TFW ecosystems. This suggests that the biological processes of NR, primarily plant uptake and denitrification, are limited by hydrological delivery mechanisms, not reaction kinetics or the supply of nitrate. These results are specific for the set of conditions studied in this ecosystem. During the winter months, NR would drop significantly due to the effects of temperature on enzyme and denitrification kinetics, even though hydrologic delivery of nitrate-rich water usually increases during the winter season.

Hydrologic flux increases as a function of inlet cross sectional area. This provides a scaling procedure to predict hydrologic flux and thus nitrate retention for the ecosystem. Seasonal variations in channel vegetation, in this case the SAV species *H. verticillata*, primarily appear to influence effective channel cross sectional area. Mass balance measurements indicate that hydrologic flux is closely related to NR. This relationship appears to apply to all channels and seasons, with the exception that NR in late spring appears to be higher than during other seasons (Fig 5.8). This increase is most likely the effect of vegetative uptake of nitrate. During late spring, vegetation height within channels is minimal, but uptake rates are high. The minimal vegetative flow resistance allows for internal movement of nitrate-rich water into marsh networks where the nitrate is immediately utilized by marsh surface macrophytes, algae, and denitrification reactions.

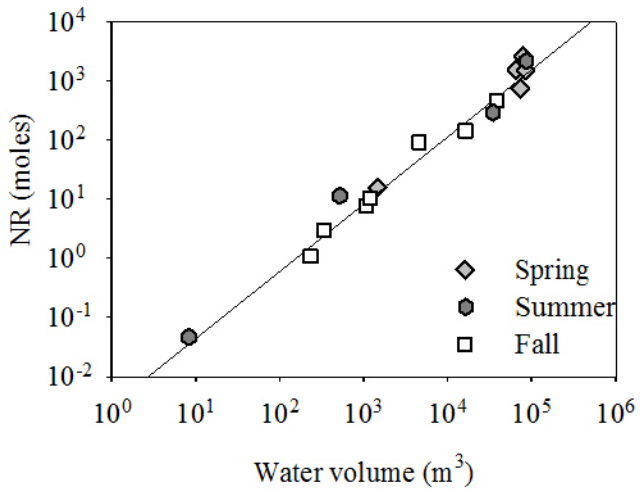

Figure 5.8. Hydrologic flux is a dominant control on NR in the upper Patuxent TFW marshes. There is little variation between NR and season: $\boldsymbol{NR = 0.0045 V_w^{1.1}}$.

5.4.1 Hydrologic flux as an emergent control on nitrate retention

The relationship of hydrologic flux to NR is an emergent property of this complex ecosystem that results from the geomorphic organization of the freshwater tidal wetlands (Fig 5.9). The motivation of this study was to determine the controls on NR (over one tidal cycle); retention includes both plant uptake and denitrification on marsh surfaces, and to a lesser extent in channels. NR is influenced by a suite of external controls; temperature and water inputs (rainfall) determine the climatic regime, and watershed loadings determine nitrate and sediment supplies. During the growing season, when this study was conducted, temperatures are elevated and rainfall is fairly consistent; therefore, the relative importance of these climatic controls diminishes. In addition, the nitrate loading data suggest ample supply of nitrate to drive nitrate processing (i.e. denitrification); therefore, the relative importance of the watershed loading as a control also diminishes. Thus, geomorphic and hydraulic characteristics of marshes exert controls on nitrate retention.

In an individual marsh system, nitrate processing is controlled by the marsh surface inundation because the water-soil interface (both on marsh surface and in channels) may be the site for nitrate processing via both macrophyte uptake and denitrification. The controls on marsh surface inundation must therefore be examined. Inundation is controlled primarily by the magnitude of hydrologic flux. In synchronous marshes, this is controlled by tidal stage; however, inlet channel geometry changes during vegetated conditions, which alters the effects of the tidal stage. During maximum vegetative flow resistance, inlet channel velocities are reduced for a given tidal stage and they decrease upstream into tidal networks. These changes in velocity and hydrologic flux, however, are predictable in this system because the SAV creates a vegetative boundary layer, and thus reduces effective channel cross sectional area. The results of this investigation continually point back to hydrologic flux/discharge as a major control on nitrate retention; therefore, this is an emergent control on nitrate retention of the Patuxent TFW ecosystem.

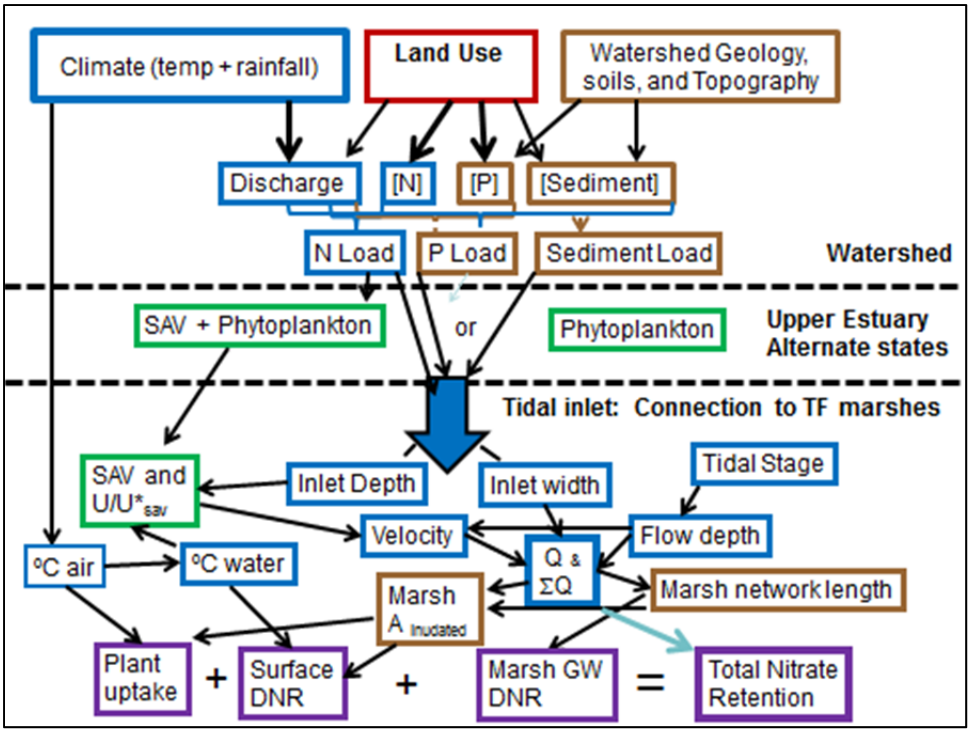

Figure 5.9. Flowchart examining the controls on nitrate retention at a variety of scales (watershed to individual tidal marsh) in a tidal freshwater ecosystem. Hydrologic flux emerges as a dominant control once critical temperature and nitrate concentrations values are reached.

5.4.2 Effects of interannual variations in streamflow on nitrate retention

In this study, the hydraulic transport of water and solutes into marsh inlets and distribution into channel networks was the emergent control on nitrate retention; however, the data supporting this relationship were only collected during the growing season and during relatively low levels of Patuxent River streamflow. In Maryland, rainfall is distributed throughout the year, but streamflow varies seasonally (Fig. 5.10) due to evapotranspirative processes (Weisman, 1977; Moore, 1997; Wittenberg and Sivapalan, 1999). Seasonal and interannual variations in temperature and storm events can generate significant variations in both stream flow and nitrate fluxes. For the Patuxent River, the highest discharges are achieved during tropical storms in the

summer/early fall months and Nor'Easter events during winter months. These storms contribute to the highest tidal stages and thus the greatest volumes of water distributed into the marshes. The timing of peak flows is temporally variable, and may not correspond with the timing of optimal NR rates. In the Patuxent ecosystem, temperatures exceed 10°C between April and September; however, this portion of the year corresponds to 45% of the nitrate loading. The majority of nitrate loading (55%) currently occurs at times when temperatures are less than 10°C (between October and March), when plant uptake and denitrification rates are at a minimum. Therefore during this time of year, the system is limited by kinetics, not water distribution. The largest N loading values occur in the winter months when NR rates are likely at their lowest, but were not directly measured in this study. Therefore, more research is necessary to determine the relative effects of temperature and hydrologic flux on NR in winter months. In addition, more research is necessary to determine the effects of climate change on both temperature and streamflow. A shift to smaller winter-spring storms and more frequent tropical storms may result in an increase in overall processing. Warming temperatures may expand nitrate processing to later in the fall and earlier in the spring, which would increase annual nitrate retention.

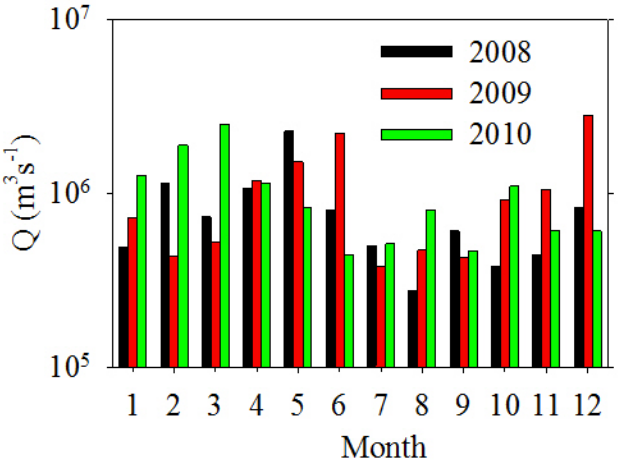

Figure 5.10. Seasonal and interannual variability in baseflow conditions of Patuxent River discharge. The high discharge values in the winter months are generally a result of winter Nor'Easter storms, and in the late summer months are a result of tropical storms. Data source: U.S. Geological Survey National Water Information System.

5.5 Expected future changes in nitrogen loading and ecosystem responses

The analysis in this paper indicates that nitrate concentrations have less of an effect on NR than hydrological flux. Although the reason for this is unclear, it suggests that nitrate concentration values do not limit NR as significantly as water distribution. According to the RIM data (Fig. 5.11), the Patuxent receives between 1 to 2 mg/L of watershed nitrate (flow-weighted). From 1985-1995 the Patuxent experienced a reduction in nitrate loading; thereafter nitrate loading values have remained fairly constant. Continued reductions in watershed nitrate would likely decrease incoming nitrate concentration in the TFW ecosystem.

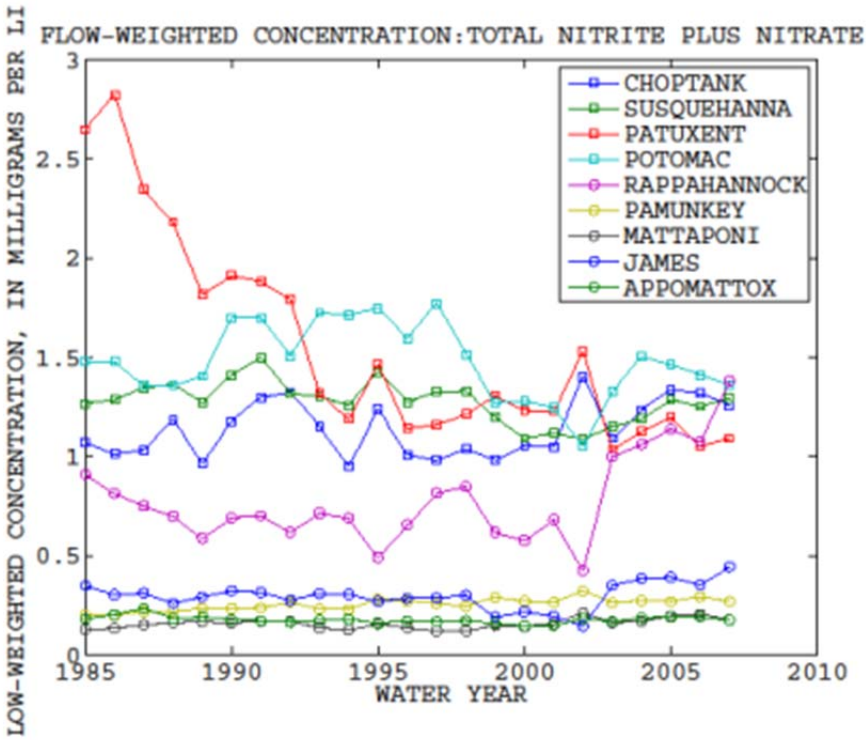

Figure 5.11. Annual flow-weighted nitrite + nitrate concentrations for contributing watersheds of the Chesapeake Bay from 1985-2007. Patuxent River concentrations have steadily decreased during this time period. Data source: U.S. Geological Survey Chesapeake Bay River Input Monitoring Program.

Although nutrient reduction is essential for improving the health of the Bay (McCarthy et al., 1977; Boynton et al., 1995; Boesch et al., 2001; Kemp et al., 2005; etc.), continued reduction in nitrate concentrations may affect nitrate retention in the tidal marshes, and shift the system into concentration-limited behavior. If nitrate concentrations are limiting, then hydrologic flux may not exert the dominant control, and all relationships would need to be reexamined. It is important to note that this critical threshold of nitrate concentration remains unknown. Study of nitrate retention in the other Coastal Plain Estuaries (e.g. Appomattox, Mattaponi, etc.) may provide such information.

Changes in nutrient concentrations are unlikely to generate simple linear ecosystem responses. Alteration of the nutrient regime may cause a shift in the dominant plant community. Lower nutrient systems are dominated by submerged aquatic vegetation, but perhaps not *Hydrilla sp*. High nutrient loads will cause a shift to macroalgal and phytoplankton dominated systems and away from SAV dominated systems (Duarte, 1995; Duarte et al., 2009). In the early 1980s, eutrophic conditions with corresponding large phytoplankton blooms were reported in the majority of tributaries of the Bay, including the Patuxent River (Fisher et al., 1988; Kemp et al., 2005). In the past 25 years, both sediment and nitrate concentrations have decreased significantly in the Patuxent River. The reductions corresponded with the initial recovery of SAV species in the 1980s in the Patuxent River (Orth and Moore, 1984; Carter and Rybicki, 1986). This suggests that the ecosystem was once dominated by phytoplankton or macroalgae, but it may be shifting into a low nutrient regime that supports SAV. It is not clear how the system adjusts to these changes, or at what N concentrations these shifts take place.

5.6 Application of this approach to other RIM Systems

The USGS RIM data provides water and nutrient flux information on other river systems of the Coastal Plain. As outlined in the introduction, the Patuxent River is similar to other Coastal Plain rivers that contain extensive tidal freshwater wetlands. TFW ecosystems in tidal rivers throughout the Mid-Atlantic Coastal Plain display similar geomorphic characteristics. This study demonstrates the feasibility of the mass balance approach for characterizing nitrate retention; however, before application to other systems, a number of considerations must be made.

First, the marsh morphology must be examined. Extensive TFW ecosystems are found along these Coastal Plain river systems. Next, the incoming river N concentrations should be similar to the Patuxent River, not be below the threshold that induces nitrate-limited behavior. In the period since 1985, inorganic nitrate concentrations from the Patuxent River have dropped significantly; values now have similar ranges to the Potomac, James, Rappahannock and Susquehanna Rivers. It is important to note that values are flow-weighted; therefore, river size must also be considered. The Pamunkey, Appomattox, Mattaponi, and James Rivers have significantly lower nitrate concentrations than the Patuxent. They also have lower discharges, so they might behave in a similar manner to the Patuxent, or they might be nitrate-limited. Finally, other watershed variables such as sediment loads, river size (contributing watershed area), and river velocities must also be examined because they might affect the behavior of the system. For example, the Rappahannock marshes have similar marsh size distributions to the Patuxent, but they are showing signs of erosion. Based on the criteria discussed above, the Choptank River marshes appear to be most comparable to the Patuxent marshes, but salinity regimes might be different.

The geomorphic-hydrologic relationships established through this study are empirical results and must be tested before applied to other systems. Field work is necessary to determine channel area to surface width relationships. Additionally, hydraulic measurements are necessary to adjust existing geomorphic-hydrologic (e.g. area to Q_{max} and Q_{max} to volume) relationships. It is likely that each river system and its associated tidal marshes may have significant differences from other systems.

5.7 Future work and synthesis

As is true for most research projects, there are many unanswered questions generated from this study. In particular, I think that the following research topics are worthy of future research attention:

1. What proportion of nitrate retention occurs via plant assimilation?

Plant assimilation has been established as an important sink in nitrate retention (Bowden, 1986; Bowden, 1987; Mitsch and Gosselink, 2007); however, it remains one of the most difficult pathways to quantity. Previous studies have approached quantification of nitrogen removal by emergent macrophytes through chemical stoichiometry and biomass studies (e.g. Tanner, 1996), or experimental chamber studies (e.g. Chambers et al., 1992); however, this approach fails to incorporate the *in situ* importance of the hydrologic flux (nitrate uptake under shear flows).

A large proportion of nitrate assimilation may also be through uptake by the SAV species *Hydrilla verticillata* (Kennedy et al., 2009). This relationship is likely quite dynamic and involves uptake from shear flows, development of vegetative boundary layers, and possibly important controls of mononi on mixing nitrate-rich flows into the vegetative boundary layer. During SAV maximum, a vegetative boundary layer forms; this layer traps water into the SAV canopy. Over time, the trapped water likely is depleted of nitrate, which may in turn limit SAV growth. This depends on the initial nitrate concentration of the trapped water, possible mixing

during changes in tidal flow directions, and the characteristics of the vegetative boundary layer.

2. What are the long-term effects of the invasive species *Hydrilla verticillata*?

The results of this study demonstrate the strong influence of SAV plant growth on hydrologic flux. It was also observed, however, that SAV growth declined by mid-summer. This may be due to sedimentation and/or negative feedbacks on nitrate availability to *Hydrilla* sp. as a result of the development of the vegetative boundary layer. A portion of the particulate load that settles on SAV is likely organic matter, which is reflected by the organic nitrogen concentrations. The RIM data suggest that organic nitrogen loads can be as high as 65% of the total nitrogen load into the Patuxent during summer months.

Sediment and particulate organic matter are carried into tidal channel networks via tidal discharge. During peak SAV growth, the discharge is greatly impeded; the low velocities and shallow depths to the SAV layer facilitate settling and trapping of particulate organic matter and sediment in dense canopies. Therefore, during maximum SAV conditions, sediment loads are likely deposited onto SAV beds, rather than on the marsh surface. Qualitative observations support this idea, but more work is necessary to quantify sedimentation on marsh surfaces and within SAV canopies.

3. What effect will climate change have on nitrate retention rates?

A warming climate could lead to widespread ecosystem changes. In the TFW ecosystem, climate change is manifested through sea level rise, increased frequency and magnitude of peak discharges, a shift in the timing of these maximum levels, and lower summer baseflow levels. The effects of sea level rise have been modeled for tidal wetland ecosystems (Moore et al., 1997; Mulholland, 1997; Meyer, 1999; Craft et al., 2009; Najjar et al., 2010; etc.). Greater volumes of water will flood marsh surfaces as a consequence of increases in both sea level and tidal range. The tidal marshes may be slowly submerged if marsh surface accumulation rates cannot keep pace with sea-level rise. If this occurs, the tidal network channels will become less important as delivery vehicles for N processing. In subsiding freshwater wetlands of the Chesapeake Bay, the interior tidal networks appear to be the first areas affected by sea level rise. These interior channels appear to respond by widening and marsh loss results in the development of interior ponds (Kearny et al., 1988).

Next, the increased frequency and magnitude of peak discharges will affect the TFW ecosystem differently depending on the time of year when the peaks occur. During the summer months, increased magnitude and frequency of flooding may enhance NR. On the other hand, if the floods occur during the winter months when vegetation is dormant and NR processes are not optimal, the large flood pulses may scour the unconsolidated soils on the marsh surface.

Alternatively, if there is a shift to warmer temperatures with less precipitation, summer baseflow levels may decrease (Gibson et al., 2005). This would cause water temperatures to increase, which would have a myriad of negative effects on the

ecosystem health (Karr, 1991) including: lower dissolved oxygen levels, reduced survival of larval fishes, unsuitable habitat for sensitive species, etc.

Although future work is necessary to understand the dynamic tidal freshwater ecosystem, this research project has identified controls on nitrate retention. The culmination of this project will hopefully aid researchers in understanding the governing relationships for scaling nitrate retention to the ecosystem level in tidal freshwater wetlands.

Appendix A:
List of symbols
(A-S)

Symbol	Description
A	Arrhenius rate constant
a	Average incoming nitrate concentration
A_c	Cross sectional area
A_c'	Effective cross sectional area (as influenced by *Hydrilla verticillata*)
A_i	Cross sectional area at time step
A_m	Marsh surface area
A_{ws}	Water surface area
b	Integrated average nitrate concentration on outgoing tide
c	Integrated averaged nitrate concentration of retained nitrate
C_i	Concentration at time step
D_A	Average inlet channel depth
D_{MAX}	Maximum inlet channel depth
DNF	Denitrification
E_a	Activation energy
g	Acceleration due to gravity
H	Mean channel depth
h	Effective mean channel depth
k	Arrhenius rate constant
L	Channel length
N	Nitrogen
N_L	Nitrogen load
N_x	Cumulative number in the power law equation
NR	Nitrate retention
NR_{rate}	Nitrate retention rate
q_i	Discharge at time step
Q	Discharge
Q_{max}	Maximum discharge measured at bankfull conditions
R	Universal gas constant
S	Water surface gradient
SAV	Submerged aquatic vegetation

List of symbols
(T-Z)

Symbol	Description
T	Temperature
$T_{inundation}$	Time of (tidal) marsh surface inundation
T_r	Tidal range
TFW	Tidal freshwater wetland
u	Local velocity
$U_{\max}$	Maximum velocity
$\overline{u}$	Mean velocity
u^*	Shear velocity
V_p	Tidal prism
V_t	Total volume
V_t'	Total volume calculated using the effective cross sectional area
W	Channel width
Z	Relative height
Zm	Height of plane of momentum absorption
Zo	Height above bed where velocity is zero

Appendix B:
At-a-station hydraulic geometry relationships

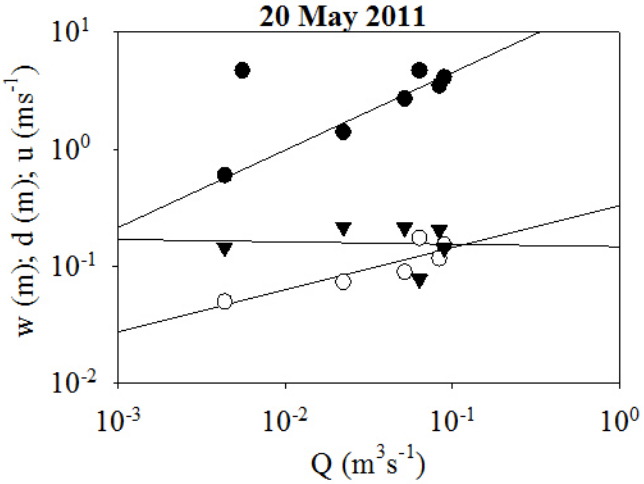

Figure 1. At-a-station hydraulic geometry relationships for Site 1 (spring): $w = 20.6Q^{0.66}$; $d = 0.33Q^{0.36}$; $u = 0.15Q^{-0.02}$.

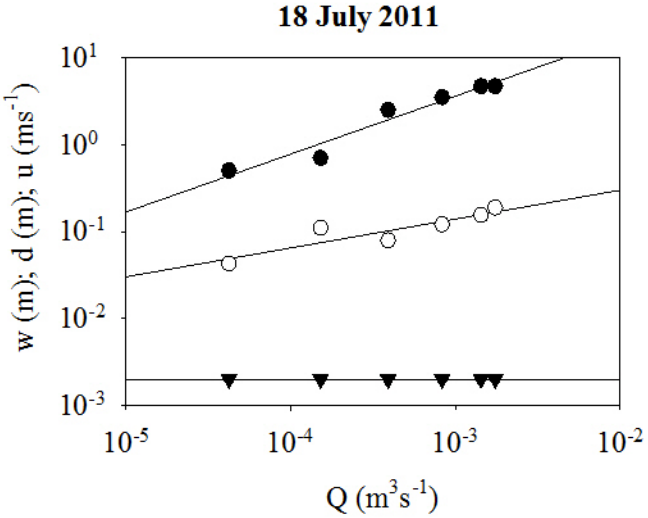

Figure 2. At-a-station hydraulic geometry relationships for Site 1 (summer): $w = 364.4Q^{0.67}$; $d = 1.38Q^{0.33}$; $u = 0.002Q^{0.0}$.

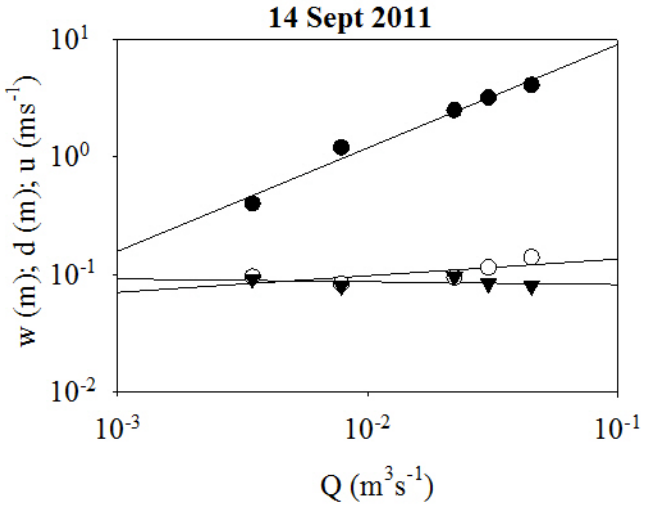

Figure 3. At-a-station hydraulic geometry relationships for Site 1 (fall): $w = 69.2Q^{0.88}$; $d = 0.19Q^{0.15}$; $u = 0.077Q^{-0.02}$.

.

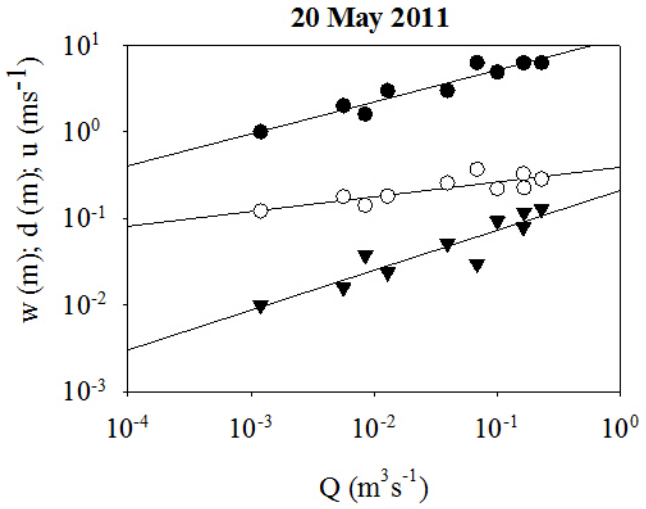

Figure 4. At-a-station hydraulic geometry relationships for Site 2 (spring): $w = 12.1Q^{0.37}$; $d = 0.39Q^{0.17}$; $u = 0.21Q^{0.46}$.

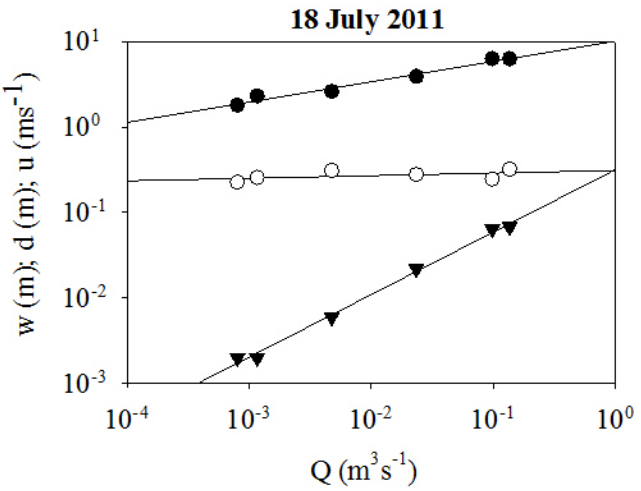

Figure 5. At-a-station hydraulic geometry relationships for Site 2 (summer): $w = 10.2Q^{0.24}$; $d = 0.31Q^{0.03}$; $u = 0.32Q^{0.73}$.

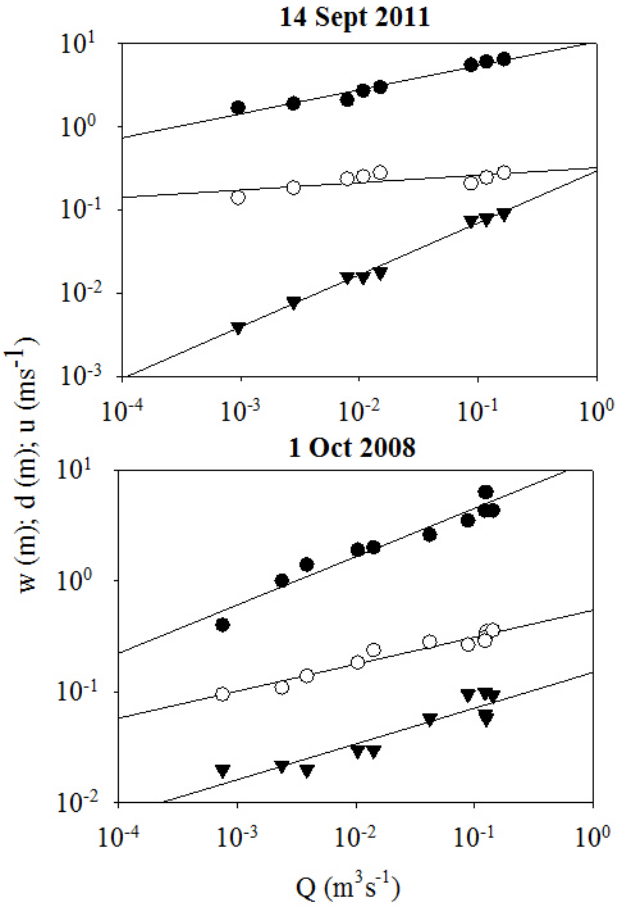

Figure 6. At-a-station hydraulic geometry relationships for Site 2 (fall): 14 Sept 2011: $w = 10.5Q^{0.29}$; $d = 0.32Q^{0.09}$; $u = 0.29Q^{0.62}$, and 1 Oct 2008: $w = 12.3Q^{0.44}$; $d = 0.54Q^{0.24}$; $u = 0.15Q^{0.32}$.

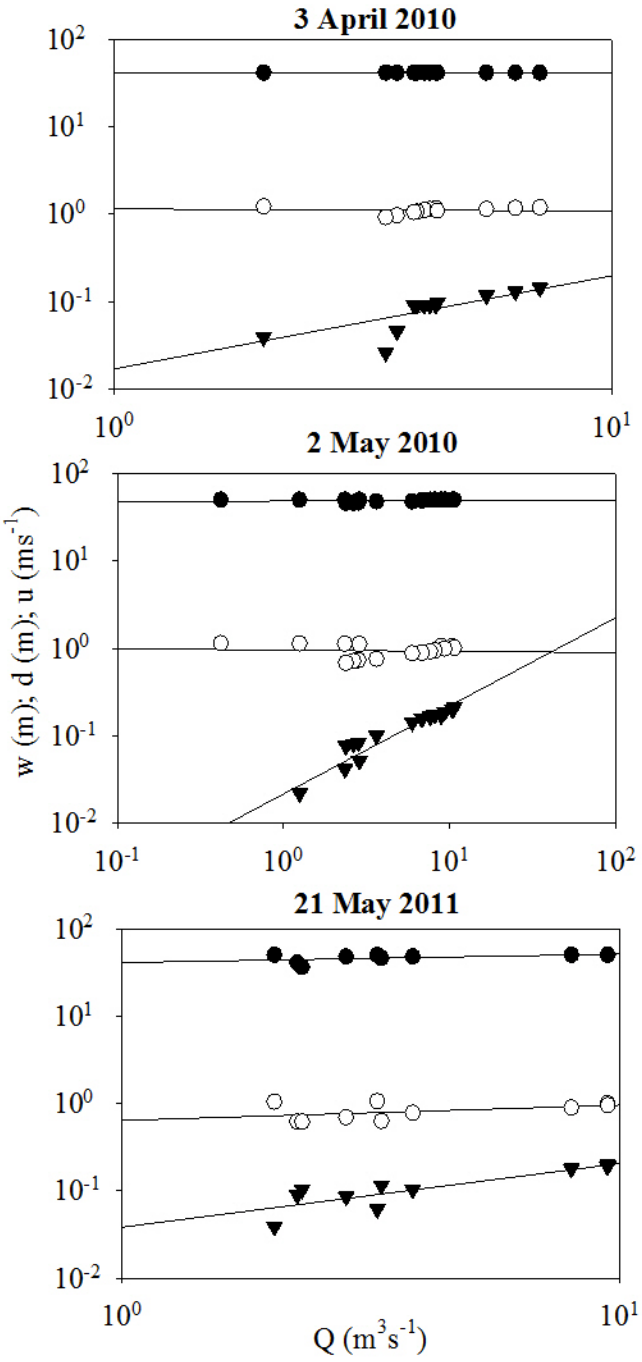

Figure 7. At-a-station hydraulic geometry relationships for Site 3 (spring): 3 April 2010: $w = 41.6Q^{0.01}$; $d = 0.86Q^{0.17}$; $u = 0.03Q^{0.83}$, 2 May 2010: $w = 48.5Q^{0.06}$; $d = 0.95Q^{0.25}$; $u = 0.02Q^{0.70}$, 21 May 2010: $w = 40.9Q^{0.1}$; $d = 0.64Q^{0.18}$; $u = 0.04Q^{0.73}$.

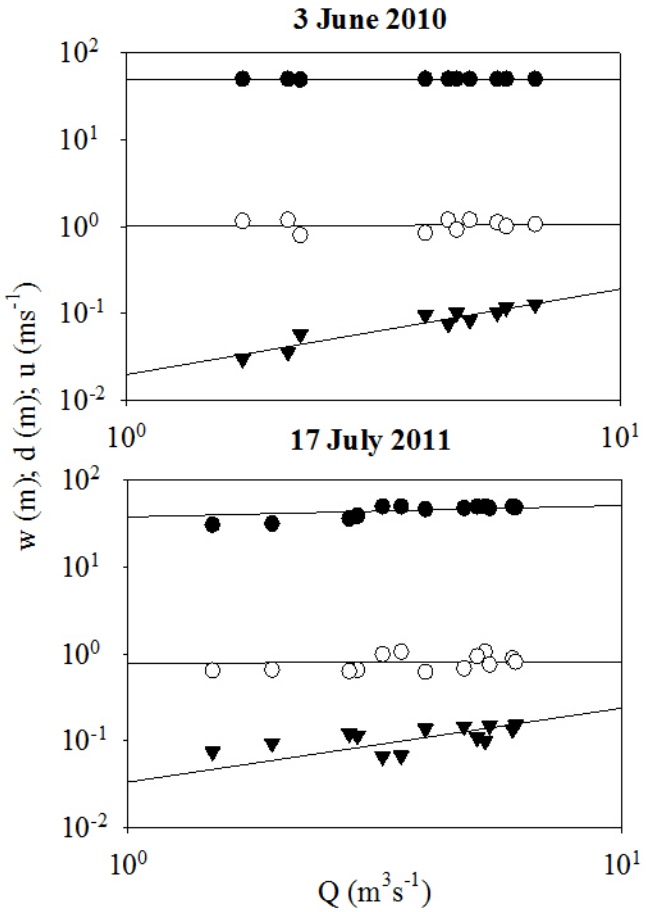

Figure 8. At-a-station hydraulic geometry relationships for Site 3 (summer): 3 June 2010: $w = 45.1Q^{0.01}$; $d = 0.65Q^{0.04}$; $u = 0.0005Q^{0.95}$; 17 July 2011: $w = 39.9Q^{0.37}$; $d = 0.84Q^{0.19}$; $u = 0.07Q^{0.44}$.

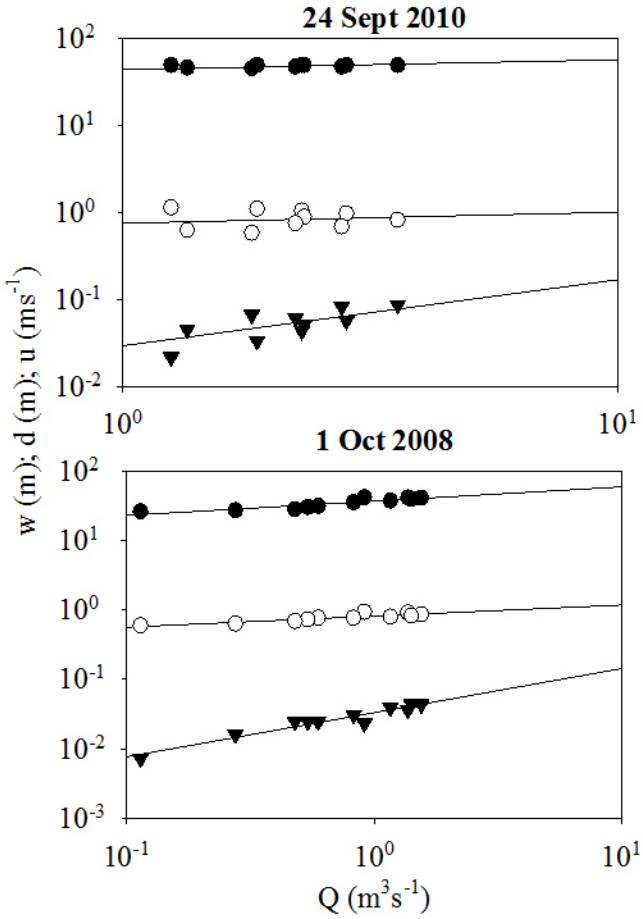

Figure 9. At-a-station hydraulic geometry relationships for Site 3 (fall): 24 Sept 2010: $w = 44.3Q^{0.12}$; $d = 0.76Q^{0.13}$; $u = 0.03Q^{0.76}$; 1 Oct 2008: $w = 36.6Q^{0.20}$; $d = 0.82Q^{0.15}$; $u = 0.03Q^{0.65}$.

References

Aber, J.D., Nadelhoffer, K.J., Stuedler, P., Melillo, J.M., 1989. Nitrogen saturation in Northern forest ecosystems: Excess nitrogen from fossil fuel combustion may stress the biosphere. BioScience 39, 378-386.

Aber, J.D., McDowell, W., Nadelhoffer, K.J., Magill, A., Berntson, G., Kamakea, M., McNulty, S., Currie, W., Rustad, L., Fernandez, I., 1998. Nitrogen saturation in temperate forest ecosystems: Hypotheses revisited. BioScience 48, 921-934.

Abdalla, M., Jones, M., Smith, P., Williams, M., 2009. Nitrous oxide fluxes and denitrification sensitivity to temperature in Irish pasture soils. Soil Use and Management 25, 376–388, doi: 10.1111/j.1475-2743.2009.00237.x

Ågren, G.I., Bosatta, E., 1988. Nitrogen saturation of terrestrial ecosystems. Environmental Pollution 54, 185-197.

Bak, P., Tang, C., Wiesenfeld, K., 1988. Self-organized criticality. American Physical Society 38, 364-374.

Bastviken, S.K., Eriksson, P.G., Premrov, A., Tonderski, K., 2005. Potential denitrification in wetland sediments with different plant species detritus. Ecological Engineering 25, 183–190.

Bayliss-Smith, T.P., Healey, R., Lailey, R., Spencer, T., Stoddart, D.R., 1979. Tidal flows in salt marsh creeks. Estuarine and Coastal Marine Science 9, 235-255.

Bedford, B.L., Walbridge, M.R., Aldous, A., 1999. Patterns in nutrient availability and plant diversity of temperate North American wetlands. Ecology 80, 2151-2169.

Betlach, M.R., Tiedje, J.M., 1981. Kinetic explanation for accumulation of nitrite, nitric oxide, and nitrous oxide during bacterial denitrification. Applied Environmental Microbiology 42, 1074-1084.

Boesch, D.F., Brinsfield, R.B., Magnien, R.E., 2001. Chesapeake Bay eutrophication: Scientific understanding, ecosystem restoration, and challenges for agriculture. Journal of Environmental Quality 30, 303–320.

Bowden, W.B., 1986. Nitrification, nitrate reduction, and nitrogen immobilization in a tidal freshwater marsh sediment. Ecology 67, 88-99.

Bowden,W.B., 1987. The biogeochemistry of nitrogen in freshwater wetlands. Biogeochemistry 4, 314-348.

Boyer, E.W., Alexander, R.B., Parton, W.J., Li, C., Butterbach-Bahl, K., Donner, S.D., Skaggs, R.W., Del Grosso, S.J., 2006. Modeling denitrification in terrestrial and aquatic ecosystems at regional scales. Ecological Applications 16, 2123-2142.

Boyer, E.W., Goodale, C.L., Jaworski, N.A., Howarth, R.W., 2002. Anthropogenic Nitrogen sources and relationships to riverine nitrogen exports in the northeastern U.S.A. Biogeochemistry 57/58, 137-169.

Boynton, W.R., Garber, J.H., Summers, R., Kemp W.M., 1995. Inputs, transformations, and transport of N and P in Chesapeake Bay and selected tributaries. Estuaries 18, 285-314.

Boynton,W.R., Hagy, J.D., Cornwell, J.C., Kemp, W.M., Greene, S.M., Owens, M.S., Baker, J.E., Larsen, R.K., 2008. Nutrient budgets and management actions in the Patuxent River Estuary, Maryland. Estuaries and Coasts 31, 623-651, doi: 10.1007/s12237-008-9052-9.

Brinson, M.M., Bradshaw, H.D., Kane, E.S., 1984. Nutrient assimilative capacity of an alluvial flood plain swamp. Journal of Applied Ecology 21, 1041-1057.

Burgin, A.J., Hamilton, S.H., 2007. Have we overemphasized the role of denitrification in aquatic ecosystems? A review of nitrate removal pathways. Frontiers in Ecology and the Environment 5, 89-96.

Busnardo, M.J., Gersberg, R.M., Langis, R., Sinicrope, T.L., Zedler, J.B., 2003. Nitrogen and phosphorus removal by wetland mesocosms subjected to different hydroperiods. Ecological Engineering 1, 287-307.

Caffrey, J.M., Sloth, N.P., Kaspar, H.F., and Blackburn T.H., 1993. Effect of organic loading on nitrification and denitrification in a marine sediment microcosm. FEMS Microbiology Ecology 12, 159-167.

Carter, V., Rybicki, N.B., 1986. Resurgence of submersed aquatic macrophytes in the tidal Potomac River, Maryland, Virginia and the District of Columbia. Estuaries 9, 368–375.

Chambers, A.M., Meyerson, L.A., Saltonstall, A., 1999. Expansion of *Phragmites australis* into tidal wetlands of North America. Aquatic Botany 64, 261-273, doi: 10.1016/S0304-3770(99)00055-8.

Chambers, R.M., Harvey, J.W., Odum, W.E., 1992. Ammonium and phosphate dynamics in a Virginia salt marsh. Estuaries 15, 349-359.

Chambers, P.A., Kalff, J., 1984. Depth distribution and biomass of submersed aquatic macrophyte communities in relation to Secchi depth. Canadian Journal of Fisheries and Aquatic Sciences 42, 701-709.

Chen, Y.-C., Chiu C.-L., 2002. An efficient method of discharge measurement in tidal streams. Journal of Hydrology 265, 212-224.

Christensen, J.P., Murray, J.W., Devol, A.H., Codispoti, L.A., 1987. Denitrification in continental shelf sediments has a major impact on the oceanic nitrogen budget. Global Biogeochemical Cycles 2, 97-116.

Claassen, N., Barber, S.A., 1974. A method for characterizing the relation between nutrient concentration and flux into roots of intact plants. Plant Physiology 54, 564-568.

Cooper, A.B., 1990. Nitrate depletion in the riparian zone and stream channel of a small headwater catchment. Hydrobiologia 202, 13-26.

Cooper, A.B., Cooke, J.G., 1984. Nitrate loss and transformation in 2 vegetated headwater streams. New Zealand Journal of Marine & Freshwater 18, 441-450.

Cornwell, J.C., Kemp, W.M., Kana, T.M., 1999. Denitrification in coastal ecosystems: methods, environmental controls, and ecosystem level controls, a review. Aquatic Ecology 33, 41-54.

Correll, D.L., 1997. Buffer zones and water quality protection: General principles. *In*: Buffer Zones: Their Processes and Potential in Water Protection, N.E. Haycock, T.P. Burt, K.W.T. Goulding, and G. Pinay (Editors). Quest Environmental, Harfordshire, UK, pp. 7-20.

Craft, C., Clough, J, Ehman, J., Joye, S. Park, R., Pennings, S., Guo, H, Machmuller, M., 2009. Forecasting the effects of accelerated sea-level rise on tidal marsh ecosystem services. Frontiers in Ecology and the Environment **7**, 73-78.

Dalrymple, R.W., Zaitlin, B.A., Boyd, R., 1992. A conceptual model of estuarine sedimentation. Journal of Sedimentary Petrology 62, 113-1146.

Daniels, R.B., Gilliam, J.W., 1996. Sediment and chemical load reduction by grass and riparian filters. Soil Science Society of America Journal 60, 246-251.

Davidson, E.A., Seitzinger, S.P., 2006. The enigma of progress in denitrification research. Ecological Applications 16, 2057-2063.

DeLaune, R.D., Jugsujinda, A., West, J.L., Johnson, C.B., Kongchum, M., 2005. A screening of the capacity of Louisiana freshwater wetlands to process nitrate in diverted Mississippi River water. Ecological Engineering 25, 315-321.

Dennison, W.C., Orth, R.J., Moore, K.A., Stevenson, J.C., Carter, V., Kollar, S., Bergstrom, P.W., Batiuk, R.A., 1993. Assessing water quality with submersed aquatic vegetation. BioScience 43, 86-94.

Dingman, S.L., 2007. Analytical derivation of at-a-station hydraulic-geometry relations: Journal of Hydrology 334, 17-27.

Dodds, W.K., López, A.J., Bowden, W.B., Gregory, S., Grimm, N.B., Hamilton, S.K., Hershey, A.E., Martí, E., McDowell, W.H. Meyer, J.L., Morrall, D., Mulholland, P.J. Peterson, B.J., Tank, J.L., Valett, H.M., Webster, J.R., Wollheim, W., 2002. N uptake as a function of concentration in streams. Journal of North American Benthological Society 21, 206–220.

Duarte, C.M., 1995. Submerged aquatic vegetation in relation to different nutrient regimes. Ophelia 41, 87-112.

Duarte, C.M., Conley, D.J., Carstensen, J., Sanchez-Camacho, M., 2009. Return to Neverland: Shifting baselines affect eutrophication restoration targets. Estuaries and Coasts 32, 29-36.

Engelhardt, K.A.M., Ritchie, M.E., 2001. Effects of macrophyte species richness on wetland ecosystem functioning and services. Nature 411, 687-689.

Eppley, R.W., Rogers, J.N., McCarthy, J.J., 1969. Half-saturation constants for uptake of nitrate and ammonium by marine phytoplankton. Limnology and Oceanography 14, 912-920.

Eyes on the Bay., 1998. Maryland Department of Natural Resources: Water quality monitoring data. http://mddnr.chesapeakebay.net/eyesonthebay/index.cfm (March 2012).

Fagherazzi, S., Bortoluzzi, A., Dietrich,W.E., Adami, A., Lanzoni, S., Marani, M., and Rinaldo, A., 1999. Tidal networks: 1. Automatic network extraction and preliminary scaling features from digital terrain maps. Water Resources Research 35, 3891-3904.

Ferguson, R.I. 1986. Hydraulics and hydraulic geometry. Progress in Physical Geography 10, 1-31.

Ferguson, R.L., Korfmacher, K., 1997. Remote sensing and GIS analysis of seagrass meadows in North Carolina, USA. Aquatic Botany 58, 241-258.

Fisher, D.C., Oppenheimer, M., 1991. Nitrogen deposition and the Chesapeake Bay Estuary. Ambio 20, 102-108.

Fisher, T. R., Harding, L.W., Stanley, D.W., Ward, L.G., 1988. Phytoplankton, nutrients, and turbidity in the Chesapeake, Delaware, and Hudson estuaries. Estuarine, Coastal and Shelf Science 27, 61-93.

Fisher, T.R., Hagy, J.D., Boynton, W.R., Williams, M.R., 2006. Cultural eutrophication in the Choptank and Patuxent estuaries of Chesapeake Bay. Limnology and Oceanography 51, 435-447.

French, J.R., Stoddart, D.R., 1992. Hydrodynamics of salt marsh creek systems: implications for marsh morphological development and material exchange. Earth Surface Processes Landforms 17, 235–252.

Ghisalberti, M., Nepf, H., 2002. Mixing layers and coherent structures in vegetated aquatic flow. Journal of Geophysical Research 107, 1-11.

Gibson, C.A., Meyer, J.L., Poff, N.L., Hay, L.E., Georgakako, A., 2005. Flow regime alterations under changing climate in two river basins: Implications for freshwater ecosystems. River Research Applications 21, 849-864.

Greene, S.E. 2005. Nutrient removal by tidal fresh and oligohaline marshes in a Chesapeake Bay tributary. University of Maryland M.S. Thesis, College Park, MD.

Grimm, N.B., Gergel, S.E., McDowell, W.H., Boyer, E.W., Dent, C.L., Groffman, P., Hart, S., Harvey, J., Johnston, C., Mayorga, E., McClain, M.E., Pinay, G., 2003. Merging aquatic and terrestrial perspectives of nutrient biogeochemistry. Oecologia 137, 485–501, doi:10.1007/s00442-003-1382-5.

Groffman, P.M., 1994. Denitrification in freshwater wetlands. Current Topics in Wetland Biogeochemistry 1, 15-35.

Harvey, J.W., Germann, P. F., Odum,W. B., 1987. Geomorphological control of subsurface hydrology in the creekbank zone of tidal marshes. Estuarine, Coastal and Shelf Science 25, 677-691.

Healey, R.G., Pye, K., Stoddart, D.R., Bayliss-Smith, T.P., 1981. Velocity variations in salt marsh creeks, Norfolk, England. Estuarine, Coastal and Shelf Sciences 13, 535-545.

Hedin, L.O., von Fischer, J.C., Ostrom, N.E., Kennedy, B.P., Brown, M.G., Robertson, G.P., 1998. Thermodynamic constraints on nitrogen transformations and other biogeochemical processes at soil-stream interfaces. Ecology 79, 684-703.

Hemond, H.F., Nuttle, W.K., Burke, R.W., Stolzenbach, K.D., 1984. Surface infiltration in salt marshes: theory, measurement, and biogeochemical implications. Water Resources Research 20, 591-600.

Hickin, E. J., 1987. Vegetation and river channel dynamics, Canadian Geographic 28, 111-126.

Hill, A.R., 1988. Factors influencing nitrate depletion in a rural stream. Hydrobiologia 60, 111-122.

Hill, A.R., 1995. Nitrate removal in stream riparian zones. Journal of Environmental Quality 25, 743-755.

Hirsch, R.M., Moyer, D.L., Archfield, S.A., 2010. Weighted regressions on time, discharge, and season (WRTDS), with an application to Chesapeake Bay river inputs. Journal of American Water Resources Association 46, 857-880, doi: 10.1111/j.1752-1688.2010.00482.x.

Holtan-Hartwig, L., Dorsch, P., Bakken, L.R., 2002. Low temperature control of soil denitrifying communities: kinetics of N_2O production and reduction. Soil Biology and Biochemistry 34, 1797-1806.

Hooper, D.U., Vitousek, P.M., 1998. Effects of plant composition and diversity on nutrient cycling. Ecological Monographs 68, 121–149, doi: 10.1890/0012-9615(1998)068[0121:EOPCAD]2.0.CO;2.

Horton, R.E., 1945. Erosional development of streams and their drainage basins hydrophysical approach to quantitative morphology. Geological Society of America Bulletin 56, 275-370.

Howarth, R.W., Marino, R., 2006. Nitrogen as the limiting nutrient for eutrophication in coastal marine ecosystems: Evolving views over three decades. Limnology and Oceanography 51, 364-376.

Howarth, R.W., Teal, J.M., 1979. Sulfate reduction in a New England salt marsh. Limnology and Oceanography 24, 999-1013.

Ingersoll, T.L., Baker, L.A., 1998. Nitrate removal in wetland microcosms. Water Research 32, 677-684.

Intergovernmental Panel on Climate Change (IPCC), 2007. Summary for policymakers. In: Solomon, S., Qin, D., Manning, M., Chen, Z., Marquis, M., Averyt, K.B., Tignor, M., Miller, H.L. (Eds.), Climate Change 2007: The Physical Science Basis. Contribution of Working Group I to the Fourth Assessment Report of the Intergovernmental Panel on Climate Change. Cambridge University Press, Cambridge, United Kingdom and New York, NY, USA.

Jansson, M., Andersson, R., Berggren, H., Leonardson, L., 1994. Wetlands and lakes as nitrogen traps. Ambio 23, 320–325.

Järvelä, J., 2002. Flow resistance of flexible and stiff vegetation: a flume study with natural plants. Journal of Hydrology 269, 44-54.

Jenkins, M.C., Kemp, W.M., 1984. The coupling of nitrification and denitrification in two estuarine sediments. Limnology and Oceanography 29, 609-619.

Jenner, B.A., 2010, Hydraulic consequences of invasive *Hydrilla* (submerged aquatic vegetation) in tidal channels: Implications for wetland maintenance. University of Maryland Geology Senior Thesis, College Park, MD, pp. 52. http://www.geol.umd.edu/undergraduates/paper/paper_jenner.pdf .

Jenner, B.A., 2011. Geomorphic and hydrologic controls on tidal prism and inlet cross sectional area for Chesapeake Bay lagoons. University of Maryland M.S. Thesis, College Park, MD, pp. 135.

Jensen, J. P., Kristensen, P., Jeppesen, E., 1990. Relationships between nitrogen loading and in-lake nitrogen concentrations in shallow Danish lakes. Verhandlungen des Internationalen Verein Limnologie 24, 201–204.

Jordan, T.E., Correll, D.L., Weller, D.E., 1993. Nutrient interception by a riparian forest receiving inputs from adjacent cropland. Journal of Environmental Quality 22, 467-473.

Joye, S.B., Paerl, H.W., 1994. Nitrogen cycling in microbial mats: rates and patterns of denitrification and nitrogen fixation. Marine Biology 119, 285-295.

Junk, W.J., Bayley, P.B., Sparks, R.E., 1989. The flood-pulse concept in river-floodplain systems. In D.P. Dodge (ed) Proceedings of the international large river symposium. Canadian Special Publication of Fisheries and Aquatic Sciences 102, 110-127.

Kana, T.M., Darkangelo, C., Hunt, M.D., Oldham, J.B., Bennett, G.E., Cornwell, J.C., 1994. Membrane Inlet Mass Spectrometer for rapid high-precision determination of N_2, O_2 and Ar in environmental water samples. Analytical Chemistry 66, 4166-4170.

Kana, T.M., Sullivan, M.B., Cornwell, J.C., Groszkowski, K.M., 1998. Denitrification in estuarine sediments determined by membrane inlet mass spectrometry. Limnology and Oceanography 43, 334-339.

Karr, J.R., 1991. Biological integrity: a long-neglected aspect of water resource management. Ecological Applications 1, 66–84.

Kearny, M.S., Grace, R.E., Stevenson, J.C., 1988. Marsh loss in Nanticoke Estuary, Chesapeake Bay. American Geographical Society, Geographical Review 78, 205-220.

Keefe, C.W., Blodniker, K.L., Boynton, W.R., Clark, C.A., Frank, J.M., Kaumeyer, N.L., Weir, M.W., Wood, K.V., Zimmermann, C.F., 2004. Nutrient analytical services laboratory standard operating procedures. Technical Report Number SS-80-04-CBL, Chesapeake Biological Laboratory, 2004.

Kemp, W.M., Boynton, W.R., Adolf, J.E., Boesch, D.F., Boicourt, W.C., Brush, G., Cornwell, J.C., Fisher, T.R., Glibert, P.M., Hagy, J.D., Harding, L.W., Houde, E.D., Kimmel, D.G., Miller, W.D., Newell, R.I.E., Roman, M.R., Smith, E.M., Stevenson, J.C., 2005. Eutrophication of Chesapeake Bay: historical trends and ecological interactions. Marine Ecology Progress Series 303, 1-29.

Kennedy, T.L., Horth, L.A., Carr, D.E., 2009. The effects of nitrate loading on the invasive macrophyte *Hydrilla verticillata* and two common, native macrophytes in Florida. Aquatic Botany 91, 253-256 doi: 10.1016/j.aquabot.2009.06.008.

Kirchner, J.W., 1993. Statistical inevitability of Horton's laws and the apparent randomness of stream channel networks. Geology 21, 591-594.

Kirwan, M.L., Guntenspergen, G.R., 2010. Influence of tidal range on the stability of coastal marshland. Journal of Geophysical Research 115, F02009, doi:10.1029/2009JF001400.

Knapton, R.W., Petrie, S.A., 1999. Changes in distribution and abundance of submerged aquatic macrophytes in the Inner Bay at Long Point, Lake Erie: Implications for foraging waterfowl. Journal of Great Lakes Research 25, 783–798.

Knight, D.W., 1981. Some field measurements concerned with the behavior of resistance coefficients in a tidal channel. Estuarine, Coastal and Shelf Science, 12, 303-322.

Kouwen, N., 1980. Biomechanics of Vegetative Channel Linings. American Society of Civil Engineers Journal of the Hydraulics Division 106, 1085-1103.

Langland, M.J., Phillips, S.W., Raffensperger, J.P, Moyer, D.L., 2005. Changes in streamflow and water quality in selected nontidal sites in the Chesapeake Bay Basin, 1985-2003. Scientific Investigations Report 2004-5259, 50 p.

Langeland, K.A., 1996. *Hydrilla verticillata* (L.F.) Royle (Hydrocharitaceae), "The Perfect Aquatic Weed." Castanea 61, 293-304.

Langeland, K.A., Sutton, D.L., 1980. Regrowth of Hydrilla from axillary buds. Journal of Aquatic Plant Management 18, 27-29.

Leopold, L.B., Maddock, Jr., T., 1953. The hydraulic geometry of stream channels and some physiographic implications. U.S. Geological Survey Professional Paper 252, pp. 56.

Lowrance, R., 1998. Riparian forest ecosystems as filters for nonpoint-source pollution. In: Limitations and Frontiers in Ecosystem Science, M.L. Pace and P.M. Groffman (Editors). Springer-Verlag, New York, pp. 113-141.

Maag, M., 1997. Kinetic and temperature dependence of potential denitrification in riparian Soils. Journal of Environmental Quality 26, 215–223.

Madsen, J.D., Hartleb, C.F., Boylen, C.W., 1991. Photosynthetic characteristics of *Myriophyllum spicatum* and six submersed aquatic macrophyte species native to Lake George, New York. Freshwater Biology 26, 233–240.

Madsen, J.D., Smith, D.H., 1999. Vegetative spread of dioecious Hydrilla colonies in experimental ponds. Journal of Aquatic Plant Management 37, 25-29.

Marani, M., Belluco, E., D'Alpaos, A., Defina, A., Lanzoni, S., Rinadlo, A., 2003. On the drainage density of tidal networks. Water Resources Research 39, 1040-1051, doi: 10.1029/2001WR001051.

Markewich, H.W., Pavich, M.J., Buell, G.R., 1990. Contrasting soils and landscapes of the Piedmont and Coastal Plain, eastern United States. Geomorphology 3, 417-447.

Martin, T.L., Kaushik, N.K., Trevors, J.T., Whiteley, H.R., 1999. Review: Denitrification in temperate climate riparian zones. Water, Air and Soil Pollution 111, 171-186.

Maryland Department of Natural Resources, 2012. Maryland's Environmental Resources and Land Information Network: http://www.mdmerlin.net/ (March 2012).

Mayer, P.M., Reynolds, S.K., McCutchen, M.D., Canfield, T.J., 2007. Meta-analysis of nitrogen removal in riparian buffers. Journal of Environmental Quality 36, 1172–1180, doi:10.2134/jeq2006.0462.

McCarthy, J.J., Taylor, W.R., Taft, J.L., 1977. Nitrogenous nutrition of the plankton in the Chesapeake Bay. 1. Nutrient availability and phytoplankton preferences. Limnology and Oceanography 22, 996-1011.

McClain, M.E., Boyer, E.W., Dent, C.L., Gergel, S.E., Grimm, N.B., Groffman, P.M., Hart, S.C., Harvey, J.W., Johnston, C.A., Mayorga, E., McDowell, W.H., Pinay, G., 2003. Biogeochemical hot spots and hot moments at the interface of terrestrial and aquatic ecosystems. Ecosystems 6, 301-312.

McKellar, H.N., Tufford, D.L., Alford, M.C., Saroprayogi, P., Kelley, B.J., Morris, J.T., 2007. Tidal nitrogen exchanges across a freshwater wetland succession gradient in the Upper Cooper River, South Carolina. Estuaries and Coasts 30, 989-1006.

Megonigal, J.P., Neubauer, S.C., 2009. Biogeochemistry of tidal freshwater wetlands. Coastal wetlands: An integrated approach. *In* G. Perillo, E. Wolanski, D. Cahoon, M. Brinson (eds.) Coastal wetlands: An integrated ecosystem approach. Elsevier.

Merrill, J. Z., Cornwell, J. C., 2000. The role of oligohaline marshes in estuarine nutrient cycling, in: Concepts and Controversies in Tidal Marsh Ecology, Weinstein, M. P. and Kreeger, D. A., Kluwer Academic Publ., Dordrecht, Netherlands, 425-441.

Meyer, J.L., Sale, M.J., Mulholland, P.J., Poff, N.L., 1999. Impacts of climate change on aquatic ecosystem functioning and health. Journal of the American Water Resources Association 35, 1373–1386.

Michaelis, L., Menten, M.L., 1913. Die Kinetik der Invertinwirkung. Biochemische Zeitschrift 49, 334−336.

Mitsch, W.J. and Gosselink, J.G., 2007. Wetlands. John Wiley and Sons, Hoboken, New Jersey, pp. 582.

Montgomery, D.R., 1999. Process domains and the river continuum. Journal of American Water Resources Association 35, 397-410.

Moore, M.V., Pace, M.L., Mather, J.R., Murdoch, P.S., Howarth, R.W., Folt, C.L., Chen, C.Y., Hemond, H.F., Flebbe, P.A., Driscoll, C.T., 1997. Potential effects of climate change on freshwater ecosystems of the New England/Mid-Atlantic Region. Hydrological Processes 11, 925–947.

Moore, R.D., 1997. Storage–outflow modelling of streamflow recessions with application to a shallow-soil forested catchment. Journal of Hydrology 198, 260–270.

Morris, J.T., 1980. The nitrogen uptake kinetics of *Spartina alterniflora* in culture. Ecology 61, 1114-1121.

Myrick, R.M., Leopold, L.B., 1963. Hydraulic geometry of a small tidal estuary, physiographic and hydraulic studies of rivers. U.S. Geological Survey Professional Paper 422-B, 18pp.

Mulholland, P.J., 1992. Regulation of nutrient concentrations in a temperate forest stream: Roles of upland, riparian, and instream processes. Limnology Oceanography 37, 1512-1526.

Mulholland, P.J., Best, G.R., Coutant, C.C., Hornberger, G.M., Meyer, J.L., Robinson, P.J., Steinberg, J.R., Turner, R.E., Vera-Herrera, F., Wetzel, R.G., 1997. Effects of climate change on freshwater ecosystems of the south-eastern United States and the Gulf Coast of Mexico. Hydrological Processes 11, 949–970.

Naiman, R.J, Decamps, H., 1997. The ecology of interfaces: Riparian zones. Annual Review of Ecology and Systematics 28, 621-658.

Najjar, R.G., Pyke, C.R., Adama, M.B., Breitburg, D., Hershner, C., Kemp, M., Howarth, R.,Mulholland, M.R., Paolisso, M., Secor, D., Sellner, K., Wardrop, D., Wood, R., 2010. Potential climate-change impacts on the Chesapeake Bay. Estuarine, Coastal and Shelf Science 86, 1-20, doi:10.1016/j.ecss.2009.09.026.

Navarre-Sitchler, A., Brantley, S., 2007. Basalt weathering across scales. Earth and Planetary Science Letters 261, 321-334.

Naylor, M., Kazyak, P., 1995. Quantitative characterization of submerged aquatic vegetation species in tidal freshwater reaches of the Patuxent River Drainage Basin. Chesapeake Bay and Watershed Programs: Monitoring and non-tidal assessment. Technical Report CBWP-MANTA- EA-95-2, 27 p.

Nepf, H., Ghisalberti, M., 2008. Flow and transport in channels with submerged vegetation. Acta Geophysica 56, 753-777.

Neubauer, S.C., 2008. Contributions of mineral and organic components to tidal freshwater marsh accretion. Estuarine, Coastal and Shelf Science 78, 78-88, doi:10.1016/j.ecss.2007.11.011.

Neubauer, S.C., Anderson, I.C., Constantine, J.A., Kuehl, S.A., 2002. Sediment deposition and accretion in a Mid-Atlantic (U.S.A.) tidal freshwater marsh. Estuarine, Coastal and Shelf Science 54, 713-727.

Nichols, D.S., 1983. Capacity of natural wetlands to remove nutrients from wastewater. Journal Water Pollution Control Federation 55, 495-505.

Nixon, S.W., 1987. Chesapeake Bay nutrient budgets - A reassessment. Biogeochemistry 4, 77-90.

Nixon, S.W., 1995. Coastal marine eutrophication: A definition, social causes, and future concerns. Ophelia 41, 199-219.

Nowicki, N.L., 1994. The effect of temperature, oxygen, salinity, and nutrient enrichment on estuarine denitrification rates measured with a modified nitrogen gas flux technique. Estuarine, Coastal and Shelf Science 38, 134-156.

Odum, H.T., 1988. Self-organization, transformity, and information. Science 242, 1132-1139.

Odum, W.E., 1988. Comparative ecology of tidal freshwater and salt marshes. Annual Review of Ecology and Systematics 19, 147-176.

Odum, W.E., Odum, E.P., Odum, H.T., 1995. Nature's pulsing paradigm. Estuaries and Coasts 18, 547-555.

Orth, R.J., Moore, K.A., 1984. Distribution and abundance of submerged aquatic vegetation in the Chesapeake Bay: An historical perspective. Estuaries 7, 531-540.

Orth, R.J., Nowak, J.F., Anderson, G.F., Whiting, J.R., 1994. Distribution of submerged aquatic vegetation in the Chesapeake Bay. 1993. Virginia Institute of Marine Science, Gloucester Point, VA.

Paola, C., Straub, K., Mohrig, D., Reinhardt, L., 2009. The "unreasonable effectiveness" of stratagraphic and geomorphic experiments. Earth-Science Reviews 97, 1-43.

Parkin, T.B., Kaspar, H.F., Sexstone, A.J., Tiedje, J.M., 1984. A gas-flow soil core method to measure field denitrification rates. Soil Biology and Biochemistry 16, 323-330.

Patrick, W.H. Jr., Reddy, K.R., 1976. Nitrification-denitrification reactions in flooded soils and water bottoms: Dependence on oxygen supply and ammonium diffusion. Journal of Environmental Quality 5, 469-472.

Pasternack, G.B., Brush, G.S., 1998. Sedimentation cycles in a river-mouth tidal freshwater marsh. Estuaries 21, 407-415.

Petersen, J.E., Cornwell, J.C., Kemp, W.M., 1999. Implicit scaling in the design of experimental aquatic ecosystems. Oikos 85, 3-18.

Phemister, K., 2006. Characterization of the spatial differences in hydrological functioning in a tidal marsh, Patuxent River, MD: A framework for understanding nutrient dynamics. University of Maryland M.S. Thesis, College Park, MD.

Phillips, R.E., Reddy, K.R., Patrick Jr., W.H., 1968. The role of nitrate diffusion in determining the order and rate of denitrification in flooded soils: II. Theoretical analysis and interpretation. Soil Science Society of America Journal 42, 272-278.

Pinay, G., Black, V.J., Planty-Tabacchi, A.M., Gumiero, B., Décamps, H., 2000. Geomorphic control of denitrification in large river floodplain soils. Biogeochemistry 50, 163-182, doi: 10.1023/A:1006317004639.

Poff, N.L., Allan, J.D., Bain, M.B., Karr, J.R., Prestegaard, K.L., Richter, B.D., Sparks, R.E., Stromberg, J.C., 1997. The natural flow regime. BioScience 47, 769-784.

Pritchard, D.W., 1967. What is an estuary: Physical viewpoint. Estuaries 83, 3-5.

Rabalais, N., Turner, R.E., Wiseman, W.J., 2001. Hypoxia in the Gulf of Mexico. Journal of Environmental Quality 30, 320-329.

Reddy, K.R., Patrick, W.H., Broadbent, F.E., 1984. Nitrogen transformations and loss in flooded soils and sediments, CRC Critical Reviews in Environmental Controls 13, 273-309, doi: 10.1080/10643388409381709.

Rice, D., Rooth, J., Stevenson, J.C., 2000. Colonization and expansion of *Phragmites australis* in upper Chesapeake Bay tidal marshes. Wetlands 20, 280-299.

Rinaldo, A., Rodriguez-Iturbe, I., 1998. Channel networks. Annual Reviews Earth and Planetary Sciences 26, 289-327.

Rinaldo, A., Rodriguez-Iturbe, I., Rigon, R., Ijjasz-Vazquez, E., Bras, R. L., 1993. Self-organized fractal river networks. Physical Review Letters 70, 1222-1226.

Rinaldo A., Fagherazzi, S., Lanzoni, S., Marani, M., Dietrich, W., 1999a. Tidal networks 2. Watershed delineation and comparative network morphology. Water Resources Research 35, 3905-3917.

---, 1999b. Tidal networks 3. Landscape-forming discharges and studies in empirical geomorphic relationships. Water Resources Research 35, 3919-3929.

Rinaldo, A., Belluco, E., D'Alpaos, A., Feola, A., Lanzoni, S., Marani, M., 2004. Tidal networks: Form and function. *In*: Ecogeomorphology of Tidal Marshes, Fagherazzi, S., Blum, L., and Marani, M. (Eds.), American Geophysical Union, Coastal and Estuarine Monograph Series, 1-18.

Rybicki, N.B., Jenter, H.L., Carter, V., Baltzer, R.A., Turtora, M., 1997. Observations of tidal flux between a submersed aquatic plant stand and the adjacent channel in the Potomac River near Washington, D.C. Limnology and Oceanography 42, 307–317.

Rybicki, N.B., Landwehr, J.M., 2007. Long-term changes in abundance and diversity of macrophyte and waterfowl populations in an estuary with exotic macrophytes and improving water quality. Limnology and Oceanography 52, 1195–1207.

Sauer, V.B., Meyer, R.W., 1992. Determination of error in individual discharge measurements. U.S. Geological Survey Professional Paper 92-144, 21 pp.

Saunders, D.L., Kalff, J., 2001. Nitrogen retention in wetlands, lakes, and rivers. Hydrobiologia 443, 205–212.

Scanlon, T.M., Caylor, K.K., Levin, S.A., Rodriguez-Iturbe, I., 2007. Positive feedbacks promote power-law clustering of Kalahari vegetation. Nature 449, 209-212, doi: 10.1038/nature06060.

Schaefer, S.C., Alber, M., 2007. Temperature controls a latitudinal gradient in the proportion of watershed nitrogen exported to coastal ecosystems. Biogeochemistry 85, 333–346, doi: 10.1007/s10533-007-9144-9.

Scheffer, M., Hopser, S.H., Meijer, M-L., Moss, B., Jeppesen, E., 1993. Alternative equilibra in shallow lakes. Trends in Ecology and Evolution 8, 275-279, doi: 10.1016/0169-5347(93)90254-M.

Scott, J.T., McCarthy, M.J., Gardner, W.S., Doyle, R.D., 2008. Denitrification, dissimilatory nitrate reduction to ammonium, and nitrogen fixation along a nitrate concentration gradient in a created freshwater wetland. Biogeochemistry 87, 99-111.

Seitzinger, S.P., 1988. Denitrification in freshwater and coastal marine systems: ecological and geochemical significance. Limnology and Oceanography 33,702-724.

---, 1994. Linkages between organic matter mineralization and denitrification in eight riparian wetlands. Biogeochemistry 25, 19-39.

Seitzinger, S.P., Nielsen, L.P., Caffrey, J., Christensen, P.B., 1993. Denitrification measurements in aquatic sediments: A comparison of three methods. Biogeochemistry 23, 147-167.

Seitzinger, S.P., Nixon, S., Pilson, M.E.Q, Burke, S., 1980. Denitrification and N_2O production in near-shore marine sediments. Geochimica et Cosmochimica Acta 44, 1853-1855, 1857-1860.

Seitzinger, S.P., Styles, R.V., Boyer, E.W., Alexander, R.B., Billen, G., Howarth, R.W., Mayer, B., van Breemen, M., 2002. Nitrogen retention in rivers: Model development and application to watersheds in the Northeastern U.S.A. Biogeochemistry 57/58, 199-237.

Seitzinger, S.P., Harrison, J.A., Böhlke, J.K., Bouwman, A.F., Lowrance, R., Peterson, B., Tobias, C., van Drecht, G., 2006. Denitrification across landscapes and waterscapes: A synthesis. Ecological Applications 16, 2064-2090.

Seldomridge, E., 2009. Importance of channel networks on nitrate retention in freshwater tidal wetlands, Patuxent River, MD. University of Maryland M.S. Thesis, College Park, MD, pp. 118.

Seldomridge, E., Prestegaard, K., 2011. Is denitrification kinetically-limited or transport-limited in tidal marshes? Applied Geochemistry 26, S256-S258, doi: 10.1016/j.apgeochem.2011.03.117.

Seldomridge, E., Prestegaard, K.L., 2012. Use of geomorphic, hydrologic, and nitrogen mass balance data to model ecosystem nitrate retention in tidal freshwater wetlands. Biogeosciences 9, 1407-1437, doi: 10.5194/bgd-9-1407-2012.

Sferratore, A., Billen, G., Garnier, J., Thery, S., 2005. Modeling nutrient (N, P, Si) budget in the Seine watershed: Application of the Riverstraher model musing data from local to global scale resolution. Global Biogeochemical Cycles 19, GB4S07.

Sheibley, R.W., Jackman, A.P., Duff, J.H., Triska, F.J., 2003. Numerical modeling of coupled nitrification-denitrification in sediment perfusion cores from the hyporheic zone of Shingobee River, MN. Advances in Water Resources 26: 977-987.

Shreve, R.L., 1967. Infinite topologically random channel networks. Journal of Geology 75, 178-186.

Simpson, R.L., Good, R.E., Leck, M.A., Whigham, D.F., 1983. The ecology of freshwater tidal wetlands. BioScience 33, 255- 259.

Smullen, J.T., Taft, J.I., Macknis, J., 1982. Nutrient and sediment loads to the tidal Chesapeake Bay system, p. 147-258. *In* United States Environmental Protection Agency, Chesapeake Bay Program. Technical Studies: A Synthesis. Washington, D.C.

Snyder, N.J., Mostaghimi, S., Berry, D.F., Reneau, R.B., Hong, S., McClellan, P.W., Smith, E.P., 1998. Impact of riparian forest buffers on agricultural nonpoint source pollution. Journal of the American Water Resources Association 34, 385-395.

Solorzano, L., 1969. Determination of ammonia in natural waters by the phenolhypochlorite method. Limnology and Oceanography 14, 799-801.

Sørensen, J., 1978. Denitrification rates in a marine sediment as measured by the acetylene inhibition technique. Applied and Environmental Microbiology 36, 139-143.

Stanford, G., Dzienia, S., Vander-Pol, R.A., 1975. Effect of temperature on denitrification rate in soils. Soil Science Society of America Proceedings 39, 867-870.

Strahler, A.N., 1952. Hypsometric (area-altitude) analysis of erosional topology. Geological Society of America Bulletin 63, 1117-1142.

Tanner, C.C., 1996. Plants for constructed wetland treatment systems - A comparison of the growth and nutrient uptake of eight emergent species. Ecological Engineering 7, 59-83, doi:10.1016/0925-8574(95)00066-6.

Temmerman, S., Bouma, T.J., Govers, G., Wang, Z.B., de Vries, M.B., Herman, P.M.J., 2005. Impact of vegetation on flow routing and sedimentation patterns: Three-dimensional modeling for a tidal marsh. Journal of Geophysical Research 110, 1-18.

Testa, J.M., Kemp, W.M., Boynton, W.R., Hagy, J.D., 2008. Long-term changes in water quality and productivity in the Patuxent River Estuary: 1985 to 2003. Estuaries and Coasts 31, 1021-1037, doi: 10.1007/s12237-008-9095-y.

Thom, A., 1971. Momentum absorption by vegetation. Quarterly Journal of the Royal Meteorological Society 97, 414-428.

Tiedje, J.M., 1988. Ecology of denitrification and dissimilatory nitrate reduction to ammonium. p. 179-244. *In* A.J.B. Zehnder (ed), Environmental Microbiology of Anaerobes. John Wiley and Sons, N.Y.

Tischner, R., 2000. Nitrate uptake and reduction in higher and lower plants. Plant, Cell & Environment 23, 1005–1024, doi: 10.1046/j.1365-3040.2000.00595.x.

Turner, R.E., Rabalais, N.N., 2003. Linking landscape and water quality in the Mississippi River Basin for 200 years. BioScience 53, 563–72.

Turner, R.E., Howes, B.L., Teal, J.M., Milan, C.S., Swenson, E.M., Goehringer-Toner, D.D., 2009. Salt marshes and eutrophication: An unsustainable outcome. Limnology and Oceanography 54, 1634-1642.

United States Geological Survey, 2009. Chesapeake Bay River Input Monitoring Program: http://va.water.usgs.gov/chesbay/RIMP/index.html (March 2012).

United States Geological Survey, 2012. National Water Information System: http://waterdata.usgs.gov/nwis (March 2012).

Van, T.K., Haller, W.T., Bowes, G., 1976. Comparison of the photosynthetic characteristics of three submersed aquatic plants. Plant Physiology 58, 761-768.

VanNess, E.H., Scheffer, M., van den Berg, M.S., and Coops, H., 2002. Dominance of charophytes in eutrophic shallow lakes—when should we expect it to be an alternative stable state? Aquatic Botany 72, 275–296.

Vidon, P., 2010. Riparian zone management and environmental quality: A multi-contaminant challenge. Hydrological Processes 24, 1532–1535, doi:10.1002/hyp.7740.

Vidon, P., Dosskey, M.G., 2008. Testing a simple field method for assessing nitrate removal in riparian zones. Journal of the American Water Resources Association 44, 523-534, doi: 10.1111/j.1752-1688.2007.00155.x.

Wallenstien, M.D., Myrold, D.D., Firestone, M., Voytek, M., 2006. Environmental controls on denitrifying communities and denitrification rates: Insights from molecular methods. Ecological Applications 16, 2143-2152.

Weisman, R.N., 1977. The effects of evapotranspiration on streamflow recession. Hydrological Science Bulletin XXII, 3, 371–377.

Wigington, P.J., Griffith, S.M., Field, J.A., Baham, J.E., Horwath, W.R., Owen, J., Davis, J.H., Rain, S.C., Steiner, J.J., 2003. Nitrate removal effectiveness of a riparian buffer along a small agricultural stream in Western Oregon. Journal of Environmental Quality 32, 162-170.

Windolf, J., Jeppesen, E., Jensen, J.P., Kristensen, P., 1996. Modelling of seasonal variation in nitrogen retention and in-lake concentration: a four-year mass balance study in 16 shallow Danish lakes. Biogeochemistry 33, 25–44.

Wittenberg, H., Sivapalan, M., 1999. Watershed groundwater balance estimation using streamflow recession analysis and baseflow separation. Journal of Hydrology 219, 20–33.

Wolf, K.L., Ahn, C., Noe, G.B., 2011. Microtopography enhances nitrogen cycling and removal in created mitigation wetlands. Ecological Engineering 37, 1398-1406.

Wollheim, W.M., Vörösmarty, C.J., Peterson, B.J., Seitzinger, S.P., Hopkinson, C.S., 2006. Relationship between river size and nutrient removal. Geophysical Research Letters 33, L06410.

Yu, K., DeLaune, R.D., Boeckx, P., 2006. Direct measurement of denitrification activity in a Gulf coast freshwater marsh receiving diverted Mississippi River water. Chemosphere 65, 2449-2455.